8129436

SMITH, LINDA SUSAN

A NEW VAPOR DENSITY TECHNIQUE FOR STUDYING PROTON DONOR - ACCEPTOR INTERACTIONS IN THE GAS PHASE

The University of Oklahoma PH.D. 1981

University Microfilms International 300 N. Zeeb Road, Ann Arbor, MI 48106

THE UNIVERSITY OF OKLAHOMA

GRADUATE COLLEGE

A NEW VAPOR DENSITY TECHNIQUE FOR STUDYING PROTON DONOR - ACCEPTOR INTERACTIONS IN THE GAS PHASE

A DISSERTATION

SUBMITTED TO THE GRADUATE FACULTY

in partial fulfillment of the requirements for the

degree of

DOCTOR OF PHILOSOPHY

BY

LINDA SUSAN SMITH

Norman, Oklahoma

1981

A New Vapor Density Technique

for Studying

Proton Donor-Acceptor Interactions

Approved by

Dissertation Committee

ACKNOWLEDGEMENT

I am very grateful to the many people who contributed to my research program. I appreciate the time and consideration the members of my advisory committee gave to my graduate exam and this dissertation. I am particularly grateful for the assistance of Dr. Lloyd Lee in preparing for the graduate exam and for the opportunity to study statistical thermodynamics with him.

There were several undergraduates who helped collect data for one of the systems studied in the dissertation research and I would like to express my thanks to them: Dale Christian, William Hartsell, Mohit Nanda, Richard Shahan, and Kevin Stellner.

Dr. Ed Tucker's contribution to this research cannot be overstated and is greatly appreciated. His knowledge of instrumentation is amazing and I have learned many practical laboratory techniques from him.

The contributions of my sister, Donna Bushong, to my progress as a graduate student has been both professional and personal. She is a dearest friend and a wonderful sister; her patience and friendship will never be forgotten.

Every successful graduate student owes much of that success to his or her advisory professor; I am no exception. I hope that my approach to chemical problems and the degree of professionalism in my work is a reflection of the daily example of Dr. Sherril Christian. He is greatly respected by his many co-workers and I feel privileged to know him and share that respect.

Thank you, Dr. Christian.

The completion of

this dissertation is dedicated to

my husband,

with love.

TABLE OF CONTENTS

TABLE OF CONTENTS cont.

TABLE OF CONTENTS cont.

LIST OF TABLES

LIST OF TABLES cont.

LIST OF TABLES cont.

LIST OF ILLUSTRATIONS

LIST OF ILLUSTRATIONS cont.

LIST OF ILLUSTRATIONS cont.

CHAPTER I

INTRODUCTION

i. General

The perfect gas is characterized by the equation of state, PV = nRT. The ideal behavior of solutions

$$A(gas) \rightleftharpoons A(solution)$$

is described by Raoult's law[1]

$$P_A = P_A^\circ X_A$$

and Henry's[2] law

$$P_A = K_H X_A .$$

P_A is the pressure of component A, P_A° is the vapor pressure of component A, and X_A is the mole fraction of component A in solution. K_H is the Henry's law constant.

In nature, pure fluids or mixtures of fluids do not ordinarily exhibit ideal behavior. Some examples of this nonideality are molecular association in the vapor phase, the existence of azeotropes in binary liquid-vapor mixtures, and the

varying degree of complexation dependent on the environment of the complexing species in solutions.

Adequate theories of the nature of the interactions contributing to non-ideal behavior are important with respect to a variety of scientific studies. Rectification of liquids and separation of mixtures of liquids through distillation require information on the liquid-vapor equilibrium behavior of the system. In order to understand biological systems, information about solvent effects is necessary to characterize the interactions in protein association or enzymatic reactions. Tertiary recovery of oils involves solubilizing hydrocarbons into an aqueous medium via surfactant molecules or the solubilization of hydrocarbons by carbon dioxide as it flows past oil-filled capillaries in rocks or clay. And, from a very fundamental standpoint, experimental data on molecular association in the vapor phase may be analyzed and compared with statistical mechanical or quantum mechanical theories of molecular association for the purpose of confirming or rejecting the theoretical models.

J. Willard Gibbs[3] discussed nonideal behavior in the vapor phase in terms of "convertible components" as early as 1875. In his discussions of gas mixtures of formic acid, acetic acid, phosphorus pentachloride, and nitrogen dioxide, Gibbs recognized the existence of other species in equilibrium with the monomer[4]

$$2HCOOH \rightleftharpoons (HCOOH)_2$$

$$2CH_3COOH \rightleftharpoons (CH_3COOH)_2$$

$$PCl_5 \rightleftharpoons PCl_3 + Cl_2$$

$$2NO_2 \rightleftharpoons N_2O_4$$

and assumed that each group of species obeys the ideal gas law. An imperfect gas may be considered to be an equilibrium mixture of readily interconvertible monomers, dimers, trimers, etc.[5]

In condensed-phase systems, deviations from Raoult's law or Henry's law are measures of the nonideality due either to solvent-solute interactions or solute-solute interactions. Early discussions of the nature of these interactions resulted in polemics in the literature[6] between those who attributed deviation from Raoult's law to physical (nonspecific) interactions between molecules[7,8] and those who attributed deviations from Raoult's law to chemical (specific) associations between molecules.[9] According to Dolezalek,[9] all deviations from Raoult's law are due to the formation of chemical bonds between solute and solvent molecules (negative deviations) or solute and solute molecules (positive deviations). On the other side of the controversy, van Laar[7] ascribed deviations from Raoult's law to effects of a nonspecific nature (i.e. interactions between molecules which occur through physical interactions not involving the formation of chemical bonds.) At the time of their controversy, G. N. Lewis had not yet proposed his more general theory for acid-base interactions, namely the donation of a pair

of electrons by one species to another species, nor had London[12] described the dispersion forces; the former theory applies to specific interactions, the latter to nonspecific interactions.

More recent proponents of the chemical interaction school of thought claimed that actual bonds do exist between molecules of a covalent[13] or ionic[14] nature. A specific interaction may be dicussed in terms of the specific chemical nature of the molecules involved and their capacity for chemical combination (e.g. hydrogen bonds).[15] The idea that the deviation is only due to the formation of chemical bonds has been proven incorrect by the adherence of many gases to the principle of corresponding states.

A rule of thumb proposed by Redlich[16] to differentiate between "physical" and "chemical" interactions spectroscopically in condensed phases is:

if, in a solution, the frequency of a particular line or band continuously changes on changing the concentration, the shift is due to a "physical" interaction with the environment;

if one line gradually becomes less intense while a different line appears and becomes stronger, a "chemical" equilibrium is assumed to exist between two distinct species.

(A discussion of spectral techniques to study molecular association is presented in section iv.).

In more general terms, interactions which satisfy the valence bond theory forces[17] are considered chemical if

a) bonds, when formed, have a natural angle between them;

b) bonds involve electrons with paired spins, and with a charge-cloud localized in the region of the bond;

c) saturation of valence completes the octet of electrons;

d) excitation of an electron from one orbital to another will often result in an increase in the number of bonds an atom can form.

These bonds may be either electrostatic or covalent in nature or some combination of electrostatic and covalent forces. Van der Waals or polarization forces are weak compared with valence forces. "In general, we do not consider the weak van der Waals forces between molecules as leading to chemical bond formation."[18] Thus, the individuality of the molecule remains intact.

Methods for separating the second virial coefficient into specific and nonspecific contributions are varied. (The second virial coefficient is dicussed in section iii.) One such separation[10] was attempted by measuring the vapor phase association of the non-polar homomorph of acetonitrile, namely propane. The second virial coefficient for this association is labelled B (non-polar). This B (non-polar) is then subtracted from the observed second virial coefficient for the vapor phase association of acetonitrile to yield a virial coefficient, B (polar), for specific interactions.

$$B(\text{observed}) = B(\text{non-polar}) + B(\text{polar})$$

Another method employs the Berthelot equation[19] to calculate B (non-polar), which is then subtracted from B(observed) for a polar vapor to yield a measure of the specific interaction contribution, B (polar). This second method is analogous to attributing the specific interaction to the deviation of a curve of the reduced temperature verses the reduced observed second virial coefficient from the curve relating to the principle of corresponding states. This division is somewhat arbitrary and contrary to one of the purposes of obtaining an experimental virial coefficient, that is to compare it with virial coefficients calculated from the statistical mechanical or quantum mechanical theories. In any case, molecules are believed to interact with one another, but for the most part, the intermolecular forces involved are small compared with the interatomic forces within molecules.

Both physical and chemical interactions are responsible for deviations from ideality; these chemical inteactions are not as strong as covalent or ionic bonds whose energies of interaction are about 50-100 kcal/mole. For studies of imperfect vapors, it seems reasonable to assume that all deviations are due strictly to formation of discrete dimers, trimers, tetramers, etc. as has often been assumed in the past.[5,20] A criticism of this assumption suggests that the contribution of the imperfection of the monomer to the deviations from ideality is ignored leading to an overestimation of the degree of dimerization.[21] It will be the

assumption of this writer that all species behave ideally in the vapor phase.

Although there have been many studies of nonelectrolyte association in the solution phase,[20] a composite understanding of the types of physical or chemical interactions is not available since the degree of complexation is affected by the solvent environment. Attempts have been made to predict the effects of solvent on complexation through the use of a single parameter, α[22-25]"By a two-step process involving the vapor as an intermediate state, it is possible to predict the changes in ΔE° and ΔG° for the association reaction as the medium is changed from one solvent to another."[22]

$$\alpha = \Delta E^\circ_{\substack{DA \\ v \to s}} / (\Delta E^\circ_{\substack{D \\ v \to s}} + \Delta E^\circ_{\substack{A \\ v \to s}})$$

and

$$\alpha' = \Delta G^\circ_{\substack{DA \\ v \to s}} / (\Delta G^\circ_{\substack{D \\ v \to s}} + \Delta E^\circ_{\substack{A \\ v \to s}})$$

for the reaction

$$D + A \rightleftharpoons DA.$$

The parameter, α, is approximately equal to α' for a given solvent. D is a donor molecule and A is an acceptor molecule; DA is a molecular complex. The value of methods for predicting the effects of media on complex formation are: [24]

(1)comparison with theory will be facilitated if reliable techniques evolve for converting thermodynamic information

about complex formation in condensed phases into information about the corresponding gaseous state;

and (2) an understanding of the role of solvents in altering properties of complexes wil be essential in future attempts to provide a molecular explanation of biological and industrial systems in which electron donor-acceptor complexes are important.

Tautomeric equilibrium data provide evidence of the effect of the environment on molecular species. For example, "the long-accepted idea that 2-pyridone is more stable than 2-hydroxy-pyridine has recently been shown to result from differences in solvation between the two isomers."[26-29] In fact, there appears to be no significant difference in stability between the two tautomers in the vapor phase.

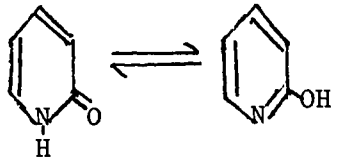

Although some solvents have in the past been labelled "inert", there are, in fact, no such solvents. This is evidenced by the change in association constants of methanol and triethylamine in a series of solvents and in the vapor phase.[30] (See Table I-1.)

The vapor phase is the only inert solvent nature has to offer and should be exploited for its simplicity. The need to investigate molecular association in the vapor phase without complicating solvent effects has been recognized by many

investigators in this field.[20,24,28,30-32] For this reason, this study will be an investigation of molecular association in the vapor phase for the purpose of understanding the origin of interactions causing deviations from ideality without the complications of solvent effects.

TABLE I-1

Solvent Effects

on Forming the 1:1 Complex: Triethylamine - Methanol

Solvent	Dielectric Constant	$-\Delta E$ (kcal/mole)
vapor	1	7.6
CCl_4	2.24	6.0
C_6H_5Cl	5.71	4.3
CH_2Cl_2	9.08	3.0

ii. Molecular Complexes

Nonpolar molecules, such as cyclohexane and benzene,[33,34] interact in the vapor phase to produce noticeable deviations from ideality. From F. London:[12] "Though it is, of course, not possible to describe this interaction mechanism in terms of our customary classical mechanics, we may still illustrate it in a kind of semi-classical language. If one were to take an instantaneous photograph of a molecule at any time, one would find various configurations of nuclei and electrons, showing, in general, dipole moments. In a spherically symmetrical rare gas molecule, as well as in our isotropic oscillators, the average over very quickly varying dipoles, represented by the zero-point motion of a molecule, produces an electric field and acts upon the polarizability of the other molecules and produces these induced dipoles, which are in phase and in interaction with the instantaneous dipoles producing them." This results in the formation of instantaneous clusters of molecules (usually no larger than the dimer for nonpolar gases) which may be called "complexes" or "aggregates". One would not choose to describe these complexes as molecules since the forces holding them together are much weaker than the intramolecular forces between the atoms of each monomer. The complex may not be bound together at all in the chemical sense; rather, the nuclei of the two monomers are at an equilibrium distance apart such that the energy

monomers are at an equilibrium distance apart such that the energy of the dimer is lower than the sum of the energy of the individual monomers. The dimer behaves as a single unit rather than two single units, thus creating the nonideal behavior.

The principle of corresponding states is obeyed by nonpolar vapors but does not hold for polar vapors.[21] The interactions between polar molecules involve the forces described by London (above) for nonpolar molecules, in addition to the more directional permanent electrical moments (e.g. dipole-dipole, dipole-quadrupole, etc.) and, in some instances, transfer of charge or hydrogen bonding. As mentioned earlier, efforts have been made to quantitatively separate the nonpolar contributions from polar contributions. Lambert, et al.[35] divided hydrocarbons into two classes. Class I represented nonpolar hydrocarbons in which the intermolecular forces were believed to be insufficient for the formation of dimers and only give rise to the general acceleration of molecules approaching one another. Class II described polar hydrocarbon behavior in which dimerization occurred.

Intermolecular forces are of two types: long-range (van der Waals) forces [36] and short-range (valence or chemical) forces.[16,38] The forces binding molecular complexes are usually weaker than valence forces (though hydrogen bonding has been described in terms of valence bond theory [16]). Long-range forces are of four types:[36]

1) electrostatic forces (important when two polar molecules interact),

2) induction forces (which occur when a polar molecule and a nonpolar molecule interact),

3) London forces (or dispersion forces, as described above, are important between two non-polar molecules),

4) resonance forces (which occur between two identical molecules.)

Polar molecules form complexes due to van der Waals forces alone or due to a hybrid of long-range and short-range forces as is the case in charge-transfer complex formation and hydrogen bonded complexes.

The theory of charge-transfer complexes is based on the concept of the isolated donor, acceptor, and complex.[39] The terms charge-transfer (CT) and electron donor-acceptor (EDA)[40] appear to be interchangeable with respect to complex origin.[41] However, some complexes to which either name has been applied are not bound by an actual transfer of charge. These complexes are probably due to long-range van der Waals forces and electrostatic interactions. When an actual intermolecular charge-transfer transition involving electron transfer from the donor to the acceptor occurs, an electronic absorption in addition to the absorption of the components is often observed.[41]

Weiss,[14] in 1942, called attention to the relation between complexing and the electron affinity of acids and the

ionization potential of bases. In 1923, G. N. Lewis generalized the acid-base concept to define an acid as any substance, in its ground state, able to accept a "lone pair" of electrons from another molecule, designated a base. A further modification of the acid-base concept is made by introducing the description electron donor-acceptor (EDA). EDA complexes involve the transfer of a single electron rather than a "lone pair" of electrons. The rates of formation of CT complexes and decomposition into the components are so high that the reaction appears to be instantaneous by normal techniques. The enthalpy of formation is usually on the order of a few kcal/mole.[41]

The hydrogen bond was proposed by A. Werner,[43] in 1902, (although he did not use the term hydrogen bond) to explain the chemical nature of ammonium hydroxide.

$$H_3N\ldots H\text{-}OH \rightleftharpoons H_3N\text{-}H\ldots O\text{-}H$$

A few years later, P. Pfeiffer[44] explained the structure of carboxylic acid as a cyclic dimer involving two hydrogen bonds.

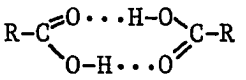

In 1920, W. M. Latimer and W. H. Rodebush[45] explained the structure of water as follows:

> "Water ... shows tendencies both to add and give up hydrogen, which are nearly balanced. Then...a free pair of electrons on one water molecule might be able to exert sufficient force on

a hydrogen held by a pair of electrons on another water molecule to bind the two molecules together.... Indeed the liquid may be made up of large aggregates of molecules, continualy breaking up and reforming under the influence of thermal agitation. Such an explanation amounts to saying that the hydrogen nucleus held between two octets constitutes a weak 'bond'."

L. Pauling[47] made the prediction, which won acclaim from many scientists, that the significance of the hydrogen bond for physiology would be found to be greater than that of any other single structural feature. Indeed, there have been many studies on hydrogen bonded systems where the hydrogen bond is intermolecular and causes dimer formation or extended association, or where the hydrogen bond is intramolecular and the hydrogen atom is bound to two atoms of the same molecule. Hydrogen bonds are also known in ionic crystals (e.g. the anion, $(FHF)^-$, exists as a distinct charged unit in the KHF_2 crystal.[16])

In the case of molecular association studies, hydrogen bonded complexes have been studied to a far greater extent than complexes held together by less-specific interactions. This is most probably due to the higher degree of association found in hydrogen bonded systems which might be detected more easily by some experimental techniques. And, as Pauling predicted, hydrogen bonded systems are very important to biochemical studies.

Hydrogen bonding may be classified as a specific interaction between atoms or functional groups in which:[49]

1) the strength is higher than that of dispersion forces alone;

2) it is directed along a hydrogen atom; and

3) the association demonstrates some kind of characteristic angular dependence.

Most usually hydrogen bonds occur when the hydrogen on one molecule is attached to oxygen or nitrogen and comes in contact with an oxygen, nitrogen, fluorine, or, sometimes, chlorine atom of another molecule. In order that the electrostatic energy will be greatest, the units must approach as closely as possible. The bonded hydrogen atom permits closest approach of the O, N, F, or Cl atom on the other molecule without the introduction of large repulsive energy terms due to unbound electrons. It is necessary to have electronegative atoms at either end of the hydrogen, again, because small size readily permits a close approach of the two molecules.[16] Weaker hydrogen bonds such as

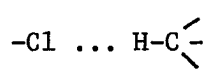

-Cl ... H-C<-

are stabilized mainly through electrostatic interactions with very little resonance character.[16]

The enthalpy of formation for

O ... H-O- , F ... H-F, or N...H-N

hydrogen-bonds is about -4 to -7 kcal/mole. For the weaker hydrogen bonds, such as C-H...N, $\Delta H = -3$ kcal/mole.[51]

iii. Equations of State and the Second Virial Coefficient

Various modifications to the equation of state for perfect gases have been implemented to arrive at an equation of state which more closely represents real gases. The first significant attempt to interpret the deviations of a real gas from the ideal gas law was made by van der Waals[52] in 1873. He proposed an equation of state which accounts for the attractive forces between molecules, a/V^2, and the finite volume occupied by the molecules, b.

$$P = RT/(V-b) - a/V^2 .$$

Another 2-parameter equation of state, known as the Berthelot equation,[19] relates the van der Waals' a and b to critical constants,

$$PV = RT + (b - a/RT^2)P,$$

where $R=32P_cV_c/9T_c$; $a=16P_cV_c^2 T_c/3$; $b=V_c/4$. The Berthelot equation describes nonpolar gases at low pressures very well.[35]

A fairly universally accepted equation of state in which the parameters can be related to macroscopic behavior and microscopic properties is the virial equation of state. "The reason for the special importance of the virial equation of state is that it is the only equation of state known which has a

thoroughly sound theoretical foundation. There is a definite interpretation for each virial coefficient in terms of molecular properties."[32] The equation expresses the deviations from the perfect gas equation and is written as a power series in either density or pressure. Written as a power series in pressure, the equation is of the form

$$PV/RT = 1 + BP^2 + CP^3 + DP^4 + \ldots$$

where the coefficients of expansion, B, C, D, ..., are the second, third, fourth, ... virial coefficients.

The theoretical foundations for the virial equation of state were developed after the acceptance of the equation for experimental use. The virial coefficients may be derived either through classical or quantum mechanics.[53] The dependence of the second virial coefficient on temperature is fairly simply related to the intermolecular potential, U(r), as follows:[54]

$$B(T) = -2\Pi N \int_0^\infty \{ \exp(-U(r)/kT) - 1\} r^2 dr$$

where r is the intermolecular radius, k is the Boltzman constant, and N is the number of molecules in the system. The quantity in brackets {} must be averaged over all orientations of both molecules for each value of r.

The second virial coefficient physically represents the formation of dimers. At low temperatures,[56] collisions between pairs of molecules are strongly influenced by long-range

attractive intermolecular forces, and such pairs may spend considerable time in one another's vicinity. These pairs are, in effect, molecular complexes and the existence of these transient dimers reduces the pressure below the ideal gas value, thus B is negative. At a much higher temperature, the collisions are more energetic and short-range repulsive forces become more important. At the temperature where the repulsive forces balance the attractive forces, the second virial coefficient is zero. This is known as the Boyle point.[57] As the temperature increases beyond the Boyle point, the repulsive forces become more important than the attractive forces and the second virial coefficient becomes positive. At still higher temperatures, the curve B(T) hits a maximum and begins to decrease, indicating that the collisions have become so energetic that the molecules begin to feel the "softness" of each other's cores.

The geometry of a molecule can not be inferred from the second virial coefficient;[5] however, molecular orbital calculations have been made on many systems in attempts to determine the most stable conformation of dimers and trimers.[58-62] Oftentimes, two different geometries are presented as the most stable structures as in the case of the acetone dimer. Two stable dimers according to ab initio molecular orbital calculations for acetone are:[60]

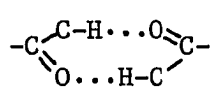

or

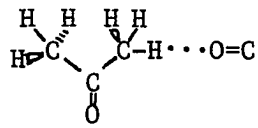

where a very weak hydrogen bond of the type C=O...H-C is found to be involved in the interaction between two monomers. Two geometries are proposed for formaldehyde dimers,

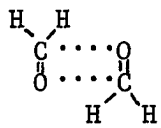

(1)

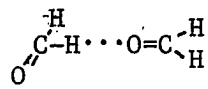

(2)

Geometry (1) involves dipole-dipole interactions and geometry (2) involves a weak hydrogen bond, again, of the type C-H...O=C. For formaldehyde, geometry (2) is the more stable.

In the case of 2,2,2-trifluoroethanol (TFE), Curtiss, Frurip, and Blander[58] studied the self-association in the vapor phase using thermal conductivity measurements and found evidence of only monomeric and dimeric species. Ab initio molecular orbital calculations were carried out on four possible dimer structures and their results showed the most stable dimer to be a cyclic structure,

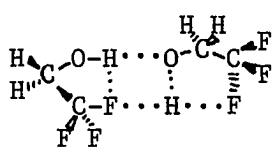

They concluded that a cyclic structure of the dimer was compatible with their experimental findings; namely, no species larger than the dimer contributes to the nonideal behavior of TFE. Vapor-density experimental evidence is strong for higher order species being present in TFE vapor at pressures greater than two-thirds of the vapor pressure of TFE.[63,64]

The virial equation of state is used in the chemical association model or mass action model. The one assumption of this model is that all deviations from ideal behavior in a gas are due to the fromation of dimers, trimers, tetramers, etc. No attempt is made to separate physical effects from chemical effects. Each virial coefficient is related to an equilibrium constant as follows.[65]

$$B = -K_2$$

$$C = 4K_2^2 - 2K_3$$

$$D = -20K_2^3 + 18K_2K_3$$

etc.

K_i is the formation constant for the reactions

$$iA \overset{K_i}{\rightleftharpoons} A_i$$

where $K_i = A_i / A^i$.

The fugacity, f, of a vapor is a concept introduced for convenience.[2] From the ideal gas law, the chemical potential, μ, or Gibbs free energy, ΔG, is related to pressure in the following equation,

$$\Delta\mu = \Delta G = RT\ln(P_1/P_2).$$

For real gases, the fugacity is defined by the expression

$$\mu = \mu^{\circ} + RT\ln(f)$$

with the requirement that

$$\lim_{\rho \to 0} f/P = 1.$$

For the chemical association model, the fugacity is equivalent to the pressure of the monomer.

A discussion of the various experimental methods used in studying molelcular association follows.

iv. Experimental Methods

A few instrumental techniques dominate experimental studies of molecular association in the vapor phase. These include spectrophotometric techniques, vapor density (or P-V-T) studies, and measurements of thermal conductivities.

Although vapor density studies were used for early studies of molecular association,[3,4] there are few reliable vapor density data in the literature until about twenty years ago. Spectroscopic techniques seemed the method of choice.

A method of studying the hydrogen bond was developed by Wulf, Hendricks, Hilbert, and Liddel[66-72] in the 1930's. Substances of interest were dissolved in carbon tetrachloride and investigated using infrared spectroscopy. Around the same time, Badger and Bauer [73] adopted this method to study hydrogen bonding in the vapor phase. Molecules containing an O-H bond exhibit a vibration in the neighborhood of 3500 cm^{-1} corresponding to the O-H stretching and the first overtone at about 7000 cm^{-1}. Hilbert, Wulf, Hendricks, and Liddel studied compounds in which strong hydrogen bond formation was known to exist and found these compounds exhibit weak and diffuse absorption bands in the 7000 cm^{-1} region rather than a sharp peak.

Brackmann[74] used spectroscopy to study charge-transfer complexes recognizing that an absorption spectrum of an electron donor and electron acceptor retains the absorption bands of the components, modified to a greater or lesser extent by the presence of the complex, and one or more absorption bands characteristic of the complex. Mulliken and co-workers[39,75-77] wrote a series of papers on the spectra of molecular complexes, further elucidating the phenomenon of charge transfer between electron donor and acceptor molecules.

Determination of thermodynamic properties from spectral data is based on the assumption that each individual species, either electron donor, electron acceptor, and complex or monomer, dimer, trimer, etc., obeys Beer's law.[78] This is quite reasonable for vapor phase studies.[20] In addition, for each species, i, the extinction coefficient or molar absorptivity, a_i^λ, must be determined at a particular wavelength, λ. The equilibrium constant K_2 for the reaction $A + D \rightleftharpoons AD$ is determined from the equation consistent with Beer's law,

$$A_\lambda = a_A^\lambda P_A + a_D^\lambda P_D + a_{AD}^\lambda K_2 P_A P_D.$$

$K_2 = P_{AD}/P_A P_D$ and P_i is the partial pressure of component i. A_λ is the absorbance. Additional terms may be added to the equation to account for higher order aggregates such as trimer, tetramer, etc. Determination of so many parameters is a problem and, so, dimers are usually the highest order complex accounted for.

In addition to infrared and ultraviolet spectroscopy, nuclear magnetic resonance[79] and, to a lesser extent, fluorimetric[80] spectroscopy have been used to investigate molecular association in solution phase. IR, UV, and NMR[81] spectroscopy have all been used for vapor phase molecular association studies as well.

The variation of thermal conductivity with pressure is a function of gas imperfection.[82] The increase in the thermal conductivity with increasing pressure indicates the presence of associated species in the vapor. "Thermal conductivity is the transport of thermal energy resulting from the existence of thermal gradients in the gas."[83] Energy is transferred very rapidly, from the center of one molecule to another when the two molecules collide. When a linear steady-state temperature distribution is attained in a medium, a constant rate of heat flow, Q, is required to maintain the temperature difference ΔT. For sufficiently small values of ΔT the following relation holds:

$$Q/A = \lambda \Delta T/X.$$

The heat flow per unit area, A, is proportional to the temperature decrease in the distance X. The constant of proportionality, λ, is the thermal conductivity of the medium.[114]

Thermal conductivity data analysis is rather involved and will be presented here only very briefly. Data are collected as pressure versus thermal conductivity coefficient at several

temperatures. The thermal conductivity coefficient is related to the pressure of the monomer, P_1, in the equation

$$\lambda = \lambda_f + \lambda_R ,$$

where only λ_R is dependent on pressure change and may be written

$$\lambda_R = (PD_{12}/RT)(\Delta H_2^2/RT^2)\ K_2 P_1/(1 + 2K_2 P_1)^2 ,$$

where D_{12}, the binary diffusion coefficient, must be calculated from kinetic theory[83] or obtained from a least squares fit of the product PD_{12} as an empirical function of the temperature:[58] $PD_{12} = aT^{3/2} + b$. The heat of formation of the dimer, ΔH_2, and the equilibrium constant at a given temperature, K_2, are determined from this equation. The pressure dependence of λ_f, known as the "frozen" thermal conductivity coefficient, is very small (about 2% of the pressure at saturation for 2,2,2-trifluoroethanol[58]) and may be corrected for.

There are many different methods used in thermal conductivity measurements. These are discussed by Touloukian et al.[84] along with their advantages and disadvantages and conditions under which optimal results might be expected. The methods most often cited in experimental sections of thermal conductivity studies of molecular association in the literature are the hot-wire method and the parallel-plate method. According to Touloukian et al.,[84] care must be taken:

(1) to avoid loss of energy by convection or radiation,

(2) to reduce the effect of temperature jump at the cell-sample interface due to unequal heating of the wall,

(3) to account for the small temperature drop across the wall of the cell,

(4) and, in the hot-wire method, to align the wire along the axis of the cell to avoid nonconcentric isotherms.

As an overall assessment of the hot-wire method, Touloukian and co-authors say "this method may be regarded as being capable of high precision in the hands of an experienced operator sufficiently patient to disentangle and eliminate the various corrections." Of the parallel-plate method they warn "the apparatus is difficult to set up and laborious in the measurement of heat input" however, "for measurements (of thermal conductivity) as a function of the density of the gas, the parallel-plate method is the most appropriate since losses due to convection are low."

Vapor density techniques involve the measurement of the gas or vapor density (weight/volume) at a given pressure and temperature and then "counting" the molecules in the vapor by, for example, the calculation of the molecular weight from the ideal gas law

$$M = wRT/PV$$

where w is the weight of the sample. Deviations from the ideal behavior of vapors are evidenced by an apparent increase in the molecular weight with increasing pressure.

An early vapor density or pressure-volume-temperature (P-V-T) apparatus was designed by Burnett.[85] The Burnett procedure involves the expansion of a gas of known pressure in a chamber of known volume into a smaller chamber of known volume. After each expansion the two chambers are isolated from each other and the smaller one evacuated. Consequently, a series of related pressures are collected and exhibit the behavior

$$P_r V_L = z_r nRT$$

and

$$P_{r-1}(V_L + V_S) = z_{r-1} nRT$$

where V_L and V_S are the volumes of the large and small chambers, respectively, and z_r is the compressibility factor.

Since the time of Burnett, the precision of pressure gauges has improved greatly. Thus, modern day versions of the Burnett apparatus, such as that used by Farnham,[64] are capable of measuring deviations from ideality not detectable by the original apparatus. A new version of an automated vapor denstiy apparatus designed by Tucker and Christian[86] was built for the present study and will be described in the Experimental chapter.

A criticism of vapor density techniques is that "PVT data are expected to be more sensitive to the presence of dimers than to the presence of higher polymers."[59] The results of this study indicate that no single species predominates near the vapor pressure for the association of TFE and, in each system, higher

polymers are accounted for by fitting the data to an equation including a stepwise equilibrium constant.

The "counting" procedure of P-V-T studies provides a very straightforward method of data analysis and calculation of the second virial coefficient, higher-order equilibrium constants, and heats of association. Fewer parameters are required to describe the non-ideal behavior than are required in spectral studies and the experimental technique is much simpler than in thermal conductivity measurements.

The adsorption of vapors onto glass and metal surfaces has been studied by many people[64,87,88] and presents a very real problem with any of the experimental techniques mentioned here. Failure to adequately account for adsorption will lead to erroneously large equilibrium constants. A method to study adsorption has been used in the present work and will be discussed in the Experimental chapter.

v. Survey of Vapor Phase Association Data

One cannot say that molecular association in the vapor phase has received little attention. Time and again people investigating association in the solution phase complain about the lack of reliable vapor phase data in the literature and suggest that attention and efforts in future studies be turned to the collection of such data. The key word here is "reliable". This writer has found an impressive quantity of vapor phase data in her review of the literature. Unfortunately, there are large discrepancies between calculated heats of association, equilibrium constants, and, very importantly, exactly what species must be taken into account (i.e. dimer, trimer, and higher polymers.)

Before the nature of the interactions involved in molecular complexes may be explored, one must be confident of the data collected. Since the degree of deviation is quite small in some gases, it is expected that highly precise methods of detecting such complexes are necessary, and instrumentation capable of such precision has only been available for the past twenty or so years.

For extensive tables of vapor phase data collected from the literature, the reader is referred to Touloukian et al.[84] for

thermal conductivity coefficients or Dymond and Smith[55] for virial coefficients of pure gases and mixtures of gases.

The present work investigates the self-association of acetone, 2,2,2-trifluoroethanol, and the heteroassociation of acetone or TFE with water, methanol, ethanol, or 2-butanol. Table I-2 provides references to work on TFE and Table V-1 provides references to vapor studies of acetone, to date, along with the experimental conditions and instrumental methods used.

Methanol[30,51,59,64,81,82,89-92] and acetone gas phase associations have been studied by many scientists. They are both industrially important chemicals and have physical characteristics conducive to vapor phase studies, namely their relatively high vapor pressures. Acetone is an excellent prototype for characterizing interactions of ketones. From molecular orbital calculations, these interactions appear to be due to dipole-dipole interactions or the formation of weak hydrogen bonds. In methanol, hydrogen bonding stabilizes the formation of associated species.

Ethanol[42,96] and 2-butanol[97,98] have not been studied quite as extensively as methanol. Hydrogen bonds stabilize associated species in these alcohols, also. Ethanol doesn't have quite so high a vapor pressure as methanol, however there is still enough of a pressure range at ambient conditions to study ethanol self-association. The vapor pressure of 2-butanol is somewhat prohibitive in studying its self-association and, indeed, at such

TABLE I-2

REFERENCES TO 2,2,2-TRIFLUOROETHANOL STUDIES

Reference	Experimental Technique	Temperature	Model	$K_2(torr^{-1})$	$K_3(torr^{-2})$	$\Delta H_2(\frac{cal}{mole})$	$K_\infty(torr^{-1})$
58	Thermal Conductivity	64.85°C-111.95°C	1-2	$3.2X10^{-4}$(a)		-4753.	
64	PVT-Burnett apparatus	15°C-35°C	1-3		$7.46X10^{-7}$	-13620.	
This work	PVT	25°C	1-2-∞	$2.11X10^{-5}$			0.0141
			1-3-∞		$2.71X10^{-7}$		0.01001

(a) Extrapolated to 25°C.

low pressures, it is doubtful that a significant amount of deviation from ideality is detectable.

The structure of water presents a very intriguing problem in the liquid phase and is the subject of many investigations using either experimental or theoretical (i.e. statistical mechanics[100]) techniques to arrive at an adequate theory. In the vapor phase,[101] water has one of the same limitations as 2-butanol in becoming an attractive compound for self-association studies, that is its low vapor pressure. Adsorption problems are also greater with water vapor than with the simple alcohol vapors.

Vapor phase associations of TFE are valuable for two reasons:[58]

(1) Experimental and theoretical determinations of the strength of the attraction between TFE molecules will provide insight into the effect of CF_3 substituents on alcohol associations, and

(2) its potential use as a working fluid in power cycles makes investigations of its thermodynamic properties industrially useful.[103]

The electronegative inductive effect of the fluorine atoms makes the hydroxylic hydrogen atom considerably more acidic than the corresponding hydrogen atom in hydrocarbon alcohols. The presence of the CF_3 group reduces the basicity of the hydroxylic group[104]

and therefore makes TFE more acidic relative to water or the simple alcohols.

Acetone, on the other hand, is basic compared to water or the simple alcohols. The association in the acetone-R-OH mixtures and TFE-R-OH mixtures will be investigated for their similarities and differences in hopes of finding some answers to the question of the nature of interactions in the vapor phase and what effects contribute to the stability of molecular complexes.

CHAPTER II

OBJECTIVES AND APPROACH

The purpose of this study are threefold:

(1) Provide reliable molecular association data of the pure vapor phase systems of acetone and 2,2,2-trifluoroethanol and for the binary gas mixtures of acetone or 2,2,2-trifluoroethanol with water, methanol, ethanol or 2-butanol.

(2) Provide liquid-vapor equilibrium data for the binary systems of point (1).

(3) Provide insight into the nature of the molecular association in the vapor phase.

The method of approach to achieve these objectives will utilize vapor density measurement techniques at 25°C for the TFE systems and at different temperatures between 15°C and 45°C for the acetone systems.

Two assumptions are used in treating the data:

(1) All nonideal behavior is attributed to the presence of associated species and

(2) each individual species obeys the ideal gas law.

From this basis, heats of association and equilibrium constants are calculated and liquid-vapor equilibrium curves inferred.

CHAPTER III.

EXPERIMENTAL

i. General

The association of 2,2,2-trifluoroethanol with itself and with water, methanol, ethanol, and 2-butanol will be referred to as the TFE association system. The association of acetone with itself, water, methanol, ethanol, and 2-butanol will be referred to as the acetone association system. The data for these two systems were collected using two different vapor density apparatuses.

The TFE association system was studied first using a manually operated vapor density apparatus. Both vapor association data and liquid-vapor equilibrium data were collected at 25°C only. The acetone association system was studied using an automated version of the aforementioned vapor density apparatus. Vapor association data for the acetone system were collected at seven different temperatures between 15° C and 45° C. The liquid-vapor equilibrium data were collected at 25°C only.

The experimental methods of data collection will be divided into two sections describing, first, the manually

controlled vapor density apparatus and, secondly, the automated vapor density apparatus.

ii. Chemicals

2,2,2-Trifluoroethanol (99.9+%, Gold Label from Aldrich Chemical Company, Inc.) was distilled and degassed under vacuum over molecular sieve, which had been previously heated and dried. The dried TFE was stored in an evacuated, heated reservoir connected directly to the inlet port.

Acetone[105] (99.9%, Analytical Reagent Grade from Mallinckrodt, Inc.) was refluxed with potassium permanganate for about 3 1/2 hours. Additional $KMnO_4$ was added and the mixture refluxed until a purple color persisted. After the acetone was filtered from the brown manganese oxide precipitate, magnesium sulfate was added to the acetone and the solution allowed to set in a stoppered flask overnight. The solution was then filtered and fractionally distilled on a 30-plate Oldershaw column.

Water was doubly distilled in a Barnstead Sybron Fi-Streem still. It was degassed and stored in a vessel accessible to the sample flask through a valve.

Methanol (absolute, low in Acetone, Reagent Grade from J. T. Baker Chemical Co.) was dehydrated[106] by reaction with magnesium methylate. About 50 ml of methanol, 5 g of dry magnesium turnings and 0.5 g of resublimed iodine were refluxed until the iodine disappeared and hydrogen gas was evolved. Methanol was then

added to the methoxide and the mixture refluxed for 30 minutes. The product was then fractionally distilled on a 30-plate Oldershaw column; the first 25 ml of distillate were discarded.

Ethanol (absolute, Reagent Quality from U.S. Industrial Chemicals Co.) was refluxed with sodium and ethyl phthalate and then fractionally distilled on a 30-plate Oldershaw column to remove traces of water.[107] 2-Butanol (Aldrich analyzed, Aldrich Chemical Co.) was doubly distilled on a 30-plate Oldershaw column.

All distilled organic liquids, with the exception of TFE, were stored in vapor contact with $CaSO_4$. All liquids were degassed before use by alternately freezing and warming the liquid while directly pumping on the liquid.

iii. Temperature Control

Temperature control was achieved by submerging the sample flask in a tank of water. The temperature of the water was controlled by a Sargent-Welch Thermonitor Model ST. The Thermonitor sensing probe, a thermistor, was submerged in the water and the Thermonitor provided proportional voltage output to the heating source. These heating sources were of two types. In the first apparatus, 200 watt painted lightbulbs were submerged in the water bath. In the second apparatus, siliconized heating mats from Economy Gauge Co. were attached to the outside walls of the water tank with silicone glue. Cool water, at a temperature 5-15 degrees below the experimental temperature, was circulated through a copper coil submerged in the water tank. The cool water was thermostatted and housed in a Haake constant temperature circulator. To prevent excessive loss of heat due to evaporation of the water or convection through the tank walls, the water surface was covered with styrofoam chips and the sides of the tank insulated by styrofoam sheets. With these precautions, it was quite easy to maintain experimental temperatures to precisions of better than 0.01°C over the temperature range of 15°C to 45°C.

iv. Manually Operated Vapor Density Apparatus

A diagram of the apparatus is shown in figure III-1. The pressure readings are made with a Texas Instrument fused quartz precision pressure gauge with a Bourdon-type transducer capable of precision within a few microns. The Texas Instrument pressure gauge was calibrated against a Mensor Pressure Gauge which had recently been calibrated at the factory. Data were collected as gauge readings and these readings converted to actual pressures using a sixth-order polynomial equation of the type:

$$\text{pressure} = aG + bG^2 + cG^3 + dG^4 + eG^5 + fG^6 ,$$

where G is the gauge reading.

A reproducible kink in the data indicated that small flaws existed in the gears of the pressure gauge. These kinks were calculated at intervals of 2.5 torr over a range of 0-60 torr by fitting the self-association vapor data of 2,2,2-trifluoroethanol to an appropriate model using a least squares optimizing routine. Any deviations between the model and the actual data were attributed to the existence of kinks. These differences were then subtracted from the heteroassociation data of the TFE association system at corresponding pressures. A list of kink corrections are given in Table IV-3.

MANUALLY OPERATED

VAPOR-DENSITY APPARATUS

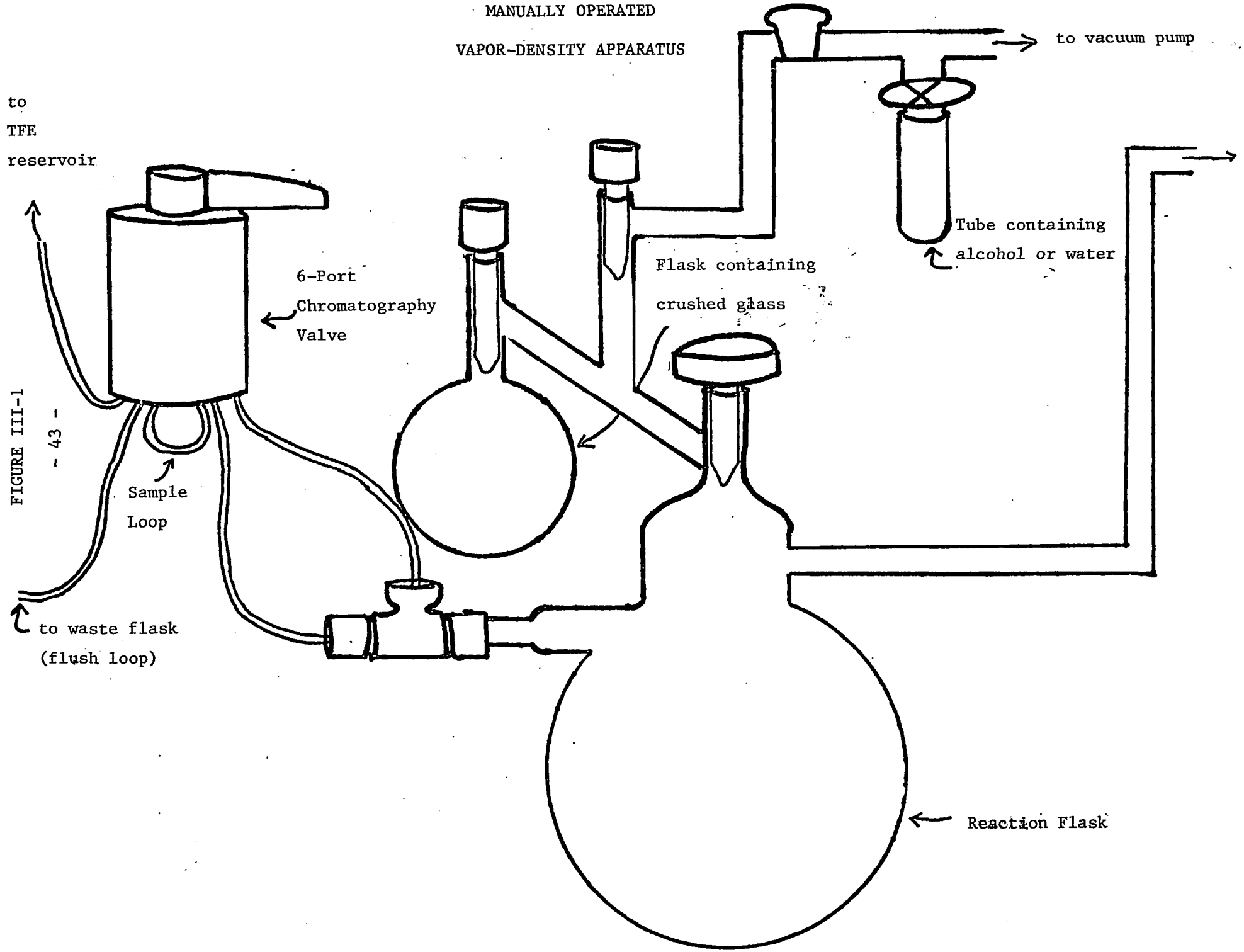

FIGURE III-1

The reaction flask is made of Pyrex glass and the interior surface has been treated with $(CH_3)_3ClSi$ in hopes that this would decrease the adsorption of the vapors to the glass walls. (The adsorption problems will be discussed at the end of this section.)

A thick-walled Pyrex glass capillary tube leads from the reaction flask to the pressure gauge. The length of this tubing not submerged in the constant temperature water bath is wrapped with heating tape to prevent any condensation of the vapor in the tube. The thick-walled capillary tubing converges into a non-rigid thin-walled spiral of glass tubing connected directly to the Bourdon tube. The reference side of the pressure gauge is kept evacuated and checked periodically with a digital Granville-Phillips pressure gauge.

Before each experiment, the sample flask is evacuated through a glass manifold connected to a Sargent-Welch vacuum pump via a liquid nitrogen cold trap. A Teflon stopcock isolates the sample flask.

A six-port chromatography valve (Valco Instruments Co.) connects the heated reservoir containing TFE to the sample flask via an external sample loop. (See figure III-2). These connections are made of 1/16th inch od stainless steel tubing. Swagelok fittings with Teflon ferrules are used to connect the metal tubing to the glass tubing. By means of a duo-position switch, the loop

FIGURE III-2

6-PORT CHROMATOGRAPHY VALVE DIAGRAM

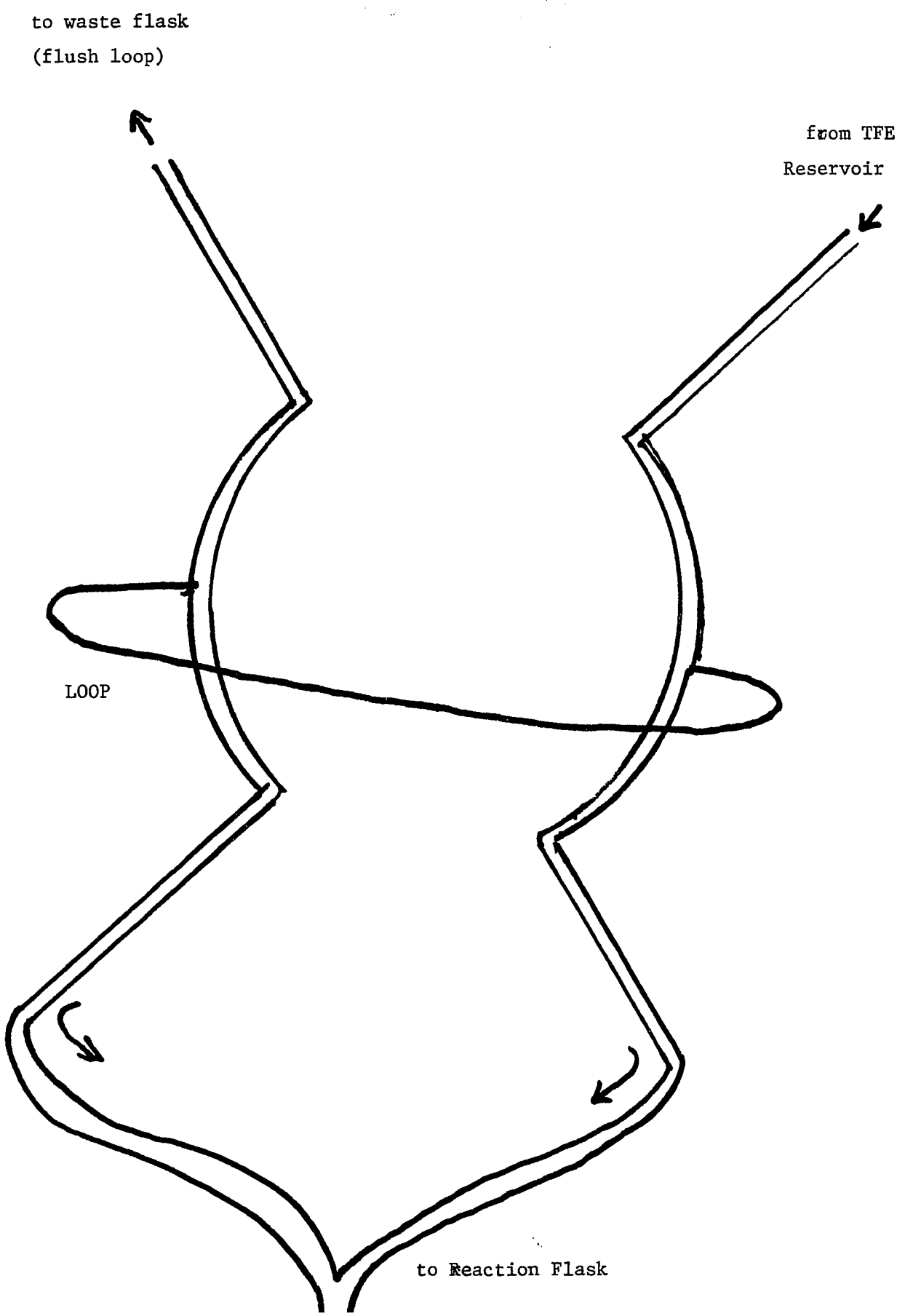

is either open to the TFE reservoir, during which time it fills with liquid TFE, or open to the evacuated sample flask, and the liquid TFE in the loop is vaporized into the flask. The volume of the loop is known to within 0.02 μl and introduces a volume of TFE with excellent reproducibility. The resulting TFE pressure is 5.283 +- 0.004 torr per increment assuming the behavior of the vapor is ideal. The loop is submerged in the same water bath as the sample flask and is, therefore, kept at 25.00°C.

In a typical heteroassociation experiment, the sample flask is evacuated to a pressure of a few microns. The hetero-component, either water, methanol, ethanol, or 2-butanol, is stored in a tube attached to the vacuum manifold and isolated by a Teflon stopcock. The hetero-compound is degassed and then distilled into the sample flask, the flow rate being controlled by the stopcock. When the desired amount of component is in the sample flask, between 2.5 and 20 torr, the sample flask is isolated and the initial pressure recorded. TFE injections are made by means of the switch on the chromatography valve, first opening the loop to the TFE reservoir for 30 seconds, then switching the loop opening to the sample flask side and vaporizing the increment into the sample mixture. After five minutes, the mixture will have reached equilibrium and the gauge reading is recorded. Injections are repeated in this fashion until the increase in pressure due to the addition of another increment is suddenly much smaller due to vapor condensation. At this point, one hour per increment is necessary to reach equilibrium.

Injections can be made until the pressure of the mixture in the sample flask reaches the vapor pressure of TFE at 25° C. At this pressure, the liquid TFE in the loop will no longer vaporize into the sample flask.

For the purpose of data analysis, the data set is divided into two parts. The data collected before vapor condensation are analyzed for vapor phase association and to obtain equilibrium constants. The data collected once condensation begins are used to infer liquid-vapor equilibrium curves.

The tube attached to the vacuum manifold in which the hetero-component is stored is calibrated to 0.01 ml. A known volume of component may be introduced to the sample flask in excess of the vapor pressure of the component by heating the tube and forcing all of the liquid into the sample flask. Using this technique, additional liquid-vapor equilibrium data are collected by introducing large amounts of the hetero-component to the sample flask and injecting samples of TFE into the flask. This provides liquid-vapor equilibrium data in the region where the mole fraction of TFE is small.

As mentioned earlier, adsorption is a problem in vapor phase studies. In order to quantify the decrease in pressure due to adsorption, a small flask filled with paper-thin crushed Pyrex glass is connected to the sample flask by a glass tube equipped

with a Teflon stopcock to close off the vacuum manifold and a Teflon stopcock to isolate the small flask. The surface area of the crushed glass has been carefully measured geometrically. The total surface area of the interior wall of the small flask plus the crushed glass is about ten times the surface area of the interior wall of the sample flask.

An expansion ratio, r, between the two flasks is calculated by introducing dry air into the sample flask, recording the pressure, p_1 , and then opening the stopcocks between the sample flask and evacuated small flask and measuring the pressure, p_2. Thus the ratio is: $r = p_1/p_2$. An expansion ratio is then calculated for each of the chemicals of interest to the TFE association system and for the various mixtures of TFE plus hetero-component. The ratios exhibited little deviation from the dry air ratio, with the exception of the ratio calculated for the TFE-water mixture. At partial pressures of water greater than 19.5 torr water, an increment of TFE caused 0.12 torr of water to desorb from the glass walls. To eliminate this problem, vapor-density studies of the water-TFE system were carried out with water partial pressures of less than 15 torr.

iv. Automated Vapor Density Apparatus

The basic design of this apparatus is similar to that of the manually operated vapor density apparatus. A 6-port chromatography valve is again used to inject increments of sample to an evacuated sample flask submerged in a temperature-controlled water bath. See figure III-3.

Pressure measurements are made by a Paroscientific quartz crystal pressure transducer kept at a constant temperature to within .05 degrees. The pressure transducer emits a frequency which varies about 2.5 kHz over a range of zero to one atmosphere of pressure. The output from the pressure transducer is connected to the input of a Racal-Dana 9904 frequency counter via a regulated power supply (from Acopian Tech. Co.).

The pressure transducer was calibrated against a Texas Instrument fused quartz precision pressure gauge and a calibration equation converting frequency to pressure was obtained. The frequency counter displays seven significant figures and outputs binary coded decimal data via a 28-way edge connector. This digital information is transferred to a Rockwell AIM 65 microcomputer. Eighteen pins of the computer edge connector are connected to the corresponding eighteen pins of the frequency counter. Four of these pins transfer one digit of the frequency reading in binary code from the frequency counter to the computer.

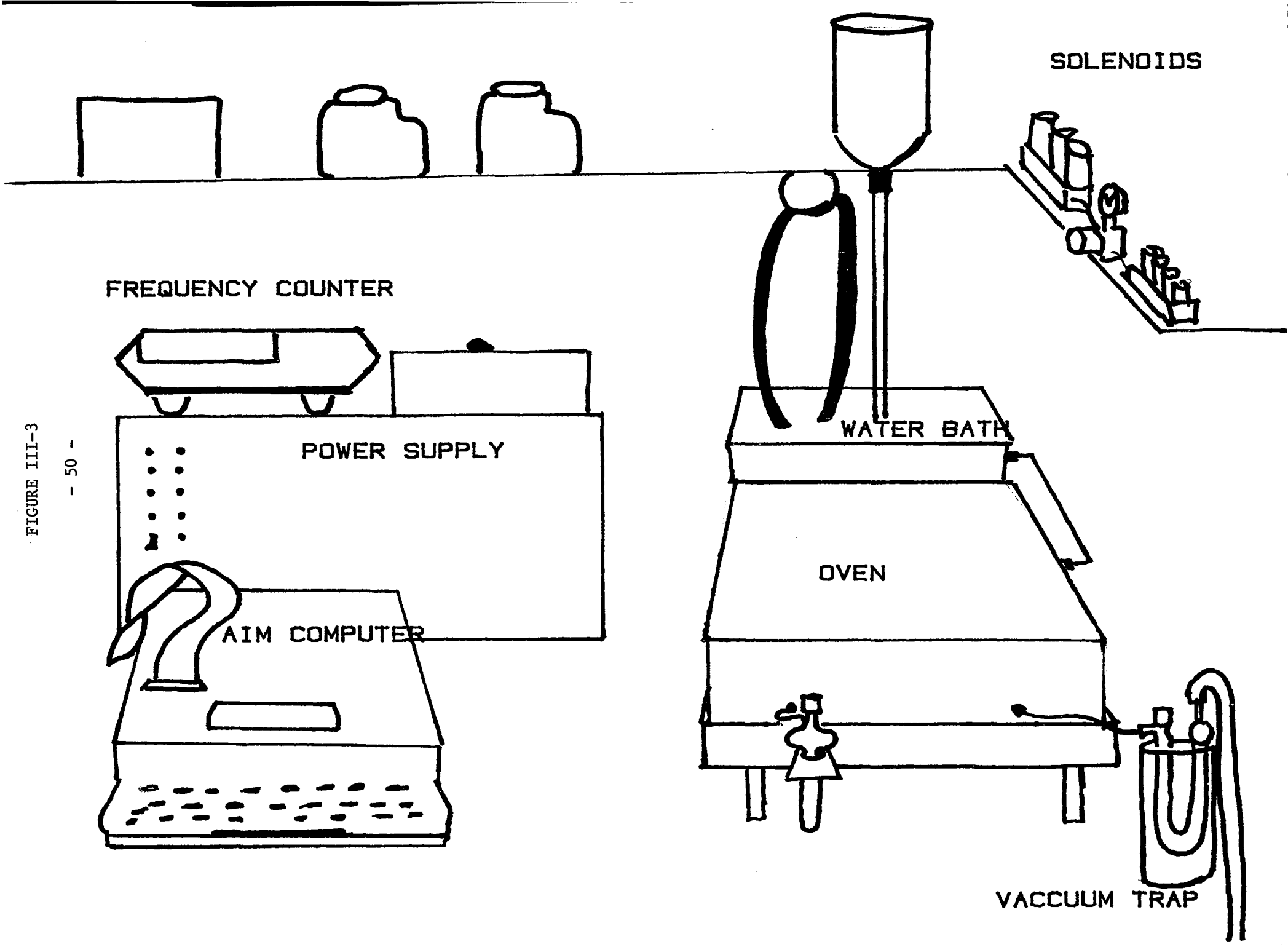
SOLENOIDS
FREQUENCY COUNTER
POWER SUPPLY
WATER BATH
OVEN
AIM COMPUTER
VACCUUM TRAP

FIGURE III-3

Each digit is transferred on these same four pins one after the other during a timing sequence controlled by the frequency counter. The computer then stores the seven digit frequency reading and converts it to an actual pressure from the calibration equation. Pressure values are precise to a few microns. Since there are no gears in a quartz crystal pressure transducer, the problem of "kinks" does not arise.

Instead of stopcocks isolating different parts of the apparatus, as in the manual apparatus, bellows valves are used. The bellows valves are normally in a closed position and may be opened by applying 100 psi of pressure (a nitrogen tank is the source of pressure) on the valve. Solenoid valves control the flow of nitrogen to a particular bellows valve and are turned on or off by the computer output of +5 volts or 0 volts to the appropriate solenoid valve relay line.

The evacuated flask is a stainless steel 300cc gas cylinder. All of the connections and tubings are either stainless steel or nickel between the sample flask and the bellows valves; thus, during an experiment the vapor is not exposed to any Teflon surfaces. There are three glass reservoirs to store the different liquids being used in any experimental run. Two reservoirs may be connected to the sample flask by two different chromatography valves and the third reservoir is connected to the sample flask through a bellows valve. A vacuum manifold connects the three

reservoirs, with a stopcock isolating each reservoir. By this means, liquids are freshly degassed before use.

The chromatography valves are equipped with an actuator (Valco Instruments Co.), taking the place of the duo-position switch. Two solenoids for each actuator are turned on and off by the computer. One solenoid opens the loop to the liquid reservoir and the other solenoid opens the loop to the sample flask, again through air pressure.

The bellows valves, chromatography valves, pressure transducer, and liquid reservoir are all mounted on a 1/4 inch thick aluminum plate (See figure III-4). On the bottom side of the plate, silicone rubber heating mats are attached with silicone glue. The entire plate is in an aluminum box, insulated with a packing of cotton over the top. The heating mats are connected to a variable transformer (Ohmite) and the temperature is kept at 50.00°C +- 0.05°C by an AC Proportional Temperature Controller from Oven Industries, Inc.

A typical heteroassociation experiment requires telling the computer, via the keyboard,:

1) The pressure of water or alcohol desired,

2) The title of the particular experimental run,

3) The number of increments of acetone to be added.

The computer will then give the appropriate signals to flush the system several times with water or alcohol and pump down to the

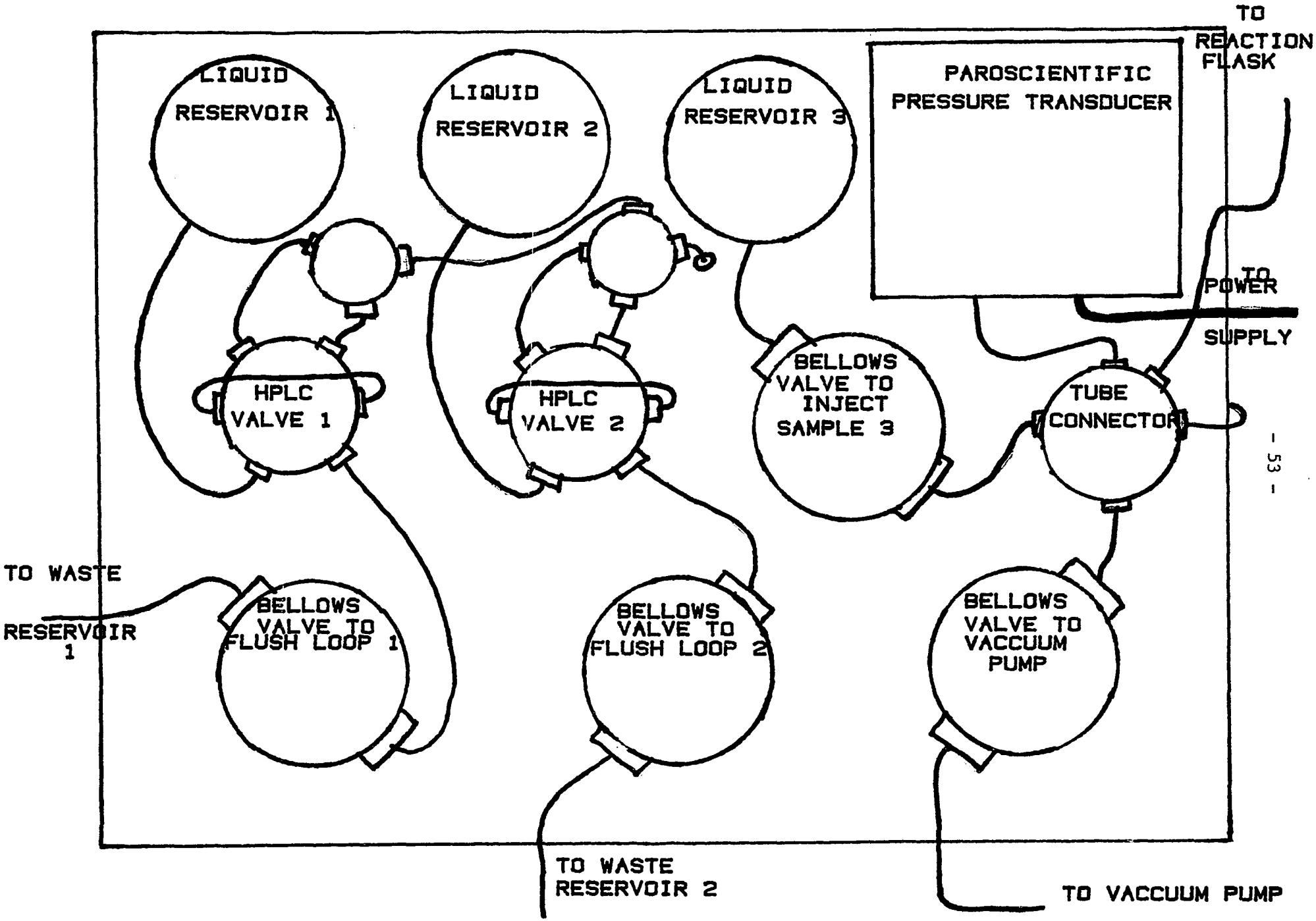
LIQUID RESERVOIR 1
LIQUID RESERVOIR 2
LIQUID RESERVOIR 3
PAROSCIENTIFIC PRESSURE TRANSDUCER
TO REACTION FLASK
TO POWER SUPPLY
HPLC VALVE 1
HPLC VALVE 2
BELLOWS VALVE TO INJECT SAMPLE 3
TUBE CONNECTOR
TO WASTE RESERVOIR 1
BELLOWS VALVE TO FLUSH LOOP 1
BELLOWS VALVE TO FLUSH LOOP 2
BELLOWS VALVE TO VACCUUM PUMP
TO WASTE RESERVOIR 2
TO VACCUUM PUMP

FIGURE III-4

pressure indicated by step (1). The title is then printed on the output paper along with the pressure of the hetero-component. Increments of acetone are injected until the number of increments indicated in step (3) is reached. After each injection, two minutes are allowed for the mixture to reach equilibrium. The computer will print the increment number, the pressure, the pressure change from the previous reading, and the frequency for each increment. After all injections are made, the sample flask is evacuated.

Since the chromatography valves are housed in the 50 degree aluminum box, the valve loops are kept at that temperature as well. This means that injections of a volatile liquid may be made up to the vapor pressure of the liquid at 50°C. This added feature of the automated apparatus allows studies on mixtures where the compound introduced into the flask initially is more volatile than the added component (e.g. the TFE-methanol system.)

Liquid-vapor equilibrium data might be collected using a slightly different procedure from that used with the manually operated apparatus. The amount of the component introduced into the flask initially may not exceed the vapor pressure of that component since the pressure is the only means by which the amount can be measured. Again, it would be desirable to collect data covering the entire range of mole fractions. Small amounts of the initial component would yield data where the mole fraction of acetone is high. Large amounts of the intitial component would

yield data where the mole fraction of acetone is low. In order to introduce large amounts of the first component, the temperature of the water bath would be raised to about 45°C; the component then would be introduced until the pressure is a little below its vapor pressure at 45°C. The pressure would be recorded and the temperature of the water bath lowered to 25.00°C, or whichever experimental temperature would be desired. The computer would be programmed to inject increments of acetone and after each increment, the pressure would be checked every four minutes. When the difference between two successive readings does not exceed four microns, the pressure would be recorded and the next injection made.

From numerous studies of pressure versus time, there appears to be little decrease in pressure the first few minutes after an injection is made. During the time it takes to perform an entire experiment, quite a significant decrease in pressure will be evident. This decrease is presumably due to adsorption of the vapor onto the walls of the sample flask. Therefore, adsorption problems can be minimized by fitting the pressure difference between increments as a function of amount injected rather than fitting the total pressure as a function of the amount injected. In this way, only adsorption occuring during the two minutes following an injection will cause error.

CHAPTER IV

DATA TREATMENT

i. Theory

According to Dalton's Law, the total pressure of a mixture is equal to the sum of the partial pressures of its components. For a mixture of associated species, the pressure is written

$$P = P_{monomer} + P_{dimer} \ldots + P_{n\text{-}mer}. \qquad \text{IV-1}$$

For each species larger than the monomer, a relationship between its partial pressure and the partial pressure of the monomer exists at equilibrium.

$$P_{dimer} = K_2 P^2_{monomer}$$

$$P_{trimer} = K_3 P^3_{monomer}$$

$$\vdots \qquad \text{IV-2}$$

$$P_{n\text{-}mer} = K_n P^n_{monomer},$$

where K_i is the equilibrium constant for the reaction

$$iX \overset{K_i}{\rightleftharpoons} X_i \qquad \text{IV-3}$$

where X is a monomeric species. Using these relationships, the total pressure may be written as a function of the partial pressure of the monomer (henceforth P_1):

$$P = P_1 + K_2P_1^2 + K_3P_1^3 + \ldots + K_nP_1^n. \qquad \text{IV-4}$$

If all of the associated species were suddenly to dissociate, the dissociated dimer would contribute twice as much pressure to the total pressure as the associated dimer. The dissociated trimer would become three monomers and would contribute three times the partial pressure of the trimer to the total pressure; in general, dissociation of an n-mer contributes n times the partial pressure of the n-mer to the total pressure. The ideal (or formal) pressure, Π, is defined by the ideal gas law

$$\Pi = nRT/V. \qquad \text{IV-5}$$

This would be the pressure of the system if no monomers associate.

The composition of a vapor may be characterized by equilibrium constants. An infinite number of equilibrium constants must be determined to use equation to model the chemical association behavior in a vapor. This equation may be modified, through certain assumptions, to different forms requiring the determination of a finite number of parameters or equilibrium constants. If a system is very nearly ideal, the pressure may be described by a monomer-dimer (1-2) model. The model equations are

$$P = P_1 + K_2P_1^2 \qquad \text{IV-6}$$

and

$$\Pi = P_1 + 2K_2P_1^2. \qquad \text{IV-7}$$

This model is sufficient to describe benzene or cyclohexane vapor.[33,34] This model has also been used to describe the behavior of acetone vapor[60] and 2,2,2-trifluoroethanol,[58] as well as other organic vapor systems.

The inclusion of a higher-order equilibrium constant in the 1-2 model yields many different combinations. Equations for a monomer-dimer-trimer model (1-2-3) are

$$P = P_1 + K_2P_1^2 + K_3P_1^3 \qquad \text{IV-8}$$

and

$$\Pi = P_1 + 2K_2P_1^2 + 3K_3P_1^3. \qquad \text{IV-9}$$

Methanol and other alcohol vapors[42] have been fit to a monomer-dimer-tetramer model (1-2-4) where the pressure and ideal pressure are defined

$$P = P_1 + K_2P_1^2 + K_4P_1^4 \qquad \text{IV-10}$$

and

$$\Pi = P_1 + 2K_2P_1^2 + 4K_4P_1^4. \qquad \text{IV-11}$$

The use of a discrete association constant, for the formation of a particular n-mer from n monomers, coupled with a

step-wise association constant, for the addition of a monomer to an n-mer, provides another set of chemical association models in which all species are accounted for using a minimum number of parameters. For example, the formation of a dimer is represented by the reaction

$$A + A \overset{K_2}{\rightleftharpoons} A_2. \qquad \text{IV-12}$$

A discrete dimer equilibrium constant, K_2, is necessary to describe this reaction. The stepwise addition of a monomer to a series of n-mers,

$$\begin{aligned} A_2 + A &\overset{K_\infty}{\rightleftharpoons} A_3 \\ A_3 + A &\overset{K_\infty}{\rightleftharpoons} A_4 \\ &\vdots \\ A_n + A &\overset{K_\infty}{\rightleftharpoons} A_{n+1}, \end{aligned} \qquad \text{IV-13}$$

is characterized by a single stepwise parameter, K_∞. The pressure of such a system is

$$P = P_1 + K_2P_1 + K_\infty P_1P_2 + K_\infty P_1P_3 + \ldots + K_\infty P_1P_n. \qquad \text{IV-14}$$

Since $P_2 = K_2P_1^2$; $P_3 = K_\infty P_1$; $P_2 = K_2K_\infty P_1^3$ and so on, equation IV-14 is rewritten in terms of monomers only,

$$P = P_1 + K_2P_1^2 + K_2K_\infty P_1^3 + \qquad \text{IV-15}$$

$$K_2K_\infty{}^2P_1{}^4+\ldots+K_2K_\infty^{n-2}P_1^n$$

or in closed form,

$$P = P_1 + K_2P_1^2/(1-K_\infty P_1) \ . \qquad \text{IV-16}$$

Similarly, the ideal pressure is

$$\Pi = P_1 + 2K_2P_1^2 + 3K_2K_\infty P_1^3 + K_2K_\infty^2P_1^4 + \ldots + nK_2K_\infty^{n-2}P_1^n \qquad \text{IV-17}$$

or in closed form

$$\Pi = P_1 + K_2P_1^2(2-K_\infty P_1)/(1-K_\infty P_1)^2. \qquad \text{IV-18}$$

Equations IV-16 and IV-18 are the mathematical form of the 1-2-infinity model.

A 1-3-infinity model includes a discrete trimer equilibrium constant and the stepwise addition equilibrium constant. In closed form, the pressure and ideal pressure are written

$$P = P_1 + K_3P_1^3/(1-K_\infty P_1) \qquad \text{IV-19}$$

and

$$\Pi = P_1 + K_3P_1^3(3-2K_\infty P_1)/(1-K_\infty P_1)^2 \ . \qquad \text{IV-20}$$

These models are modified very slightly for mixtures of vapors. The simplest heteroassociation model is analogous to the

1-2 model for a homogeneous mixture. Formation of a 1:1 dimer of component A and B,

$$A + B \overset{K_{11}}{\rightleftharpoons} AB, \qquad \text{IV-21}$$

is characterized by a 1:1 equilibrium constant, K_{11}. This constant has the same units as the self-association dimer equilibrium constant (e.g. $torr^{-1}$ in vapor phase, liter/mole in solution phase.) Pressure and ideal pressure are defined by this model to be

$$P = P_A + P_B + K_{11}P_AP_B \qquad \text{IV-22}$$

and

$$\Pi = P_A + P_B + 2K_{11}P_AP_B \qquad \text{IV-23}$$

where P_A and P_B denote the monomer pressures of components A and B, respectively.

The use of a stepwise addition equilibrium constant in a heterogeneous case can either refer to the addition of monomers of A to hetero-complexes of A and B,

$$A_xB_y + A \overset{K_\infty}{\rightleftharpoons} A_{x+1}B_y$$

$$\vdots \qquad \text{IV-24}$$

$$A_{x+n}B_y + A \overset{K_\infty}{\rightleftharpoons} A_{x+n+1}B_y,$$

or to the addition of monomers of B to hetero-complexes of A and B,

$$A_xB_y + B \overset{K_\infty}{\leftrightharpoons} A\ B$$

$$\vdots \qquad\qquad \text{IV-25}$$

$$A_xB_{y+n} + B \overset{K_\infty}{\leftrightharpoons} A_xB_{y+n+1}.$$

The subscripts y and x must be greater than zero.

A heteroassociation model analogous to the 1-2-infinity model is the 1-infinity model where a discrete dimer equilibrium constant, K_{11}, and a stepwise addition constant, K_∞, for the addition of monomer A to the complex $B(A)_i$ are represented by the equations

$$P = P_A + P_B + K_{11}P_AP_B/(1-K_\infty P_A) \qquad \text{IV-26}$$

and

$$\Pi = P_A + P_B + K_{11}P_AP_B(2-K_\infty P_A)/(1-K_\infty P_A)^2. \qquad \text{IV-27}$$

For the purpose of this study, one more model must be introduced, 1-infinity + 2:1. This is a combination of the heteroassociation model described above plus a term for the formation of B_2A,

$$2B + A \overset{K_{21}}{\leftrightharpoons} B_2A. \qquad \text{IV-28}$$

The pressure and ideal pressure are

$$P = P_A + P_B + K_{21}P_AP_B^2 + K_{11}P_AP_B/(1-K_\infty P_A) \quad \text{IV-29}$$

and

$$\Pi = P_A + P_B + 3K_{21}P_AP_B^2 + \quad \text{IV-30}$$

$$K_{11}P_AP_B(2-K_\infty P_A)/(1-K_\infty P_A)^2.$$

An infinite number of variations of chemical association models are possible. Only those used in analyzing data are presented here.

ii. Keyes Point

Vapor density data are collected over the pressure range from ~ 0 torr to the vapor pressure of the compound under investigation. As has been mentioned before and will be discussed later, adsorption effects present the major obstacle to obtaining good vapor density data. These effects become very pronounced as one reaches the vapor pressure of the compound, introducing considerable error. The problem becomes one of determining when these effects become critical.

The ratio of ideal pressure:vapor pressure is available through a series of thermodynamic relationships and certain temperature-related thermodynamic parameters of the compound under investigation. This technique was applied by F. G. Keyes in 1947.[108] Hence, this writer has adopted the name Keyes point in referring to the ratio ideal pressure:vapor pressure (Π/P). From the Clapeyron equation

$$dP/dT = \Delta H/T\Delta V, \qquad \text{IV-31}$$

where dP/dT is the variation of vapor pressure with temperature and ΔH is the heat of vaporization at the temperature T (in degrees Kelvin), one may determine the change in molar volume, ΔV. Using the ideal gas law

$$\Pi = RT/V, \qquad \text{IV-32}$$

where R is the gas constant, V is the molar volume (virtually equivalent to ΔV) and Π is the ideal pressure, one may obtain the ratio Π/P,

$$RT/PV = \Pi/P. \qquad \text{IV-34}$$

This ratio is, in fact, a measure of the degree of association at the vapor pressure of a compound. The inverse of this ratio, P/Π, is known as the compressibility ratio, Z. If $\Pi/P=1$ then the compound exhibits no nonideal behavior (i.e. no association). In the case of water, Keyes found Π/P to be 1.00152 at 25°C.[108] In other words, only 0.15% of water vapor deviates from ideality.

This number does not indicate the distribution of species sizes; that is, the relative contribution of dimer, trimer, or n-mer to the nonideality of the vapor can not be determined from this ratio. Π/P is a measure of the overall contribution of associated species to the total pressure.

The variation of vapor pressure with temperature and the heats of vaporization for acetone, methanol, and ethanol were found in the literature. Tables of Keyes points for these compounds at various temperatures are provided later in this chapter. Unfortunately, heats of vaporization data for 2,2,2-trifluoroethanol could not be found in the literature.

iii. Heat of Association

Vapor density data were collected at several temperatures over a 20°-30° range for the acetone systems. In both the homogeneous and heterogeneous acetone systems, the data at individual temperatures were fitted to a 2-parameter chemical association model, 1-2-infinity in the self-association case and 1-infinity in the heteroassociation case.

The variation of each of the two equilibrium constants with temperature may be related to a heat of association through the Clausius-Clapeyron equation:

$$\ln(K_2^{T_2}/K_2^{T_1}) = \Delta H_2(1/T_1-1/T_2)/R \qquad \text{IV-35}$$

and

$$\ln(K_\infty^{T_2}/K_\infty^{T_1}) = \Delta H_\infty(1/T_1-1/T_2)/R. \qquad \text{IV-36}$$

ΔH_2 (or ΔH_{11}) is the heat of association of the dimeric species. ΔH_∞ is the heat associated with the addition of a monomer to a complex.

The heats of association for the acetone systems were estimated from the equation:

$$\Delta H_2/R = \ln(K_2^{T_2}/K_2^{T_1})/(1/T_1-1/T_2)$$

The final values of ΔH_2 or ΔH_{11} and ΔH_∞ reported in this chapter

were determined by fitting all of the data from one system simultaneously.

iv. Determination of Liquid-Vapor Curves from PVT Data

Liquid-vapor equilibrium data were collected for the mixed TFE system at 25°C. Information about the liquid-vapor equilibrium is obtained from data taken by continuing to add TFE increments after the saturation pressure of the mixture has been reached. From total pressure/total mole fraction data, at constant temperature, the liquid mole fraction and vapor mole fraction vs. total pressure curves are derived.

The following equations relate the monomer pressure of each species and the liquid and vapor mole fractions with experimentally obtainable values, namely, total pressure and overall mole fraction:

$$P = P_B + P_{TFE} + K_3 P_{TFE}^3/(1-K_\infty P_{TFE}) + K_{11} P_{TFE} P_B/(1-K_\infty P_{TFE}) \qquad \text{IV-37}$$

$$P_B = \gamma_B X_B^L P_B^\circ \qquad \text{IV-38}$$

$$P_{TFE} = \gamma_{TFE} X_{TFE}^L P_{TFE}^\circ \qquad \text{IV-39}$$

$$X_B^V = \frac{\Pi_B}{\Pi_{total}} = (P_B + K_{11} P_B P_{TFE}/(1-K_\infty P_{TFE}))/\Pi_{total} \qquad \text{IV-40}$$

$$X_{TFE} = \frac{\Pi_{TFE}}{\Pi_{total}} = P_{TFE} + K_3 P_{TFE}(3-2K_\infty P_{TFE})/(1-K_\infty P_{TFE})^2 + K_{11} P_B P_{TFE}(2-K_\infty P_{TFE})/(1-K_\infty P_{TFE})^2 \;/\; \Pi_{total} \qquad \text{IV-41}$$

Equation IV-37 is suitable for the TFE/water system. Equation

IV-29 should replace equation IV-37 for TFE/ethanol and TFE/2-butanol. Equations IV-38 and IV-39 define the activity coefficient of the component (γ_B or γ_{TFE}). P_B° or P_{TFE}° is the pressure of the monomer at the vapor pressure of the pure species. The superscript following the mole fraction, X^V or X^L, indicates vapor phase or liquid phase, and $\bar{X}_{TFE}$ is the overall mole fraction of TFE in the system. Equation IV-41 is a form of the lever rule.

The Hansen-Miller[109,110] equations express the logartihm of the activity coefficients as a function of the mole fraction and satisfies the Gibbs-Duhem equation.[111]

$$\ln \gamma_{TFE} = (X_B^L)^2 (A + BX_{TFE}^L + C(X_{TFE}^L)^2 + D(X_{TFE}^L)^3 \ldots)$$

$$\ln \gamma_B = (X_{TFE}^L)^2 ((A-B/2) + (B-2C/3)X_{TFE}^L + (C-3D/4)(X_{TFE}^L)^2 + D(X_{TFE}^L)^3 \ldots)$$

A, B, C, and D are empirical parameters and were obtained from a non-linear least-squares analysis fitting total pressure.

v. Least-Sqares Determination of Parameters

A non-linear least squares routine, using the Marquardt algorithm[112] was employed to optimize the determination of the parameters in fitting each system of data. The routine determines the deviation between a single experimental variable and the calculated value for that variable given a particular model. All other variables are assumed to be free from error. The variable which is being fitted should, therefore, be the most uncertain variable. In the TFE association system, total pressure is the variable more subject to error. Both Π and P are equally uncertain in the acetone systems.

A parameter was included to account for the amount of TFE or acetone that is injected per increment when fitting the homogeneous data. This parameter is equal to the change in ideal pressure ($\Delta\Pi$). Total ideal pressure (Π) is this parameter multiplied by the number of increments.

For each data point, the least-squares routine calculates the uncertain variable (YC) for a given set of parameter values. The root mean square deviation (RMSD) for the entire set of data

$$\text{RMSD} = \left(\sum_{i=1}^{N}(\text{YC-EXP. VALUE})_i^2 / (\text{N-\# parameters})\right)^{\frac{1}{2}}, \qquad \text{IV-44}$$

is determined for each given set of parameter values. (N is the

number of data points.) The best set of parameter values is that which yields the lowest RMSD. The uncertainty in each parameter is also determined.

All equilibrium constants, heats of association, loop parameters, and their associated uncertainties given in the tables of this chapter are least-squares results. The calculated points plotted in the figures are also from least-squares results.

vi. - Self-Association of 2,2,2-Trifluoroethanol at 25.00 °C

Vapor density measurements of 2,2,2-trifluoroethanol (TFE) were made using the manually operated vapor density apparatus described in the Experimental section. The data set consists of twelve pressure readings and twelve incremental volumes of TFE. The pressure in the sample flask during the experiment increases from about 0.001 torr to the vapor pressure of TFE at 25.00 °C. The vapor pressure of TFE at 25.00 °C is 71.4 torr.

Replicate sets of the pressure-density measurements were collected many times to determine the reproducibility of the pressure measurements and to check the effect of different lengths of time between increments on the results. (See Table IV-1 for the experimental data.) In general, the pressure change per increment of TFE is reproduced to within 0.010 torr, out of a total pressure increment of 5.28 torr. In fact, the reproducibility of entire sets of pressure-denisty data is so good that the results may be analyzed to infer systematic errors in pressure valves determined by the bourdon-type transducer.

Figure IV-1 shows results for TFE vapor plotted as average or apparent molecular weight, M, vs. pressure. The average molecular weight is calculated from the expression $M=\rho RT/P$ where ρ is the density of the TFE vapor (determined from the known volume of the system and the known size of increments of TFE added

with the chromatography valve), R is the gas constant, T is the absolute temperature, and P is the measured total pressure.

The precise size of the loop is determined by fitting the pressure-density data to a 2-parameter association model and including a third parameter for the incremental volume size. The ideal pressure is equal to the loop parameter multiplied by the number of increments added. The loop parameter varies only slightly by changing the association model.

Several association models were used in fitting the TFE pressure-density data. The inclusion of a term accounting for the formation of species larger than the dimer or trimer in the association model descibes the experimental data much better than a model accounting for only dimers and/or trimers. Both the 1-2-inifinity and 1-3-infinity models gave equally good fits in terms of their RMSD's. The results are presented in Table IV-2. A 1-2-3-infinity model was unsuccessful in giving realistic results since one of the equilibrium constants was negative.

The differences between the measured pressures and the pressures calculated using the 1-2-infinity or 1-3-infinity association models were used as corrections for the systematic errors caused by a kink in the pressure gauge gears. A table of kink corrections was obtained for the pressure range of 0-60 torr at 2.5 torr intervals. These corrections were added to the

pressures measured in the mixed TFE-ROH systems. A list of kink corrections is in Table IV-3.

TABLE IV-1

2,2,2-TRIFLUOROETHANOL VAPOR DENSITY DATA

AT 25.000 DEGREES CELSIUS

PRESSURE (P)	IDEAL PRESSURE (Π)	P(CALC)- P(EXP)
5.292	5.286	0.006
10.593	10.572	0.023
15.879	15.858	0.025
21.123	21.144	- 0.012
26.395	26.430	- 0.017
31.687	31.716	0.004
36.948	37.002	0.004
42.180	42.288	- 0.010
47.432	47.574	0.019
52.611	52.860	0.010
57.708	58.146	- 0.025
62.775	63.432	- 0.002
67.711	68.718	0.033

FIGURE IV-1

2,2,2-Trifluoroethanol (25.00°C)

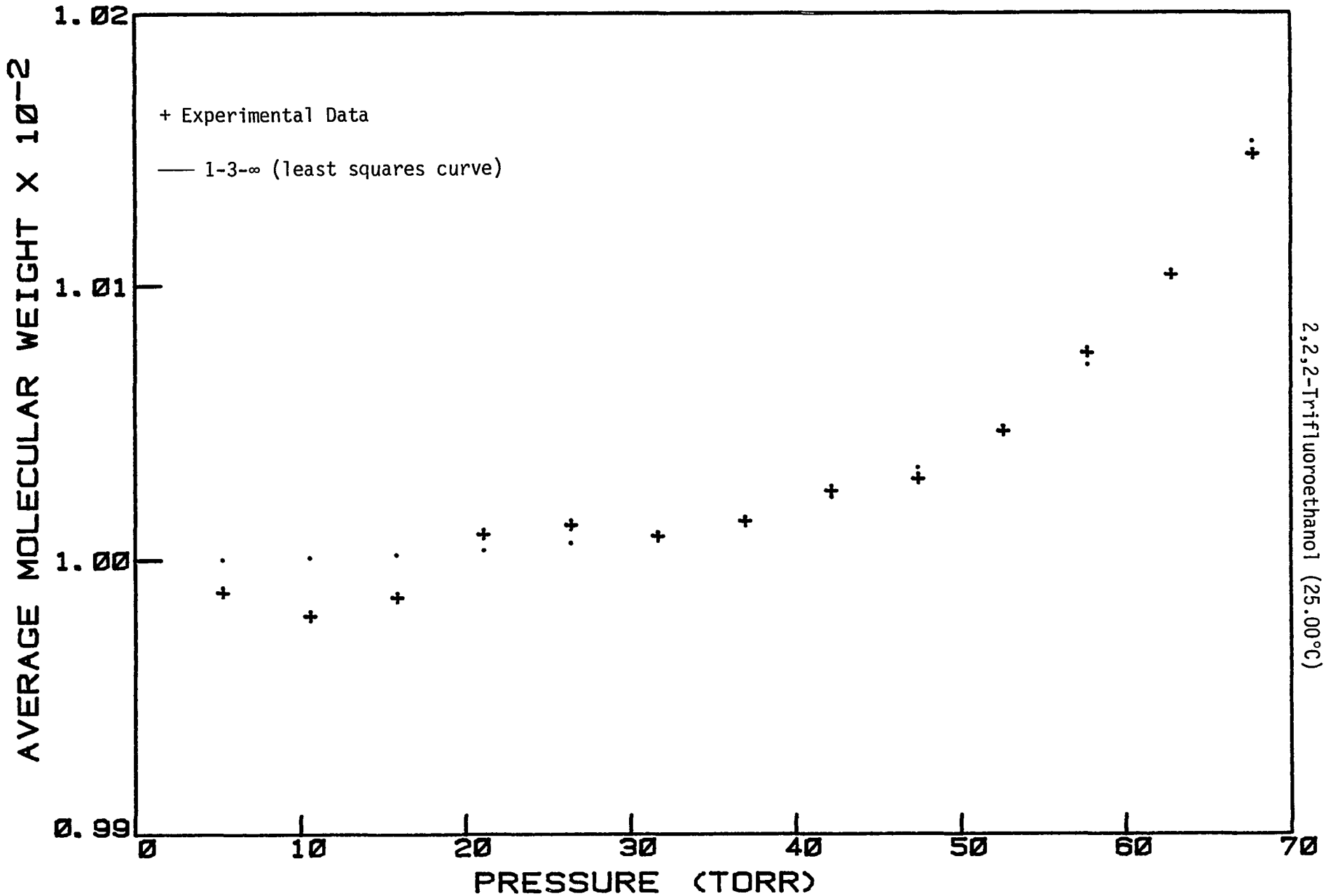

TABLE IV-2

EQUILIBRIUM CONSTANTS FOR VAPOR PHASE ASSOCIATION

OF 2,2,2 - TRIFLUOROETHANOL WITH VARIOUS COMPOUNDS

Compound	Model	RMSD(torr)	K_2(torr^{-1})	K_{11}(torr^{-1})	K_3(torr^{-2})	K_{21}(torr^{-2})	K_∞(torr^{-1})
TFE	1-2-∞	0.021	$2.11(\pm.2)\times10^{-5}$				$1.041(\pm.02)\times10^{-2}$
TFE	1-3-∞	0.021			$2.71(\pm.25)\times10^{-7}$		$1.001(\pm.02)\times10^{-2}$
Water	1 - ∞	0.027		$1.41(\pm.1)\times10^{-4}$			$1.075(\pm.04)\times10^{-2}$
Methanol	1-∞,A_2B*	0.026		$1.57(\pm.21)\times10^{-4}$		$1.09(\pm.28)\times10^{-5}$	$1.19(\pm.05)\times10^{-2}$
Ethanol	1-∞,A_2B*	0.023		$2.73(\pm.17)\times10^{-4}$		$1.82(\pm.14)\times10^{-5}$	$1.162(\pm.03)\times10^{-2}$
2-Butanol	1-∞,A_2B*	0.024		$4.62(\pm.54)\times10^{-4}$		$9.89(\pm.95)\times10^{-5}$	$1.314(\pm.06)\times10^{-2}$

* A = ROH; B = TFE

TABLE IV-3

KINK CORRECTIONS

(Obtained from 1-3-∞ Infinity model)

Kink	Gauge	Kink	Gauge
-.008	4.311	.039	35.192
-.006	4.682	.004	35.597
-.007	4.886	-.014	35.816
-.006	5.080	-.003	35.999
-.007	9.474	.001	40.349
-.017	9.857	-.011	40.730
-.033	10.076	-.003	40.924
-.022	10.260	.010	41.103
.018	14.613	-.011	45.458
-.010	15.014	-.037	45.851
-.027	15.233	-.050	46.063
-.024	15.425	-.019	46.224
.037	19.755	.029	50.482
.026	20.139	-.014	50.888
.022	20.346	-.036	51.107
.013	20.549	-.010	51.271
.022	24.925	.029	55.492
.005	25.314	.017	55.863
.017	25.505	.005	56.070
.018	25.698	.026	56.237
.021	30.073	.006	60.443
-.006	30.471	-.003	60.804
-.009	30.677	.002	61.173
-.004	30.865		

vii. Self-Association of Acetone

Pressure-density measurements for acetone were collected on the automated vapor density apparatus described in the experimental section. Data were collected at seven temperatures and analyzed similarly to the data collected for TFE self-association at 25°C. The data are presented in Tables IV-4 through IV-10.

The acetone vapor density experiments were actually conducted four times at each temperature, providing a daily check of the apparatus before proceeding with mixed vapor density experiments. Only the acetone pressure-density data collected prior to the acetone-ethanol experiments are given here; however, all acetone data were used in analyzing the behavior of acetone vapor.

The Keyes point, described earlier, provides an anchor point for the acetone vapor-density data at each temperature. Ambrose, Sprake, and Townsend [10] determined the vapor pressure of acetone as a function of temperature and fitted the data to the Antoine model:

$$\log_{10}(P/kPa) = 6.25478 - 1216.689/(T°K - 42.875)$$

Pennington and Kobe[113] studied the heats of vaporization of acetone.

$$\Delta H_{vap} = 938.7(508.7 - T^{\circ}K) \qquad \text{cal/mole}$$

The Π/P ratios, given in Table IV-11, were calculated from these equations using the method described in section IV-ii. The vapor density data are plotted as Π/P vs. P in figures IV-2 through IV-8. On each figure, the acetone Keyes point is included. The dashed line is a smooth curve from the experimental data at pressures less than about 60% of the vapor pressure to the Keyes point (i.e. the vapor pressure). At pressures larger than about 60% of the vapor pressure, the Π/P values begin to increase much more rapidly than they should to follow the smooth curve. The data deviating from the smooth curve are believed to be in error due to adsorption effects.

A choice had to be made as to which data points should be considered representative of nonideal behavior due to association. Inclusion of the data deviating from the smooth curve would yield large equilibrium constants, attributing association in the vapor to what, in fact, is most probably adsorption of the vapor to the walls of the sample flask. A monomer-dimer model would be sufficient in fitting the experimental data with pressures less than about 60% of the saturation vapor pressure. However, this neglects the obvious curvature in the Π/P vs. P plot in the region between 60% of the vapor pressure and the Keyes point. Combination of the vapor-density data up to 60% of the vapor pressure with the Keyes point should provide enough information to account for larger

aggregates and, at the same time, alleviate the enormous adsorption problem in the region near the vapor pressure. It may be assumed that the error in the Keyes point is mostly in the value of Π since this is dependent on the accuracy of the heat of vaporization. If ΔH_{vap} is known to within 10 calories, or 0.15%, the uncertainty in Π is about 0.5 torr. The vapor pressure measurements are probably as precise as pressure values obtained from the present study, i.e. about 10 microns.

Much thought went into deciding just how much importance this one anchor point should have relative to the vapor density measurements. An argument for weighting this point greater than the other data points might be its independence from adsorption effects. On the other hand, the reliability of the point may not be as good as that of the individual data points and therefore, it might not be considered as important. Using various weights on the Keyes point results in slightly different values for the equilibrium constants yielding little insight to the weight problem. Therefore, for lack of any justification to do otherwise, the Keyes point is treated exactly as any other data point when fitting the data with an association model.

The 30 °C vapor density data were fit with several different models, the results of which are in Table IV-12. All data fitting procedures included a parameter for the loop size.

$$\Pi = B(1) * I$$

Π is the ideal pressure, B(1) is the loop parameter, and I is the

number of increments injected. When fitting the data at all seven temperatures, simultaneously, the loop parameter is temperature dependent and is used in the data analysis program in the form

$$\Pi = B(1)' * T^{\circ}(K) * I.$$

The root mean square deviation is calculated using the equation

$$RMSD = \left[\frac{\Sigma\ (\Delta\Pi(exp)-\Delta\Pi(calc))^2}{\text{degrees of freedom}} \right]^{\frac{1}{2}}$$

where $\Delta\Pi(exp)$ is the loop size and $\Delta\Pi(calc)$ is the difference between the ideal pressure calculated for two consecutive points. The degrees of freedom are the number of data points fit minus the number of parameters determined.

In this particular experimental procedure, one occasionally sees an obviously bad point. Either the loop didn't completely empty when opened to the sample flask or was not completely filled with acetone when opened to the acetone reservoir flask. This error will show up in each total pressure reading in that set of data following the bad point; that is, the total pressure after n increments from one experimental run will not be consistent with the nth pressure of another experimental run in which a bad point has occurred. However, with the exception of the bad point itself, the difference between any two consecutive pressure readings is still reproducible. Therefore, fitting the data with respect to differences in pressure rather than total pressure will erase any effects of bad points. Either Π or P may be calculated since there is about as much uncertainty in either measurement, on the order of about 5 microns of

pressure. In the case of the Keyes point for each data set, the contribution to the RMSD is the difference between total Π(calc) and Π(keyes). The RMSD is actually

$$\text{RMSD} = \left[\frac{\sum_{i=1}^{N} (\Delta\Pi(\text{exp}) - \Delta\Pi(\text{calc})_i + (\Pi(\text{Keyes})-\Pi(\text{calc}))^2}{\text{degrees of freedom}}\right]^{1/2}$$

A total of 277 data points collected from seventeen vapor density experiments ranging in temperature between 15°C and 45°C were analyzed to determine the equilibrium constants at any temperature in this range and the heat of association for the formation of each species. The 1-2-infinity model is believed to best describe the data over this range, although other models give equally good fits.(See Table IV-10) Both a heat of association for the dimer and a stepwise heat of association related to the stepwise equilibrium constant were calculated using the Clausius-Clapeyron equation:

$$\ln(K_2^T/K_2^{298.15}) = \Delta H_2/R(1/T(°K)-1/298.15°K)$$

and

$$\ln(K_\infty^T \quad /K_\infty^{298.15}) = \Delta H_\infty/R(1/T(°K)-1/298.15°K)$$

where K_2^T and ΔH_2 are the dimer equilibrium constant at temperature T and the heat of association for the formation of the dimer, respectively. Likewise, K_∞^T and ΔH_∞ refer to the stepwise addition of a monomer to an n-mer where n=2,3,..., . R is the gas constant (1.9872 cal/°Kmole is the value used to obtain the data in Table IV-13.)

Five different loop parameters were needed for the seventeen experiments. During the course of data collection, modifications to the apparatus caused minor differences in the loop size, necessitating the use of different loop parameter values for different groups of experiments.

The final values for the loop sizes, equilibrium constants and heats of association calculated from the 1-2-infinity model are provided in Table IV-13.

TABLE IV-4

ACETONE VAPOR DENSITY DATA

AT 14.97 DEGREES CELSIUS

PRESSURE (P)	IDEAL PRESSURE (Π)	$\Delta\Pi$(CALC)-$\Delta\Pi$(EXP)
11.906	11.950	- 0.026
23.799	23.900	- 0.004
35.664	35.850	0.004
47.484	47.800	- 0.004
59.258	59.751	- 0.014
70.994	71.701	- 0.016
82.669	83.651	- 0.040
** 147.489	150.384	- 0.010

** Keyes point

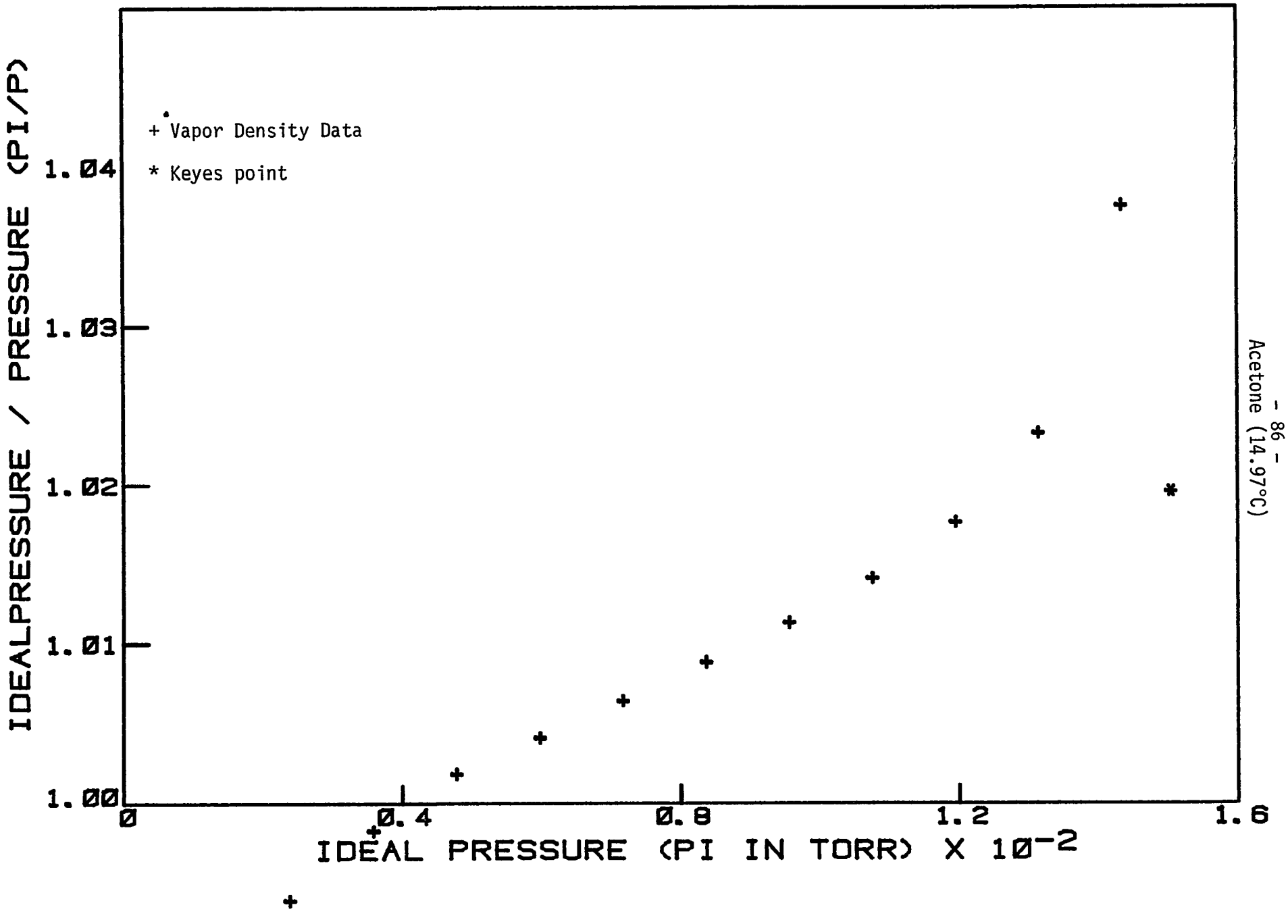

FIGURE IV-2

Acetone (14.97°C)

TABLE IV-5

ACETONE VAPOR DENSITY DATA

AT 20.00 DEGREES CELSIUS

PRESSURE (P)	IDEAL PRESSURE (Π)	$\Delta\Pi$(CALC)-$\Delta\Pi$(EXP)
12.104	12.159	- 0.038
24.208	24.317	- 0.004
36.288	36.476	0.006
48.331	48.635	0.003
60.343	60.794	0.006
72.312	72.952	- 0.003
84.244	85.111	- 0.005
96.129	97.270	- 0.017
107.967	109.429	- 0.030
** 185.553	189.746	0.009

** Keyes point

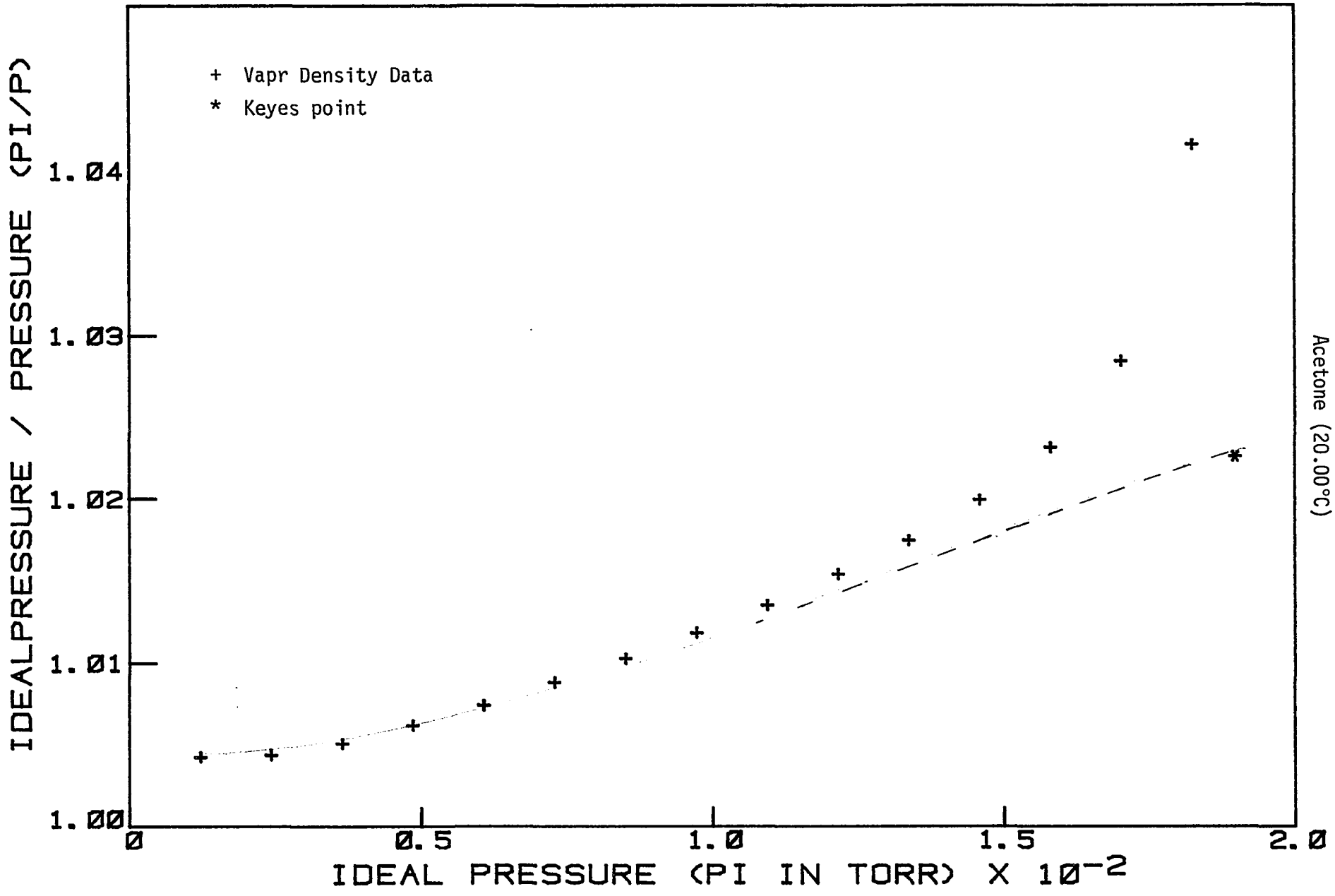

FIGURE IV-3

Acetone (20.00°C)

TABLE IV-6

ACETONE VAPOR DENSITY DATA

AT 25.00 DEGREES CELSIUS

PRESSURE (P)	IDEAL PRESSURE (Π)	$\Delta\Pi$(CALC)-$\Delta\Pi$(EXP)
12.348	12.366	- 0.002
24.676	24.732	0.010
36.983	37.098	0.021
49.252	49.465	0.015
61.492	61.831	0.019
73.699	74.197	0.018
85.863	86.563	0.008
97.997	98.929	0.011
110.088	111.295	0.001
122.136	123.661	- 0.009
134.138	136.027	- 0.022
146.088	148.394	- 0.041
** 231.040	237.047	0.017

** Keyes point

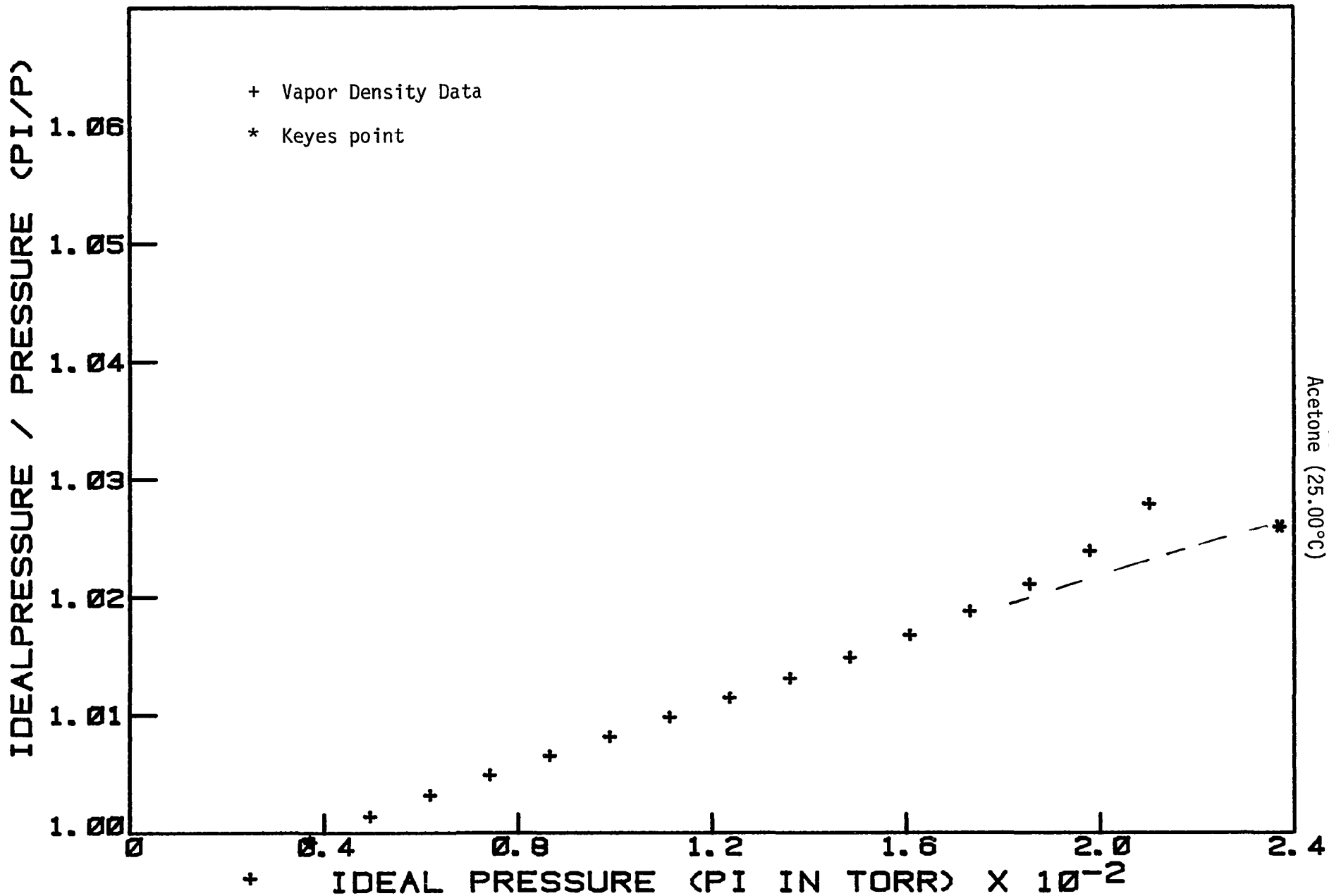

FIGURE IV-4
- 90 -
Acetone (25.00°C)

TABLE IV-7

ACETONE VAPOR DENSITY DATA

AT 30.00 DEGREES CELSIUS

PRESSURE (P)	IDEAL PRESSURE (Π)	ΔΠ(CALC)-ΔΠ(EXP)
12.528	12.574	- 0.031
25.053	25.147	- 0.003
37.567	37.721	0.016
50.043	50.294	0.009
62.501	62.868	0.021
74.917	75.441	0.010
87.309	88.015	0.017
99.666	100.588	0.014
111.986	113.162	0.008
124.277	125.735	0.010
136.531	138.309	0.005
148.743	150.882	- 0.006
160.912	163.456	- 0.017
173.053	176.029	- 0.013
185.137	188.603	- 0.039
** 285.265	293.780	0.013

** Keyes point

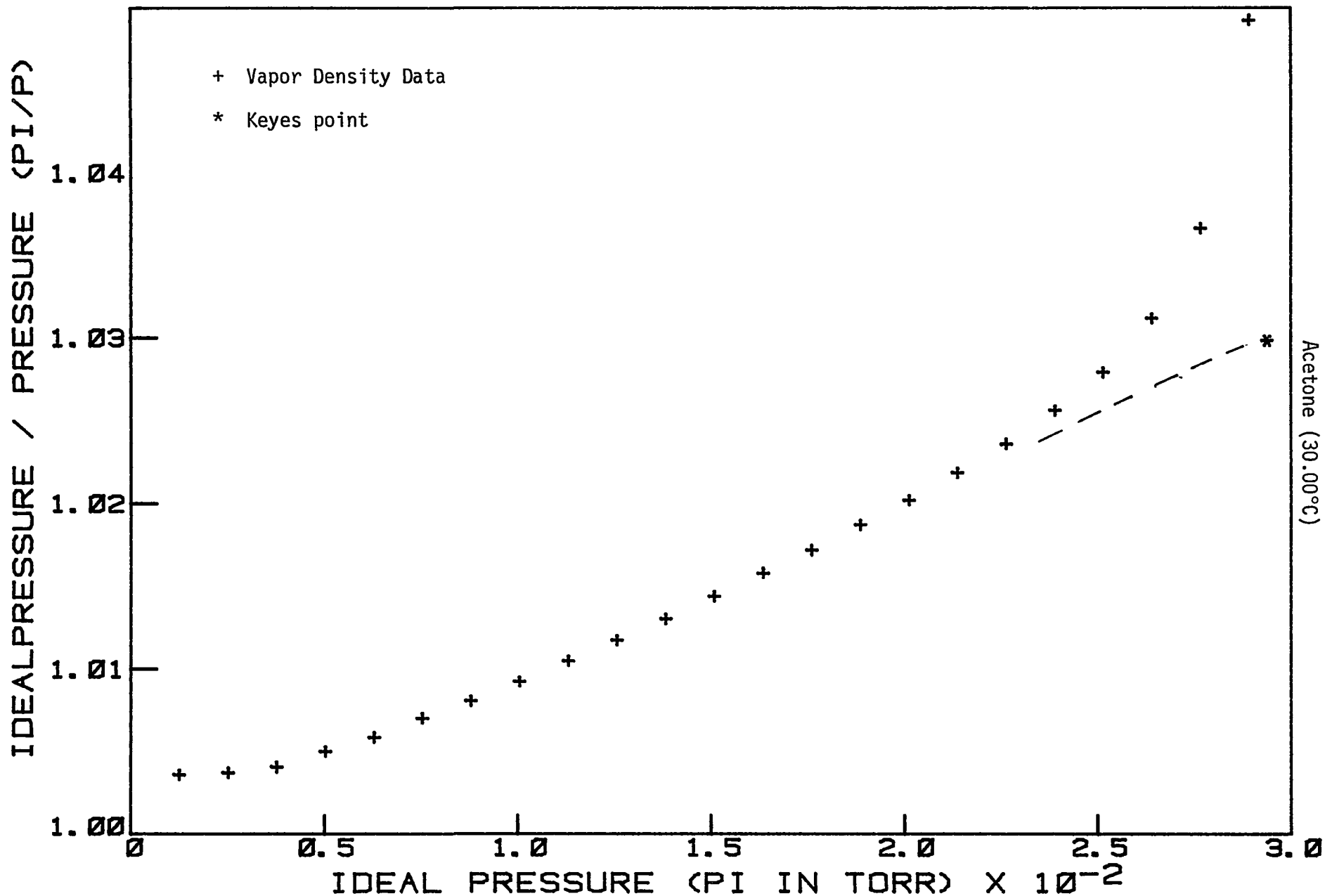

FIGURE IV-5

Acetone (30.00°C)

TABLE IV-8

ACETONE VAPOR DENSITY DATA

AT 34.79 DEGREES CELSIUS

PRESSURE (P)	IDEAL PRESSURE (Π)	$\Delta\Pi$(CALC)-$\Delta\Pi$(EXP)
12.728	12.772	- 0.030
25.456	25.544	- 0.001
38.161	38.317	0.005
50.844	51.089	0.012
63.503	63.861	0.017
76.132	76.633	0.016
88.731	89.405	0.016
101.303	102.177	0.019
113.842	114.950	0.016
126.348	127.722	0.012
138.820	140.494	0.009
151.255	153.266	0.002
163.660	166.038	0.002
176.029	178.811	- 0.004
188.367	191.583	- 0.004
200.666	204.355	- 0.013
** 346.516	358.284	0.001

** Keyes point

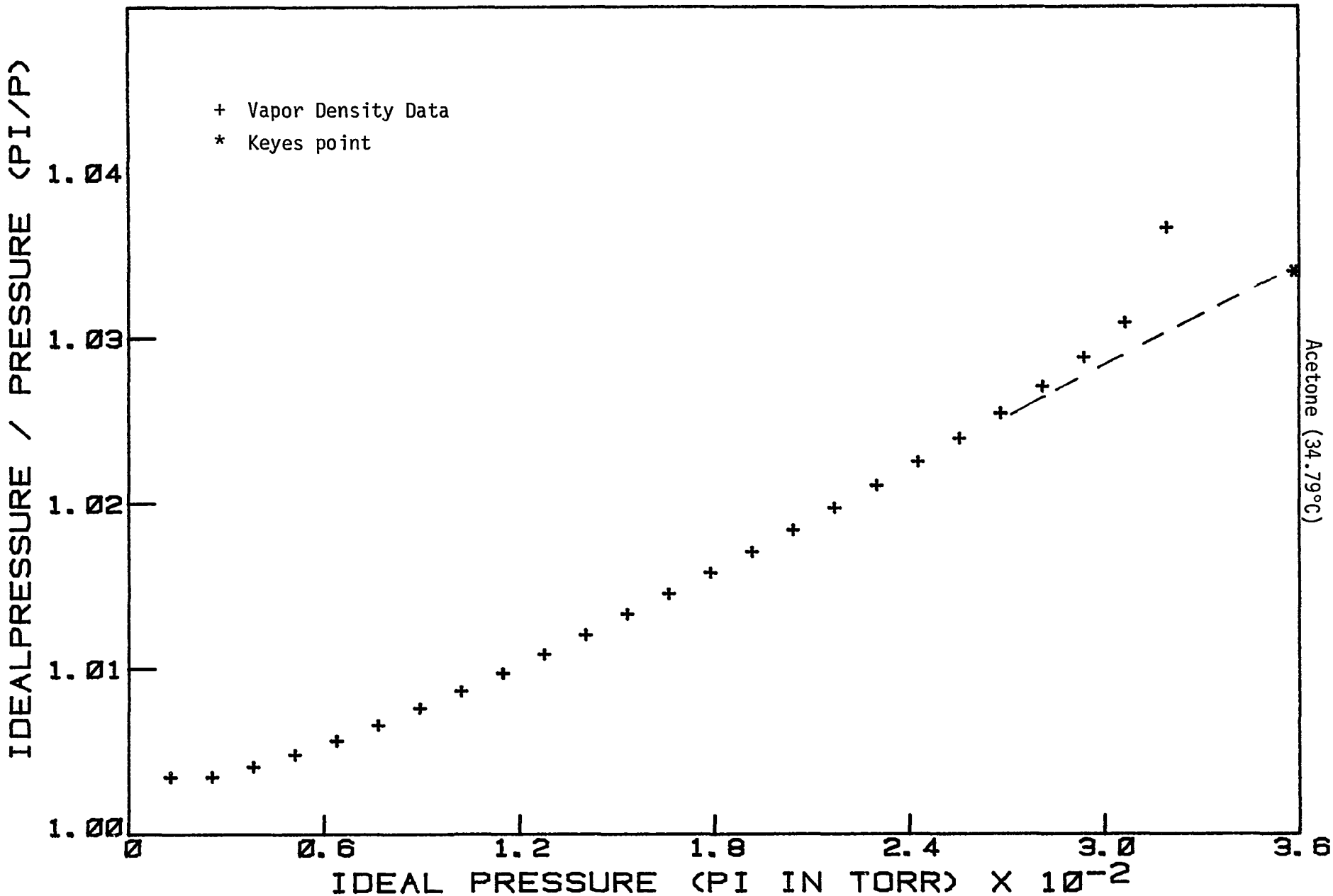

Acetone (34.79°C)

FIGURE IV-6

TABLE IV-9

ACETONE VAPOR DENSITY DATA

AT 40.06 DEGREES CELSIUS

PRESSURE (P)	IDEAL PRESSURE (π)	$\Delta\pi$(CALC)-$\Delta\pi$(EXP)
12.943	12.991	- 0.034
25.882	25.982	- 0.011
38.809	38.972	0.004
51.707	51.963	0.003
64.587	64.954	0.013
77.428	77.945	0.001
90.257	90.935	0.018
103.050	103.926	0.010
115.814	116.917	0.009
128.545	129.908	0.004
141.245	142.898	0.002
153.921	155.889	0.006
166.558	168.880	- 0.004
179.173	181.871	0.003
191.761	194.861	0.005
204.303	207.852	- 0.012
216.820	220.843	- 0.008
229.300	233.834	- 0.016
241.754	246.824	- 0.012
** 425.800	442.393	- 0.009

** Keyes point

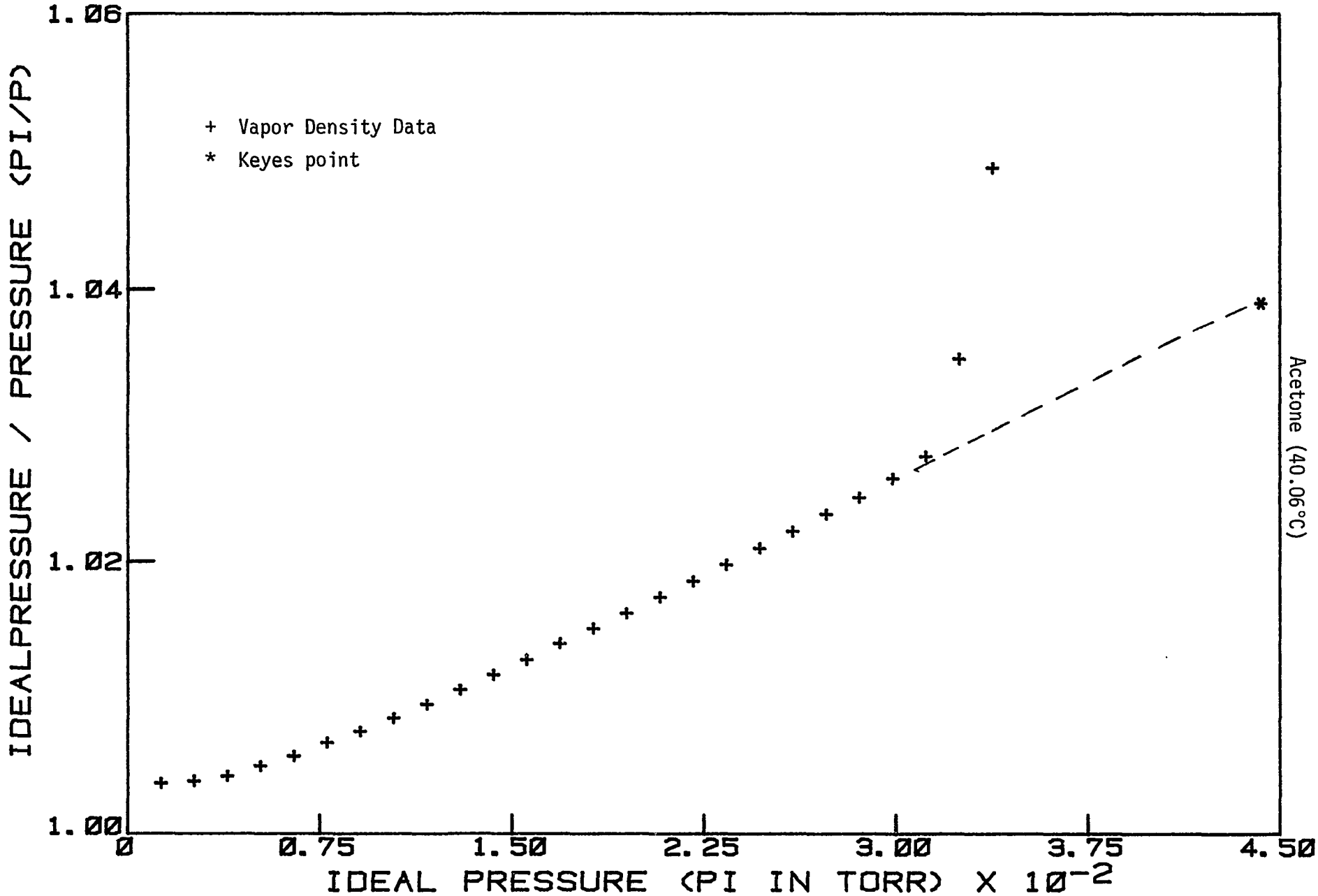

FIGURE IV-7

Acetone (40.06°C)

TABLE IV-10

ACETONE VAPOR DENSITY DATA

AT 44.96 DEGREES CELSIUS

PRESSURE (P)	IDEAL PRESSURE (Π)	ΔΠ(CALC)-ΔΠ(EXP)
13.142	13.194	- 0.039
26.287	26.388	- 0.010
39.429	39.582	0.013
52.563	52.776	0.031
65.769	65.970	0.131
78.858	79.164	0.040
91.892	92.358	0.011
104.899	105.552	0.011
117.877	118.746	0.009
130.825	131.940	0.006
143.750	145.134	0.011
156.641	158.328	0.004
169.504	171.522	0.003
182.334	184.716	- 0.002
195.140	197.910	0.001
207.910	211.104	- 0.007
220.655	224.298	- 0.004
233.371	237.492	- 0.005
246.048	250.686	- 0.017
** 512.072	534.650	0.005

**Keyes point

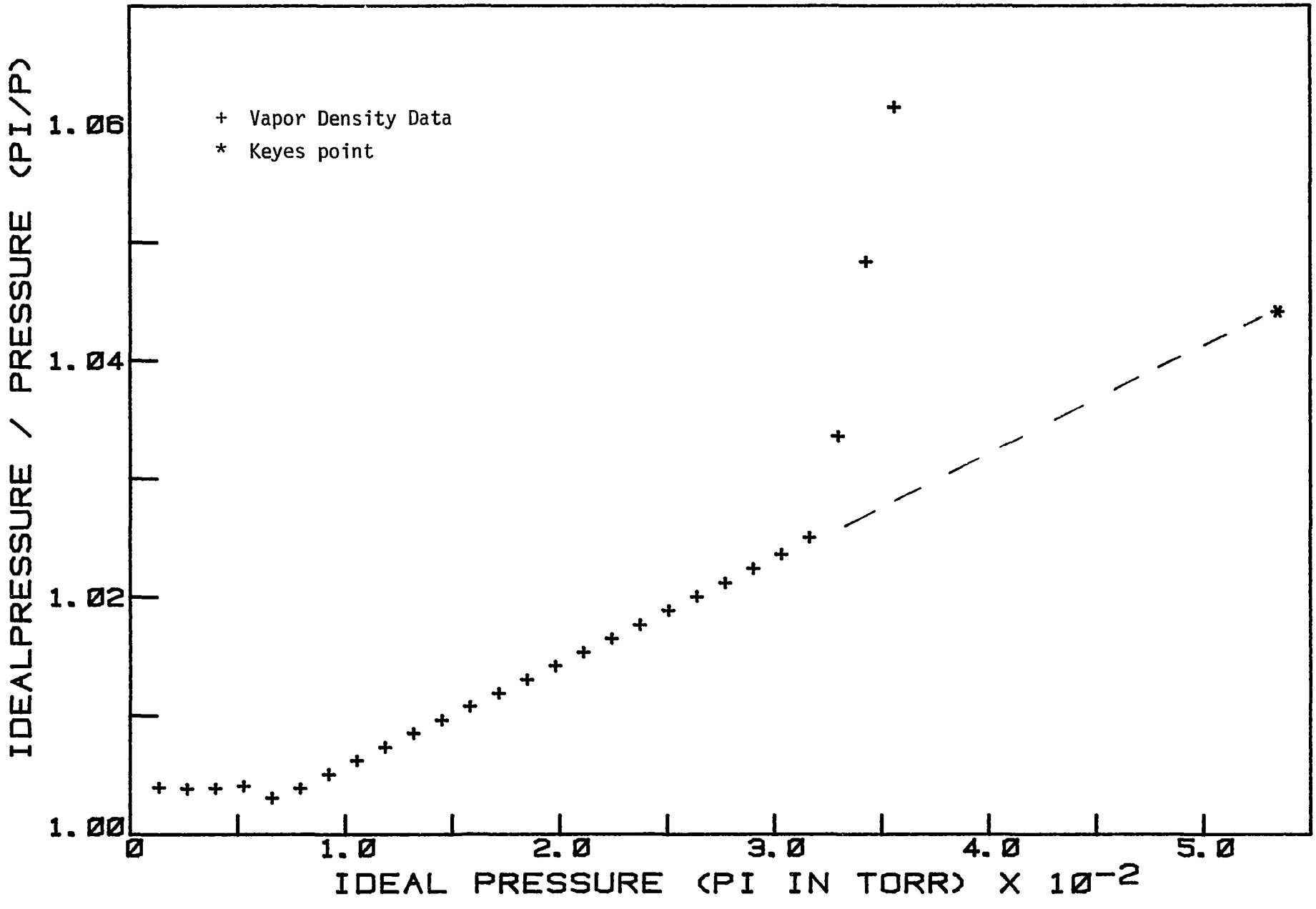

FIGURE IV-8

- 98 -

Acetone (44.96°C)

TABLE IV-11

KEYES POINTS FOR ACETONE DATA

T(°K)	$\Delta H_{vap}(\frac{cal}{mole})$	Vapor P(Torr)	Vapor II(Torr)
288.12	7536.04	147.489	150.384
293.15	7469.24	185.553	189.746
298.15	7401.88	231.040	237.047
303.15	7333.53	285.265	293.780
307.94	7267.08	346.516	358.284
313.21	7192.85	425.800	442.393
318.11	7122.71	512.072	534.650

TABLE IV-12

SELF - ASSOCIATION OF ACETONE AT 30°C

Results from Fitting Data Using Different Models

MODEL	RMSD	LOOP SIZE	$K_2(torr^{-1})$	$K_3(torr^{-2})$	$K_4(torr^{-3})$	$K_\infty(torr^{-1})$
1 - 2	.023	12.588±.007	$1.114(\pm.003)X10^{-4}$			
1 - 3	.019	12.502±.005		$1.918(\pm.004)X10^{-7}$		
1-2-3	.021	12.580±.010	$1.008(\pm.06)X10^{-4}$	$1.849(\pm.3)X10^{-8}$		
1-2-4	.020	12.571±.0002	$9.776(\pm.008)X10^{-5}$		$5.67(\pm.02)X10^{-13}$	
1 - ∞	.021	12.584±.006				$1.048(\pm.002)X10^{-4}$
1-2-∞	.019	12.575±.003	$9.551(\pm.003)X10^{-5}$			$2.590(\pm.003)X10^{-4}$
1-3-∞	.017	12.507±.007		$2.145(\pm.04)X10^{-7}$		$-2.74(\pm.4)X10^{-5}$

TABLE IV-13

EQUILIBRIUM CONSTANTS AND HEATS OF ASSOCIATION

FOR VAPOR PHASE ASSOCIATION OF ACETONE WITH VARIOUS COMPOUNDS

Compound	Model	RMSD	$K_2^{25°C}$ (torr^{-1})	ΔH_2 ($\frac{cal}{mole}$)	$K_{11}^{25°C}$ (torr^{-1})	ΔH_{11} ($\frac{cal}{mole}$)	$K_\infty^{25°C}$ (torr^{-1})	ΔH ($\frac{cal}{mole}$)
Acetone	1-2-∞	0.019	$1.034 \times 10^{-4} \pm 4 \times 10^{-7}$	3143.29 ± 34			$2.92 \times 10^{-4} \pm 7 \times 10^{-6}$	2651.34 ± 230
Methanol	1-∞	0.026			$1.58 \times 10^{-4} \pm 4 \times 10^{-6}$	2924.09 ± 354	$1.879 \times 10^{-3} \pm 9 \times 10^{-6}$	13871.91 ± 642
Ethanol	1-∞	0.020			$1.24 \times 10^{-4} \pm 2 \times 10^{-6}$	5629.38 ± 180	$3.19 \times 10^{-3} \pm 3 \times 10^{-5}$	11057.42 ± 148
2-Butanol	1-∞	0.015			$1.17 \times 10^{-4} \pm 2 \times 10^{-6}$	2646.79 215	$4.15 \times 10^{-3} \pm 4 \times 10^{-5}$	12573.47 ± 171

LOOP PARAMETERS

System	T(°C)	Loop Parameter (=$\Delta\Pi$/T°K)
Acetone/Ethanol	15°C-45°C	$0.041476 \pm 7 \times 10^{-6}$
Acetone/Methanol	15°C & 35°C-45°C	$0.033561 \pm 9 \times 10^{-6}$
Acetone/Methanol	25°C,30°C	$0.033902 \pm 1 \times 10^{-5}$
Acetone/2-Butanol	25°C	$0.035346 \pm 1 \times 10^{-5}$
Acetone/2-Butanol	30°C-45°C	$0.035601 \pm 8 \times 10^{-6}$

viii. Systems of Mixed Vapors

Eight heterogeneous vapor-density systems were studied. Data for TFE-water, TFE-methanol, TFE-ethanol, and TFE-2-butanol were collected at 25 °C only. Liquid-vapor equilibrium data were collected for each of these systems. Data for acetone-water were collected at seven temperatures over the 15 °C-45 °C range; however, little information is obtained from these data due to large adsorption problems. Data for acetone-methanol and acetone-ethanol were collected at seven temperatures over the 15 °C-45 °C range with good results. The melting point of 2-butanol is just below room temperature and so data for the acetone-2-butanol system were collected at only five temperatures over the 25° C-45° C range, also with good results.

The problems, methods, and results of data analysis will be discussed for each system, individually, in the following sections. Tables of data and results and figures for each system will follow the section describing the system.

viii-1. 2,2,2-Trifluoroethanol/Water at 25°C

Adsorption of water onto the Pyrex glass walls of the sample container was studied in several experiments where the water vapor in the sample flask was allowed to expand into a flask containing crushed Pyrex glass. The surface area of the crushed glass is ten times the surface area of the sample flask. The procedure is described more thoroughly in the experimental section. The results of this expansion indicated that water adsorption on Pyrex glass is at least ten to twelve layers thick near the vapor pressure of water. The graph of water vapor adsorbed vs. total water vapor is shown in figure IV-9. The shape of the curve is characteristic of a Brunauer-Emmett-Teller (BET) multilayer adsorption isotherm.

Addition of TFE to the flask containing water vapor decreases the amount of vapor adsorbed on the Pyrex glass. One possible reason for this phenomenon might be the displacement of several adsorbed molecules of water by a single TFE molecule.

The experimental procedure of collecting vapor density data for this mixed vapor system involves introducing an initial quantity of water vapor and then adding increments of TFE to the flask. The first increment of TFE gives a pressure increase higher than the ideal incremental pressure when the initial pressure of the water vapor is greater than about 15 torr. This is consistent

with the findings in the expansion experiment dicussed above. By introducing an increment of TFE to the flask containing water vapor, some water vapor desorbs and adds to the pressure of the mixture. To avoid this complication, the pressures of the water vapor introduced into the flask at the beginning of each of four TFE/water vapor density experiments were 2.647 torr, 5.289 torr, 7.943 torr, and 10.56 torr. These pressures are well below the region where desorption may be detected by the Bourdon type pressure transducer.

Table IV-14 gives the experimental pressure, the difference between the experimental and calculated pressures, the initial pressures of water vapor added, and the total amount of TFE added. Figure IV-10 shows the change in the incremental pressure with added TFE.

Forty-one data points were fitted using only two parameters: an equilibrium constant for the association of one water molecule with one TFE molecule and an equilibrium constant for the addition of a TFE monomer to an n-mer consisting of a single water molecule and n-1 TFE molecules. The results of this model are in Table IV-2.

In an extensive study of the thermodynamic properties of water, Keyes[108] reported the ideal pressure:vapor pressure ratio (Π/P) for water to be 1.00152 at 25°C. Although water is a highly complex liquid, its vapor is very nearly ideal. Therefore,

inclusion of a term for the self-association of water was not deemed necessary in determining the amount of association that is due to the formation of hetero-complexes or self-association. The self-association of TFE was included when fitting the mixed vapor data.

Liquid-vapor equilibrium curves were inferred from data taken after reaching the dew point. Each pair of data consists of the overall mole fraction of TFE or water and the pressure. Each experiment began with a known amount of water in the flask. Table IV-15 lists the actual data collected in the first liquid-vapor equilibrium experiment. Each pair of data consists of increment number and gauge reading. From the differences between gauge readings, one may easily detect at which increment the dew point has occurred. The differences decrease smoothly, at first, since only the vapor phase exists in the sample flask; an abrupt drop in the differences indicates that both vapor and liquid phase are present in the flask. The first liquid-vapor experiment began with 0.0166 ml of water. Thirty-two increments of TFE, or 0.1769 ml, were added over several days. Eight liquid-vapor equilibrium data points were collected. The second experiment began with 0.177 ml of water. Thirty-nine increments of TFE, or 0.2156 ml, were added during forty-eight hours and fourteen liquid-vapor equilibrium data points collected. Table IV-16 lists the twenty-two data points of pressure and overall mole fraction of TFE in addition to the calculated pressure from the NLLSQ program and the inferred mole fraction of TFE in the vapor and in the liquid

phases. Figure IV-11 is the liquid-vapor equilibrium curve for TFE/water. Values of the four parameters in the Hansen-Miller equations are given in Table IV-17 along with the parameter uncertainties and the RMSD between experimental pressures and calculated pressures.

FIGURE IV-9

Water Vapor Adsorbed in the Presence of TFE

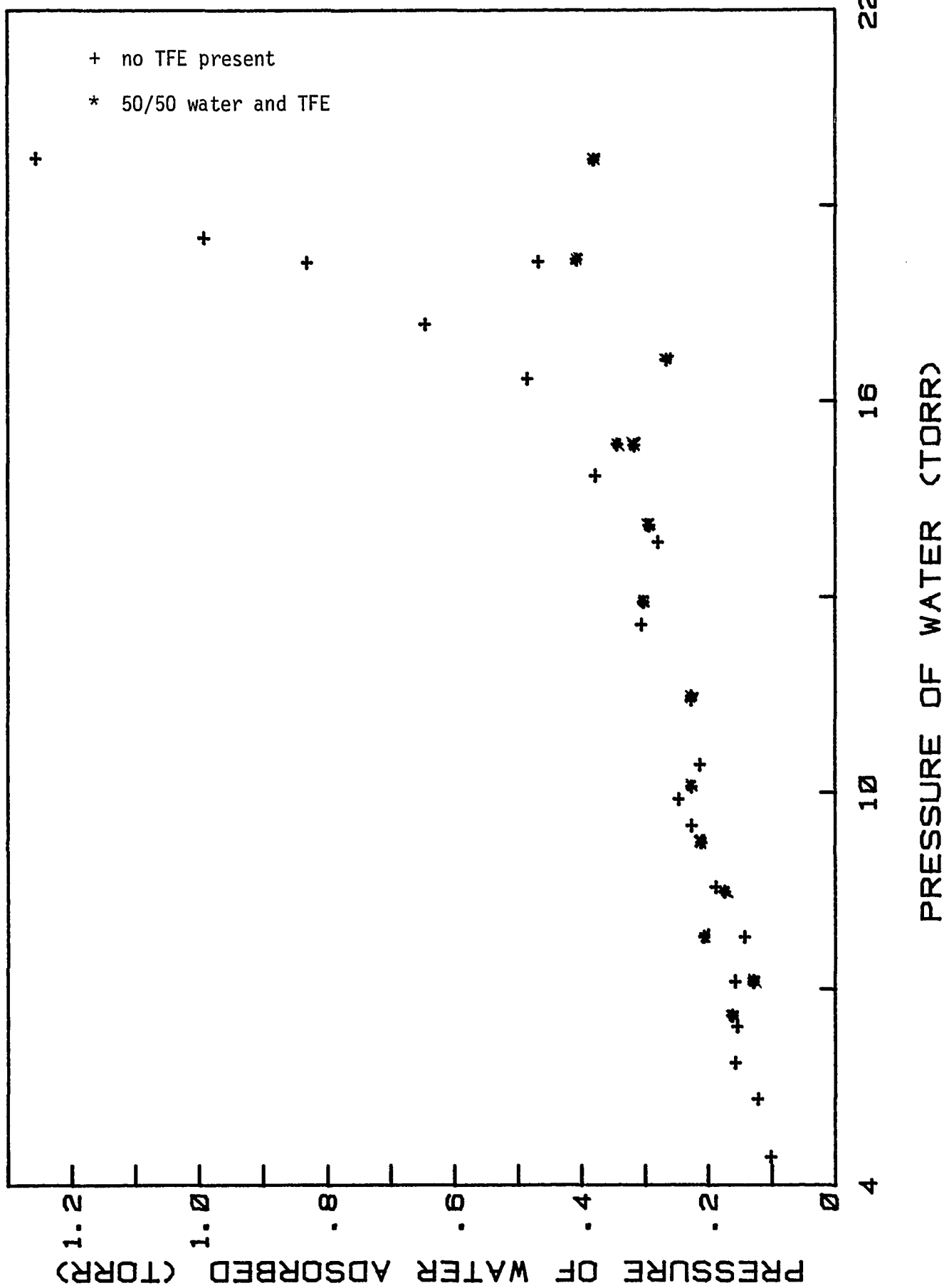

TABLE IV-14

TFE/WATER VAPOR DATA

AT 25.00 DEGREES CELSIUS

PRESSURE (P)	IDEAL PRESSURE (Π)	P(CALC)- P(EXP)
ALCOHOL PRESSURE = 2.647		
5.279	5.255	0.024
10.556	10.517	0.039
15.831	15.798	0.033
21.102	21.063	0.039
26.367	26.335	0.032
31.624	31.588	0.036
36.868	36.856	0.012
42.092	42.064	0.028
47.287	47.260	0.027
52.438	52.414	0.024
57.519	57.500	0.019
ALCOHOL PRESSURE = 5.289		
5.274	5.259	0.015
10.546	10.541	0.005
15.815	15.813	0.002
21.078	21.078	0.000
26.334	26.348	- 0.014
31.579	31.614	- 0.035
36.808	36.847	- 0.039
42.013	42.063	- 0.050
47.183	47.245	- 0.062
52.299	52.352	- 0.053
ALCOHOL PRESSURE = 7.943		
5.270	5.228	0.042
10.537	10.507	0.030
15.799	15.766	0.033
21.055	21.033	0.022
26.302	26.283	0.019
31.535	31.524	0.011
36.749	36.754	- 0.005

TABLE IV-14 cont.

TFE/WATER VAPOR DATA

AT 25.00 DEGREES CELSIUS

PRESSURE (P)	IDEAL PRESSURE (Π)	P(CALC)- P(EXP)
41.935	41.949	- 0.014
47.079	47.097	- 0.018
52.161	52.165	- 0.004
ALCOHOL PRESSURE = 10.56		
5.266	5.246	0.020
10.528	10.507	0.021
15.784	15.775	0.009
21.032	21.026	0.006
26.269	26.273	- 0.004
31.491	31.502	- 0.011
36.690	36.689	0.001
41.857	41.848	0.009
46.977	46.936	0.041
45.977	45.936	0.041

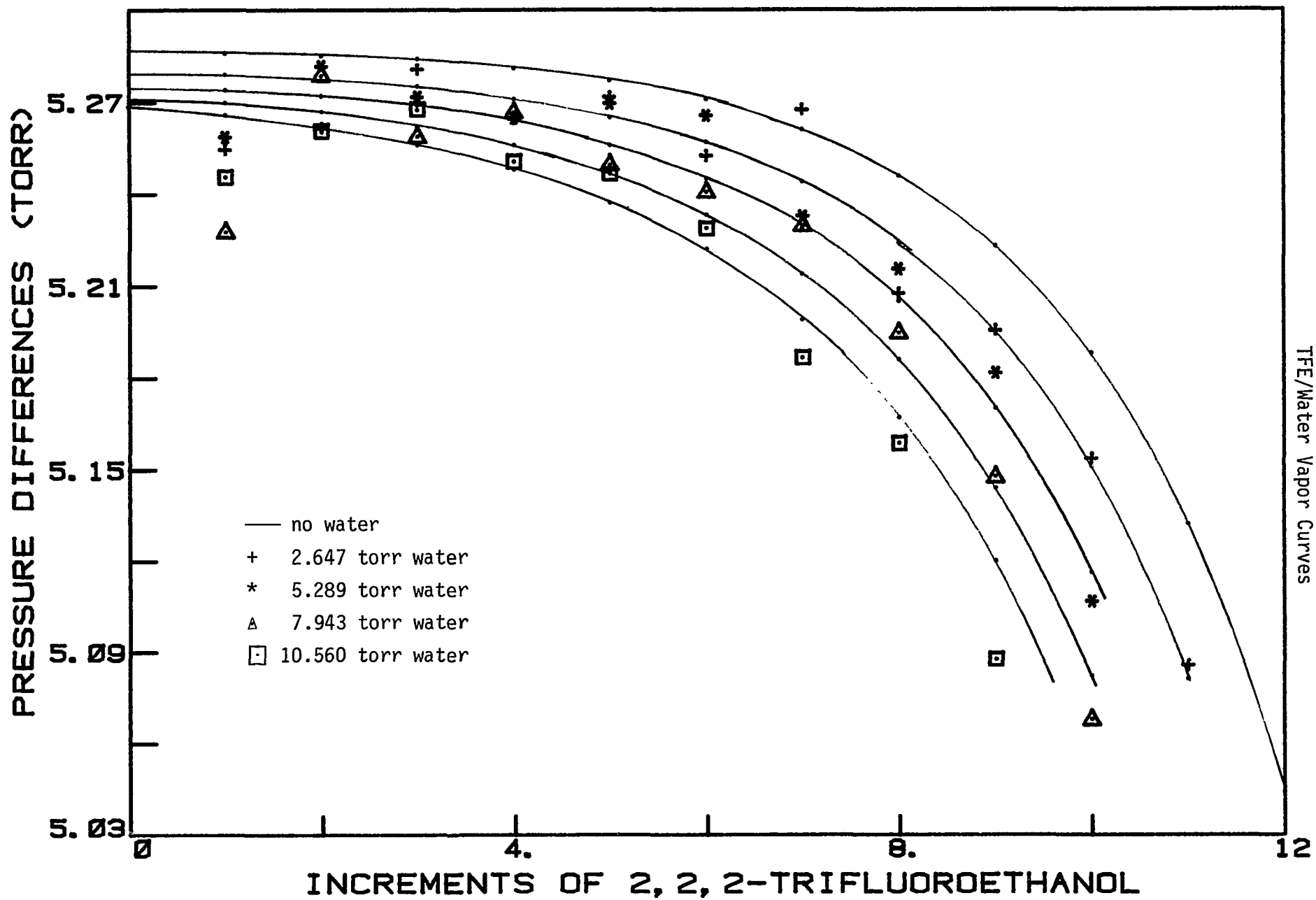

FIGURE IV-10

TFE/Water Vapor Curves

TABLE IV-15

2,2,2 - TRIFLUOROETHANOL/WATER RAW LV DATA

Inc. of TFE added	Gauge Reading	Δ Gauge
0	15.383	
1	20.562	5.179
2	25.714	5.152
3	30.871	5.157
4	35.947	5.076
5	41.125	5.178
6	46.245	5.120
7	51.279	5.034
8	56.181	4.902
9	61.011	4.830
10	63.613	2.602
11	64.355	0.742
12	64.997	0.642
15	66.205	1.208
18	66.959	0.754
22	67.245	0.286
28	67.857	0.612
30	67.890	0.033
32	68.057	0.167

TABLE IV-16

TFE/WATER LIQUID-VAPOR DATA

AT 25.00 DEGREES CELSIUS

Π(TFE)	P(EXP)	PC	P(EXP)-PC	$\bar{X}$(TFE)	X^V(TFE)	X^L(TFE)
		Π(WATER) = 168.67 TORR				
5.286	27.774	28.008	0.234	0.030	0.159	0.006
10.572	31.933	32.213	0.280	0.059	0.274	0.012
15.858	35.930	36.285	0.354	0.086	0.358	0.019
21.144	39.921	40.164	0.243	0.111	0.424	0.027
26.430	43.724	43.799	0.075	0.135	0.475	0.036
31.716	47.235	47.121	- 0.114	0.158	0.515	0.047
42.288	52.517	52.454	- 0.063	0.200	0.570	0.077
47.574	54.746	54.278	- 0.468	0.220	0.587	0.096
68.718	56.291	56.884	0.593	0.289	0.610	0.187
89.862	57.596	57.598	0.002	0.347	0.618	0.269
105.720	58.500	58.262	- 0.238	0.385	0.626	0.319
121.578	59.301	58.990	- 0.310	0.419	0.636	0.363
158.580	60.739	60.625	- 0.114	0.484	0.662	0.444
206.154	62.348	62.328	- 0.020	0.550	0.693	0.521
		Π(WATER) = 15.854 TORR				
58.146	65.950	66.378	0.427	0.786	0.793	0.715
63.432	66.610	66.892	0.283	0.800	0.810	0.743
79.290	67.850	67.881	0.031	0.833	0.846	0.799
95.148	68.625	68.459	- 0.166	0.857	0.871	0.834
116.292	68.918	68.944	0.026	0.880	0.893	0.865
148.008	69.547	69.387	- 0.160	0.903	0.915	0.894
158.580	69.581	69.492	- 0.088	0.909	0.921	0.901
169.152	69.752	69.584	- 0.168	0.914	0.926	0.907

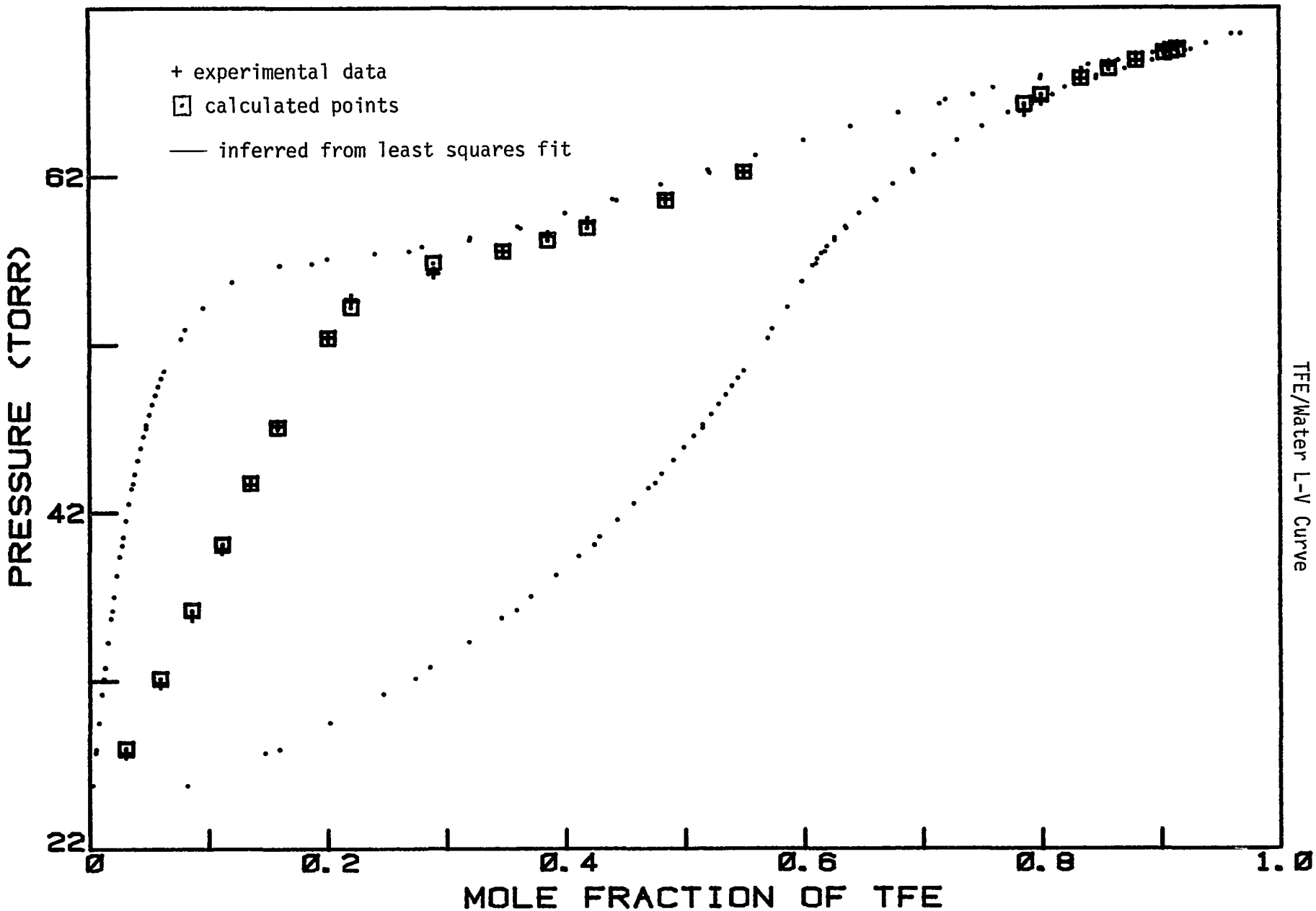

FIGURE IV-11
- 113 -
TFE/Water L-V Curve

TABLE IV-17

HANSEN - MILLER CONSTANTS
Derived from Least - Squares Analysis of
Liquid - Vapor Equilibrium Data

Binary System	A	B	C	D	RMSD
2,2,2-trifluoroethanol/water	2.50 ± 0.03	-7.34 ± 0.36	10.3 ± 1.3	-5.8 ± 1.2	0.282
2,2,2-trifluoroethanol/methanol	-0.441 ± 4.36	-6.47 ± 35	12. ± 71	-6.7 ± 42	0.398
2,2,2-trifluoroethanol/ethanol	-1.42 ± 0.07	1.65 ± 0.81	-2.6 ± 2.0	1.8 ± 1.6	0.159
2,2,2-trifluoroethanol/2-butanol	-0.933 ± 0.035	-0.45 ± 0.4	-0.04 ± 0.9	1.54 ± 0.65	0.068

viii-2. - 2,2,2-Trifluoroethanol/Methanol at 25°C

Five sets of TFE/methanol vapor density data were collected at 25.00°C on the manual vapor-density apparatus. Initial pressures of methanol were 2.647 torr, 5.214 torr, 7.94 torr, 10.52 torr, and 13.21 torr. The data and calculated pressure are given in Table IV-18. Figure IV-12 is a graph of the incremental pressure change vs. total TFE added to the flask.

In addition to a discrete dimer equilibrium constant and a stepwise equilibrium constant, a third constant representing the formation of $(\text{methanol})_2(\text{TFE})$ was necessary adequately to fit the forty-eight vapor density points. The data were adjusted with the kink corrections obtained from the TFE self-association deviations between calculated and experimental pressures. The overall fit was quite good, the RMSD between calculated and experimental total pressure being only 26 microns.

Using the Keyes method, the ideal pressure:vapor pressure ratio for methanol vapor may be calculated using heats of vaporization data from Fiock, Ginning and Holton,[46]

$$\Delta H(\text{intJ/G}) = -0.0005(240-T/°C) + 2.60875(240-T/°C) + 219(240-T/°C)$$

and the equation for vapor pressure as a function of temperature from Ambrose and Sprake,[115]

$$\log_{10}(P/kNm^{-2}) = 7.20519 - 1581.993(T/°K-33.439).$$

From these data, Π/P at 25°C is 1.02638. If one were to assume that all of the nonideal behavior is due to dimer formation, the ideal pressure would be

$$\Pi = P(\text{monomer}) + 2K_2P^2(\text{monomer})$$

and the pressure would be

$$P = P(\text{monomer}) + K_2P^2(\text{monomer}).$$

P(monomer), then, is simply $2P-\Pi$, and the dimer equilibrium constant is

$$K_2 = (\Pi-P)/P^2(\text{monomer}).$$

At 25°C, Π is 130.472 torr and the vapor pressure of methanol is 127.119, therefore K_2 is 2.1892×10^{-4} torr^{-1}. The amount of association at the highest initial pressure of methanol would only be

$$K_2*(13.21)^2 = 0.038 \text{ torr}.$$

This is assuming all deviation is due to dimer formation, which is not the case for the alcohols.[42,96] Actally, this is an overestimation of the effect of neglecting methanol association. After ten increments of TFE, the partial pressure of methanol is about 12.84 torr. The amount of dimer at this pressure is

$$K_2*(12.84)^2 = 0.036 \text{ torr}.$$

By associating methanol with TFE, only about 0.002 torr of methanol dimer has dissociated. Since the amount of methanol self-association is so small and the amount of methanol dimer dissociation during the course of the experiment is negligible, the methanol vapor is treated ideally. Nonideal behavior in the TFE/methanol system is attributed to TFE self-association and the formation of TFE-methanol dimers, TFE(methanol)$_2$ trimers, and (TFE) methanol polymers. The values of the equilbrium constants are given in Table IV-2.

Liquid-vapor equilibrium data for TFE/methanol were collected over only half of the range of TFE mole fractions. Data could not be collected at pressures greater than the vapor pressure of TFE and so the region of liquid-vapor equilibrium between the vapor pressure of TFE (71.4 torr) and the vapor pressure of methanol (127.119 torr) (i.e. mole fraction of TFE is less than 0.5) was not studied.

A partial liquid-vapor equilibrium curve is given in figure IV-13. The twenty-two liquid-vapor data points were collected from four different experiments where the initial pressure of methanol was 5.35 torr, 10.812 torr, 16.281 torr, and 40.123 torr. The data and calculated liquid and vapor mole fractions are given in Table IV-19. The RMSD between experimental and calculated pressure is 0.39 torr and the results of fitting the data to 4-parameter Hansen-Miller equations are given in

Table IV-17. An azeotrope occurs at about 66.7 torr and $0.74\overline{X}$(TFE).

TABLE IV-18

TFE/METHANOL VAPOR DATA

AT 25.00 DEGREES CELSIUS

PRESSURE (P)	IDEAL PRESSURE (Π)	P(CALC)- P(EXP)
ALCOHOL PRESSURE = 2.647		
5.276	5.253	0.023
10.551	10.514	0.037
15.823	15.790	0.033
21.091	21.055	0.036
26.352	26.327	0.025
31.603	31.573	0.030
36.840	36.819	0.021
42.055	42.056	- 0.001
47.235	47.246	- 0.011
52.361	52.403	- 0.042
ALCOHOL PRESSURE = 5.214		
5.269	5.255	0.014
10.536	10.520	0.016
15.799	15.778	0.021
21.056	21.024	0.032
26.304	26.267	0.037
31.539	31.501	0.038
36.754	36.722	0.032
41.940	41.902	0.038
47.081	47.075	0.006
52.152	52.164	- 0.012
ALCOHOL PRESSURE = 7.94		
5.260	5.231	0.029
10.517	10.491	0.026
15.768	15.743	0.025
21.011	21.013	- 0.002
26.243	26.246	- 0.003
31.459	31.477	- 0.018
36.651	36.694	- 0.043
41.807	41.868	- 0.061

TABLE IV-18 cont.

TFE/METHANOL VAPOR DATA

AT 25.00 DEGREES CELSIUS

PRESSURE (P)	IDEAL PRESSURE (Π)	P(CALC)- P(EXP)
46.907	46.981	- 0.074
ALCOHOL PRESSURE = 10.57		
5.250	5.241	0.009
10.495	10.476	0.019
15.734	15.724	0.010
20.963	20.949	0.014
26.179	26.158	0.021
31.375	31.360	0.015
36.543	36.526	0.017
41.668	41.658	0.010
46.729	46.719	0.010
51.691	51.651	0.040
ALCOHOL PRESSURE = 13.21		
5.238	5.237	0.001
10.470	10.462	0.008
15.695	15.694	0.001
20.909	20.914	- 0.005
26.107	26.134	- 0.027
31.283	31.312	- 0.029
36.426	36.445	- 0.019
41.521	41.531	- 0.010
46.543	46.520	0.023
45.543	45.520	0.023

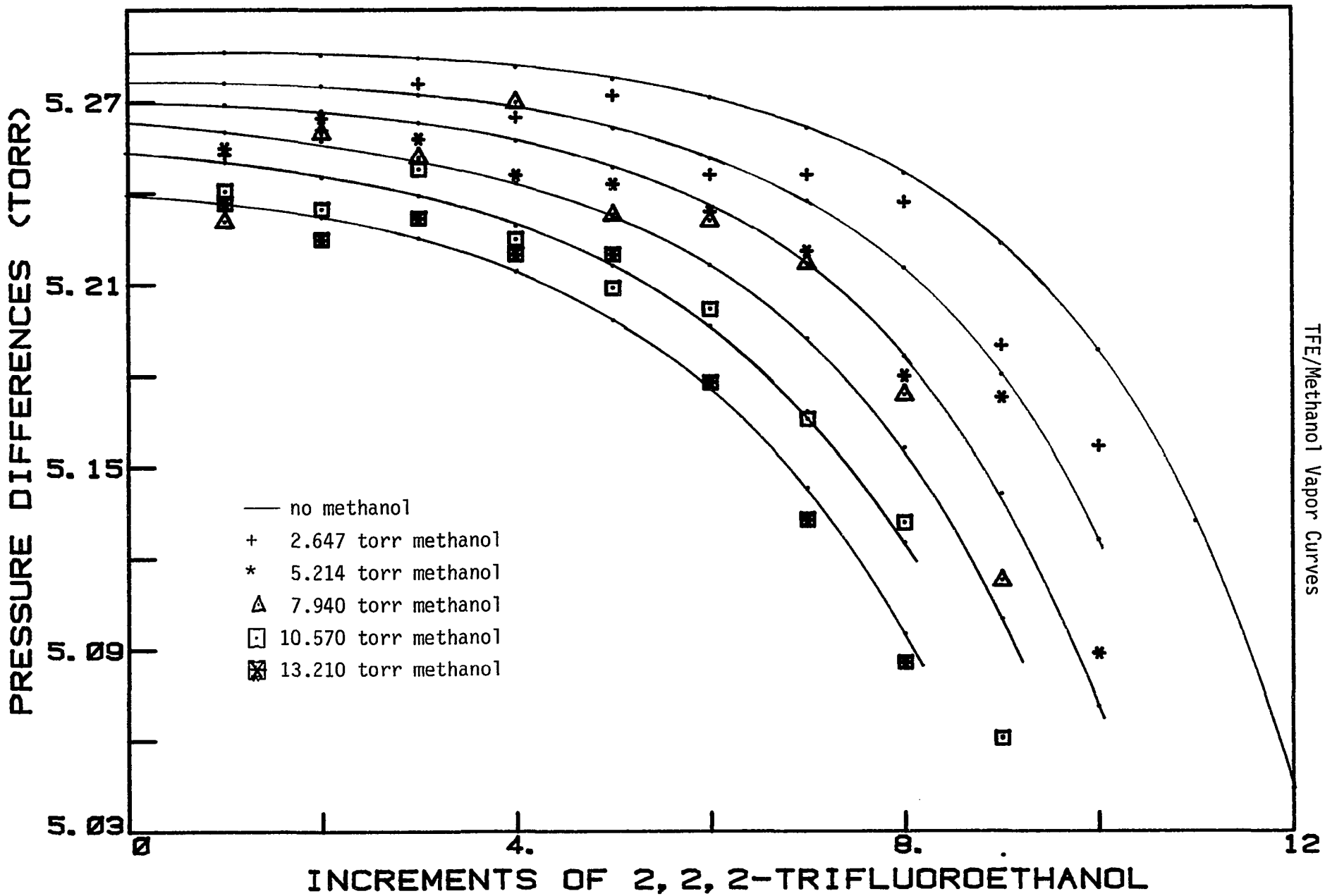

FIGURE IV-12

TFE/Methanol Vapor Curves

TABLE IV-19

TFE/METHANOL LIQUID-VAPOR DATA

AT 25.00 DEGREES CELSIUS

Π(TFE)	P(EXP)	PC	P(EXP)-PC	$\bar{X}$(TFE)	X^V(TFE)	X^L(TFE)
			Π(METHANOL) = 40.123 TORR			
47.574	68.560	68.705	0.145	0.542	0.528	0.604
74.004	67.459	67.018	- 0.441	0.648	0.636	0.667
89.862	66.630	66.677	0.047	0.691	0.685	0.698
111.006	66.481	66.591	0.110	0.734	0.736	0.733
121.578	66.459	66.636	0.178	0.752	0.757	0.748
132.150	66.439	66.714	0.275	0.767	0.775	0.762
142.722	66.541	66.813	0.273	0.781	0.791	0.774
153.294	66.497	66.925	0.429	0.793	0.805	0.786
163.866	66.642	67.044	0.402	0.803	0.818	0.796
174.438	66.730	67.166	0.436	0.813	0.829	0.805
185.010	67.111	67.288	0.177	0.822	0.839	0.814
211.440	67.396	67.583	0.186	0.840	0.860	0.833
237.870	67.668	67.854	0.185	0.856	0.876	0.849
			Π(METHANOL) = 5.351 TORR			
68.718	68.845	68.991	0.146	0.928	0.929	0.905
74.004	68.890	69.153	0.264	0.933	0.935	0.912
79.290	69.095	69.296	0.201	0.937	0.940	0.919
			Π(METHANOL) = 10.812 TORR			
68.718	68.467	67.705	- 0.762	0.864	0.867	0.840
79.290	68.817	68.038	- 0.778	0.880	0.886	0.859
			Π(METHANOL) = 16.281 TORR			
63.432	67.181	66.867	- 0.313	0.796	0.798	0.780
68.718	67.345	66.991	- 0.354	0.808	0.812	0.791
79.290	67.637	67.256	- 0.381	0.830	0.836	0.812
84.576	67.734	67.390	- 0.345	0.839	0.847	0.821

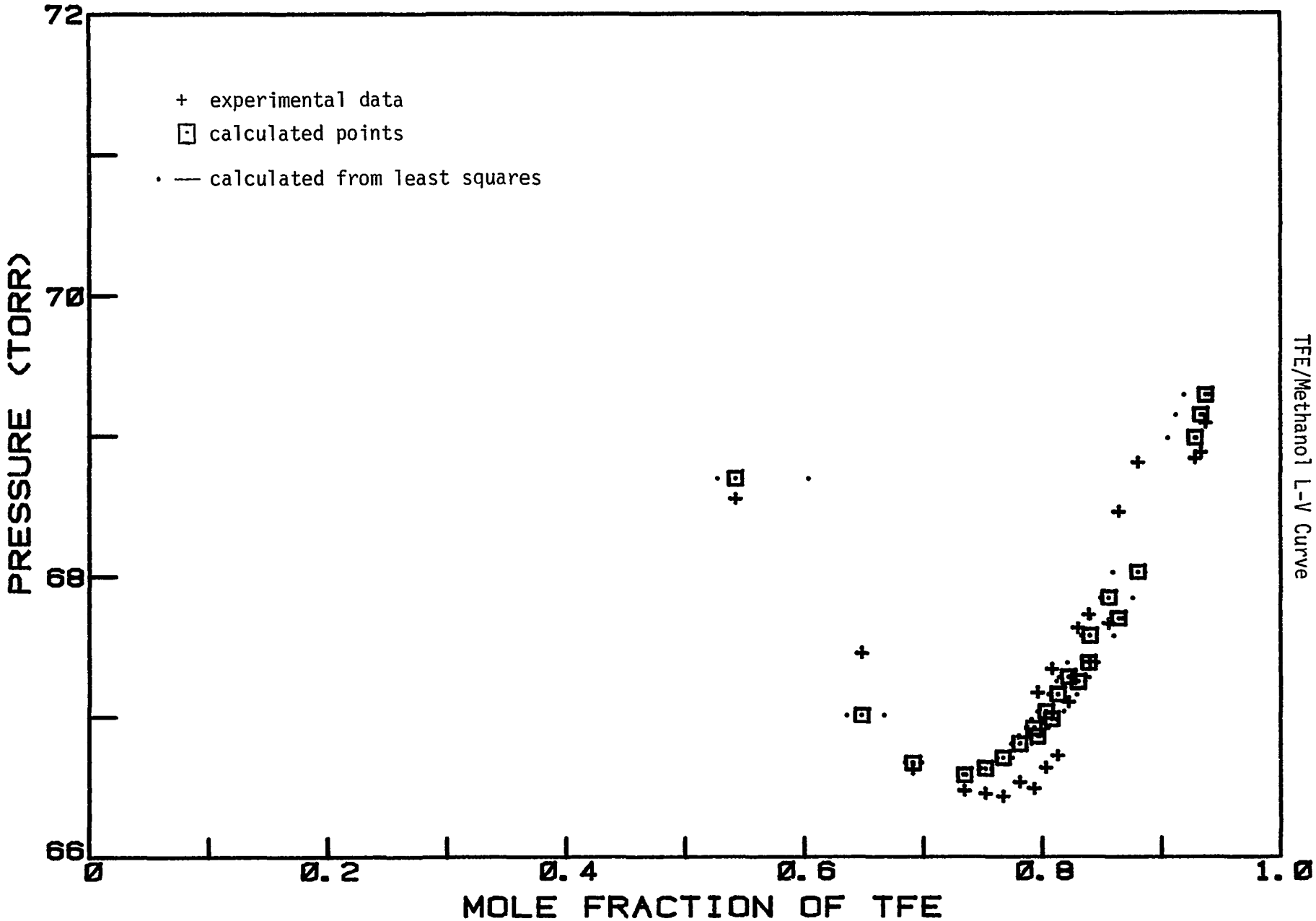

FIGURE IV-13

TFE/Methanol L-V Curve

viii-3. 2,2,2-Trifluoroethanol/Ethanol at 25° C

Vapor phase and liquid-vapor equilibrium data for the TFE/ethanol system were collected at 25.00 °C using the manually operated vapor density apparatus.

The eight sets of TFE/ethanol vapor phase data had initial ethanol pressures of 5.287 torr, 10.55 torr, 15.87 torr, 21.14 torr, 5.291 torr, 10.60 torr, 15.86 torr, and 21.15 torr. The fifty-two pressure-density data points from these eight sets were adjusted by the kink corrections and fit with a 3-parameter chemical association model. The parameters are an equilibrium constant for the formation of the TFE-ethanol dimer, an equilibrium constant for the formation of the TFE(ethanol)$_2$ trimer, and a stepwise equilibrium constant for the addition of TFE to a (TFE)$_n$ethanol polymer. The overall RMSD between experimental and calculated pressures is 0.023 torr. Table IV-2 gives the results of the NLLSQ fit.

Deviations from ideality were attributed to TFE self-association and TFE-ethanol heteroassociation. The ideal pressure:vapor pressure ratio for ethanol vapor was calculated using the equation for vapor pressure as a function of temperature[115]

$$\log_{10}(P/kNm^{-2}) = 7.24739 - 1599.039/(T/°K-46.391)$$

and the heat of vaporization at 25°C calculated from the equation[46]

$$\Delta H(\text{intJ/g}) = -0.004067(240-T/°C)^2 + 2.198(240-T/°C) + 165.83(240-T/°C)^{1/4}.$$

Π/P is 1.01344. The maximum self-association in ethanol at 25°C is only 1.3%. Using the same logic to calculate an equilibrium constant for the ethanol dimer, K_2, as was used in calculating the methanol dimer (see section V.2), K_2 for ethanol is $2.98X10^{-4}$. The maximum pressure of ethanol dimer in the vapor density experiments would be

$$2.98X10^{-4}*21.15^2 = 0.133 \text{ torr.}$$

After adding the final increments of TFE, the pressure of uncomplexed ethanol is 20.67. The dimer pressure is

$$2.98X10^{-4}*20.67^2 = 0.127 \text{ torr.}$$

Only 0.005 torr of ethanol dimer has dissociated, a negligible contribution to the total pressure. The effect of not including the association of ethanol is very small:

for the dimer: 0.0007 torr

for the TFE(ethanol)$_2$ trimer: $6X10^{-6}$ torr

for larger aggregates: 0.0002 torr.

The pressure of TFE for these calculations is 20.55 torr. The total contribution is no greater than 0.9 microns. Again, this is an overestimation of the amount of ethanol association.

Figure IV-14 is a graph of the pressure differences vs. TFE added for the first four sets of data in Table IV-20.

Forty-one liquid-vapor equilibrium data points were used from four sets of data. The initial pressures of ethanol were 10.657 torr, 15.526 torr, 10.65 torr, and 46.156 torr. The data are given in Table IV-21 along with the calculated liquid and vapor mole fractions. The data were fitted to a 4-parameter Hansen-Miller equation with an overall RMSD between the experimental and calculated pressures of 0.159 torr. Table IV-2 lists the values of the parameters. Figure IV-15 is the liquid-vapor equilibrium curve for TFE/ethanol. An azeotrope is observed at P=48.10 torr, $\bar{X}$(TFE)=0.41.

TABLE IV-20

TFE/ETHANOL VAPOR DATA

AT 25.00 DEGREES CELSIUS

PRESSURE (P)	IDEAL PRESSURE (Π)	P(CALC)- P(EXP)
ALCOHOL PRESSURE = 5.287		
5.260	5.262	- 0.002
10.516	10.520	- 0.004
15.766	15.770	- 0.004
21.008	21.019	- 0.011
26.238	26.260	- 0.022
31.451	31.472	- 0.021
36.639	36.668	- 0.029
41.791	41.810	- 0.019
46.888	46.914	- 0.026
51.902	51.903	- 0.001
ALCOHOL PRESSURE = 10.55		
5.228	5.225	0.003
10.449	10.447	0.002
15.660	15.670	- 0.010
20.858	20.869	- 0.011
26.037	26.037	0.000
31.190	31.175	0.015
36.305	36.266	0.039
ALCOHOL PRESSURE = 15.87		
5.185	5.192	- 0.007
10.361	10.394	- 0.033
15.524	15.559	- 0.035
20.669	20.687	- 0.018
25.789	25.767	0.022
ALCOHOL PRESSURE = 21.14		
5.133	5.160	- 0.027
10.255	10.289	- 0.034
15.361	15.370	- 0.009
20.446	20.406	0.040

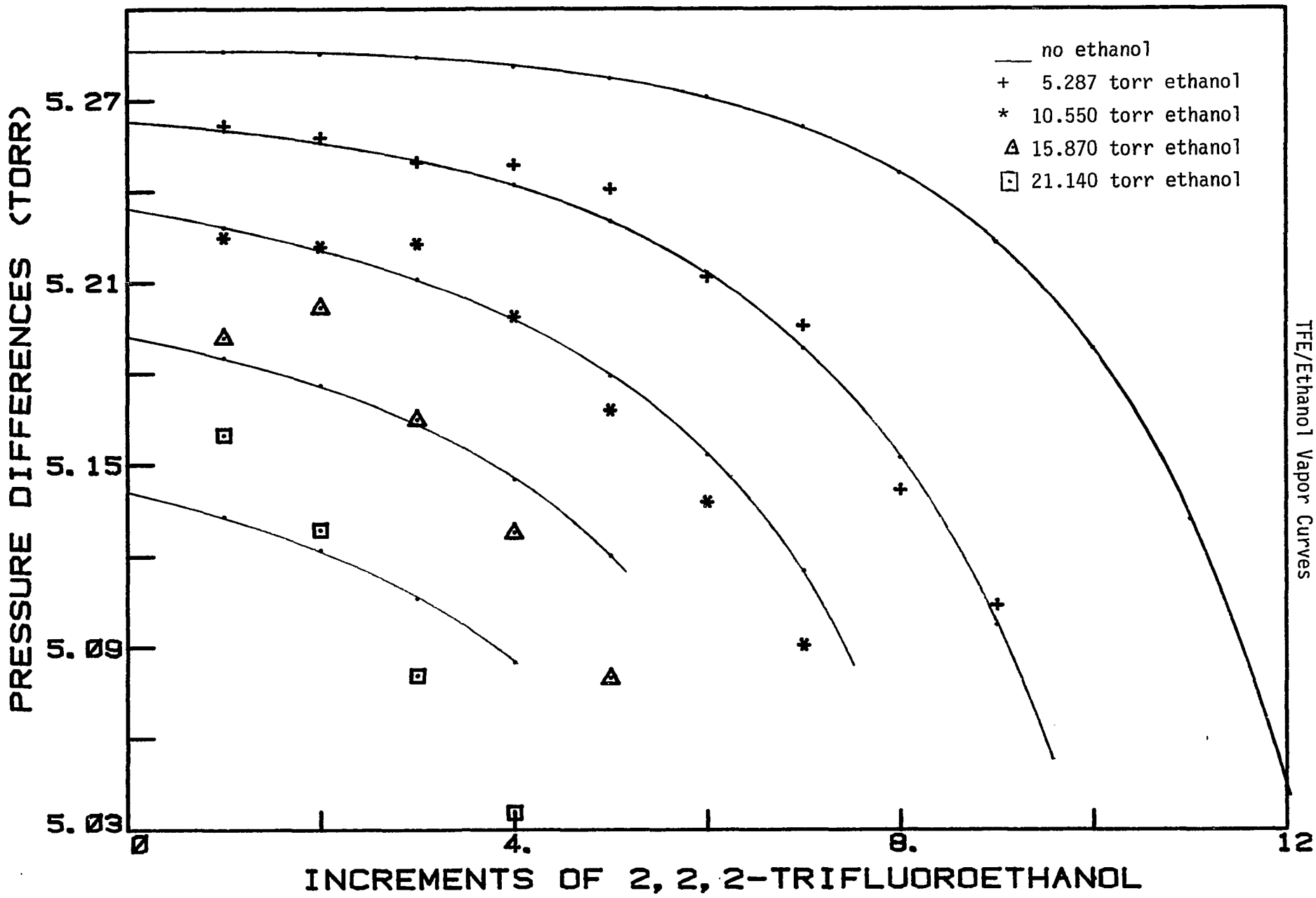

FIGURE IV-14

TFE/Ethanol Vapor Curves

TABLE IV-21

TFE/ETHANOL LIQUID-VAPOR DATA

AT 25.00 DEGREES CELSIUS

Π(TFE)	P(EXP)	PC	P(EXP)-PC	$\bar{X}$(TFE)	X^V(TFE)	X^L(TFE)
			Π(ETHANOL) = 46.156 TORR			
10.572	49.868	49.925	0.057	0.186	0.180	0.238
15.858	48.878	48.822	- 0.056	0.256	0.247	0.290
21.144	48.257	48.260	0.003	0.314	0.307	0.333
26.430	48.060	48.025	- 0.035	0.364	0.362	0.369
31.716	48.063	48.010	- 0.053	0.407	0.410	0.401
37.002	48.141	48.147	0.006	0.445	0.455	0.430
42.288	48.407	48.393	- 0.013	0.478	0.496	0.456
47.574	48.707	48.719	0.011	0.507	0.532	0.479
52.860	49.072	49.101	0.030	0.534	0.565	0.501
58.146	49.464	49.525	0.061	0.557	0.595	0.522
63.432	49.874	49.977	0.103	0.579	0.623	0.540
68.718	50.312	50.448	0.136	0.598	0.648	0.558
79.290	51.230	51.418	0.188	0.632	0.691	0.590
84.576	51.676	51.907	0.231	0.647	0.710	0.604
100.434	53.571	53.347	- 0.224	0.685	0.757	0.642
105.720	54.292	53.811	- 0.481	0.696	0.770	0.654
111.006	54.427	54.263	- 0.164	0.706	0.783	0.665
121.578	54.939	55.132	0.193	0.725	0.804	0.685
137.436	56.151	56.339	0.188	0.749	0.831	0.711
158.580	57.612	57.765	0.153	0.775	0.858	0.741
163.866	57.941	58.091	0.150	0.780	0.863	0.748
179.724	58.884	58.996	0.112	0.796	0.878	0.766
185.010	59.141	59.276	0.135	0.800	0.882	0.771
190.296	59.416	59.545	0.130	0.805	0.887	0.777
200.868	59.950	60.055	0.105	0.813	0.894	0.787
227.298	60.944	61.174	0.231	0.831	0.909	0.808
232.584	61.424	61.375	- 0.049	0.834	0.912	0.812
237.870	61.744	61.568	- 0.176	0.837	0.914	0.816
269.586	62.863	62.596	- 0.266	0.854	0.927	0.835
			Π(ETHANOL) = 10.657 TORR			
47.574	55.768	55.824	0.057	0.817	0.820	0.700
58.146	58.161	57.987	- 0.175	0.845	0.862	0.745
			Π(ETHANOL) = 15.526 TORR			
42.288	52.890	52.758	- 0.132	0.731	0.739	0.627
52.860	54.857	54.743	- 0.114	0.773	0.795	0.676

TABLE IV-21 cont.

TFE/ETHANOL LIQUID-VAPOR DATA

AT 25.00 DEGREES CELSIUS

Π(TFE)	P(EXP)	PC	P(EXP)-PC	$\overline{X}$(TFE)	X^V(TFE)	X^L(TFE)
		Π(ETHANOL) = 10.65 TORR				
47.574	55.733	55.828	0.095	0.817	0.820	0.700
52.860	57.056	56.945	- 0.111	0.832	0.843	0.724
58.146	58.240	57.991	- 0.250	0.845	0.862	0.746
74.004	60.679	60.659	- 0.020	0.874	0.902	0.798
84.576	62.043	62.056	0.013	0.888	0.920	0.825
95.148	63.188	63.193	0.005	0.899	0.933	0.847
105.720	64.165	64.116	- 0.049	0.908	0.943	0.864
116.292	64.962	64.869	- 0.093	0.916	0.951	0.879

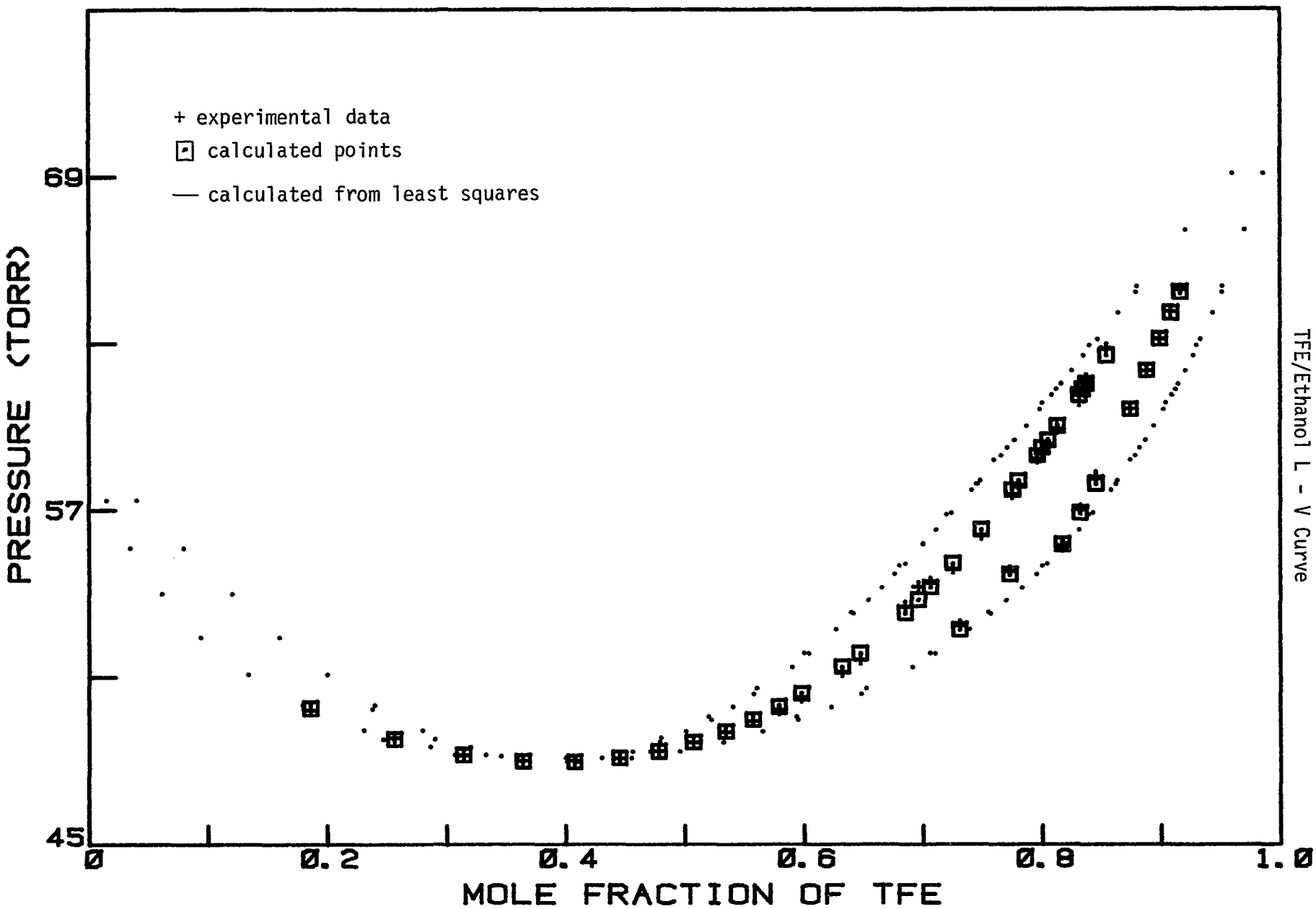

FIGURE IV-15
- 131 -
TFE/Ethanol L - V Curve

viii-4.2,2,2-Trifluoroethanol/2-Butanol at 25°C

Liquid-vapor equilibrium data and vapor density data were collected for TFE/2-butanol at 25.00°C on the manually operated vapor density apparatus.

Initial pressures of 2-butanol for the vapor density studies were 2.684 torr, 5.289 torr, 7.93 torr, 10.57 torr, and 13.21 torr. The twenty-three data points collected from the vapor density experiments are given in Table IV-22. These data are already adjusted by the kink corrections. The low vapor pressure of 2-butanol[50] (17.379 torr) limits the amount of vapor density data that may be collected with the vapor density apparatus. At a partial pressure of 13.2 torr 2-butanol, one quickly reaches the dew point of TFE/2-butanol after one or two increments of TFE.

The difference between pressure and ideal pressure is due to TFE self-association and TFE/2-butanol heteroassociation. Reliable data on the self-associaiton of 2-butanol vapor are not available in the literature. Only two to four data points could be measured before reaching the vapor pressure of 2-butanol using either of the vapor density apparatuses in this laboratory. J. D. Cox[98] measured compressibilities of 2-butanol vapor at various temperatures between 105°C and 166°C. The relationship between the second virial coefficient and temperature is

$$\log_{10}(-Bp) = 14.678 - 4.5\log_{10}(T°K).$$

Bp is the second virial coefficient in cm^3/mole. Since $-Bp=K_2$,[65] the equilibrium constant for the formation of the 2-butanol dimer at 25.00 °C is $9.2X10^{-3}torr^{-1}$. This value is calculated at a temperature 80° below the range of Cox's experimental conditions, so it is not surprising that it is much too high. A better estimate of the equilibrium constant would be to simply extrapolate from the equilibrium constants of water, methanol, and ethanol to find an approximation of K_2 for 2-butanol.

K_2 from Keyes Point

water	$1.923X10^{-4}$ $torr^{-1}$
methanol	$2.189X10^{-4}$ $torr^{-1}$
ethanol	$2.980X10^{-4}$ $torr^{-1}$

K_2 extrapolated from above values

2-butanol	$4X10^{-4}$ $torr^{-1}$

Using this value of K_2, the amount of dimer in 13.21 torr 2-butanol is 0.07 torr. Therefore, the error in neglecting the nonideal behavior of 2-butanol, following the same logic used in TFE/methanol and TFE/ethanol vapor analysis, in the vapor density studies of TFE/2-butanol is too small to affect the results of the data analysis.

Figure IV-16 is a graph of the incremental pressure differences as TFE is added. The association model includes a term for the formation of a TFE/2-butanol dimer, $(TFE)_n$2-butanol

polymer, and a TFE(2-butanol)$_2$ trimer. Values of the three equilibrium constants are given in Table IV-2.

Liquid-vapor equilibrium pressures were measured at thirty-six different mole fractions of TFE. The starting ideal pressures of 2-butanol for the five sets of data were 2.728 torr, 5.274 torr, 7.992 torr, 10.565 torr, and 46.867 torr. The liquid-vapor equilibrium data and calculated liquid and vapor mole fractions are presented in Table IV-22. The results of fitting the data to the Hansen-Miller equations are given in Table IV-17. The overall RMSD between experimental and calculated pressures is 0.068 torr. The liquid-vapor equilibrium curve may be seen in figure IV-17. No azeotrope is observed.

TABLE IV-22

TFE/2-BUTANOL VAPOR DATA

AT 25.00 DEGREES CELSIUS

PRESSURE (P)	IDEAL PRESSURE (Π)	P(CALC)- P(EXP)
ALCOHOL PRESSURE = 2.684		
5.260	5.268	- 0.008
10.516	10.513	0.003
15.766	15.773	- 0.007
21.008	21.010	- 0.002
26.237	26.250	- 0.013
31.447	31.456	- 0.009
36.629	36.643	- 0.014
41.766	41.775	- 0.009
46.830	46.837	- 0.007
ALCOHOL PRESSURE = 5.289		
5.225	5.236	- 0.011
10.444	10.470	- 0.026
15.654	15.686	- 0.032
20.851	20.869	- 0.018
26.029	26.020	0.009
31.178	31.124	0.054
ALCOHOL PRESSURE = 7.93		
5.176	5.202	- 0.026
10.345	10.394	- 0.049
15.504	15.522	- 0.018
ALCOHOL PRESSURE = 10.57		
5.115	5.140	- 0.025
10.224	10.231	- 0.007
15.322	15.263	0.059
14.322	14.263	0.059

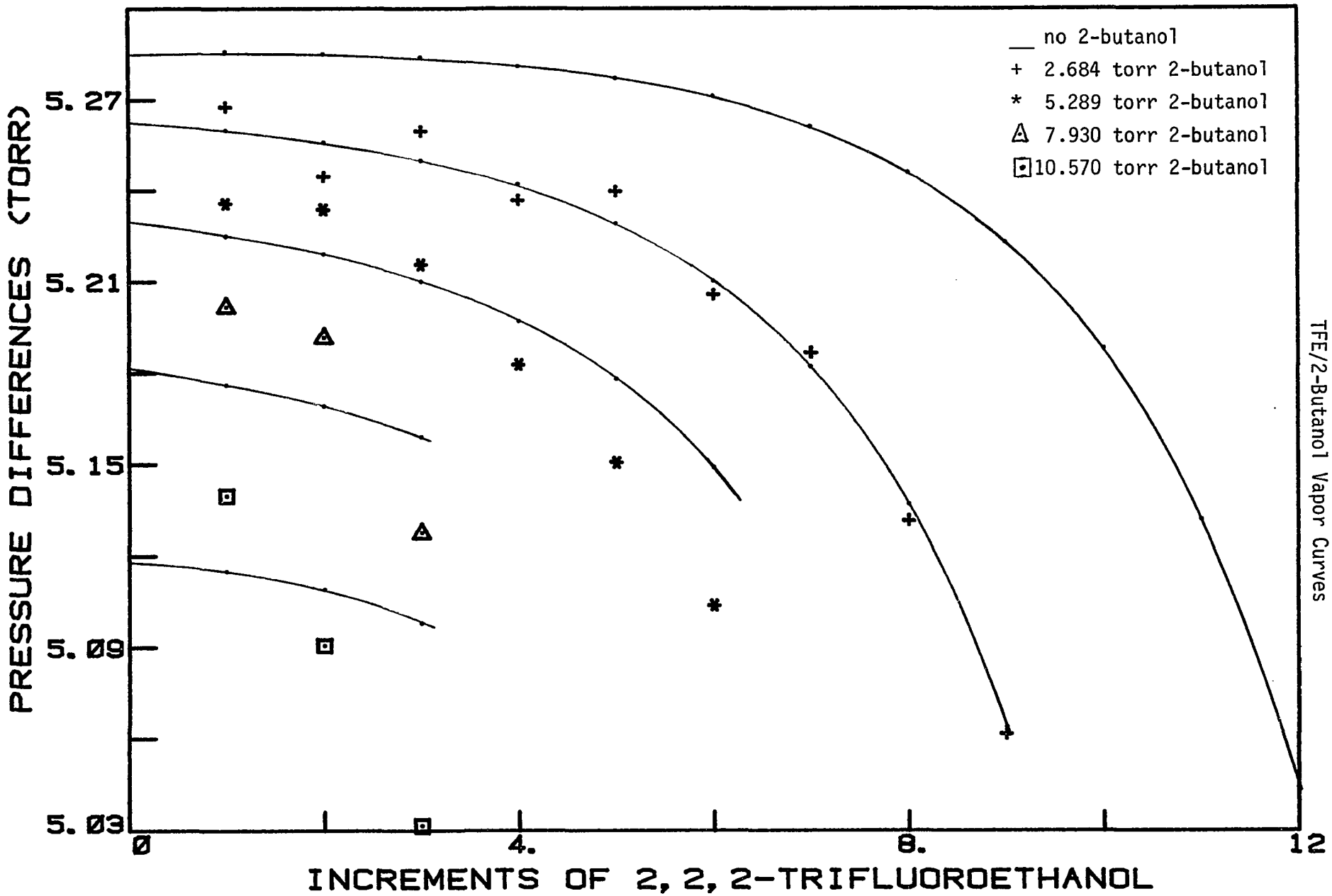

FIGURE IV-16
- 136 -
TFE/2-Butanol Vapor Curves

TABLE IV-23

TFE/2-BUTANOL LIQUID-VAPOR DATA

AT 25.00 DEGREES CELSIUS

Π(TFE)	P(EXP)	PC	P(EXP)-PC	$\bar{X}$(TFE)	X^V(TFE)	X^L(TFE)
			Π(2-BUTANOL) = 46.867 TORR			
5.286	19.233	19.180	- 0.053	0.093	0.127	0.076
10.572	20.282	20.272	- 0.009	0.170	0.236	0.138
15.858	21.412	21.445	0.033	0.236	0.329	0.190
26.430	23.898	23.941	0.043	0.339	0.478	0.275
42.288	27.908	27.869	- 0.038	0.451	0.631	0.372
63.432	33.073	33.020	- 0.053	0.552	0.756	0.467
89.862	38.873	38.863	- 0.010	0.636	0.842	0.555
111.006	42.859	42.890	0.031	0.683	0.882	0.610
148.008	48.480	48.526	0.046	0.742	0.923	0.683
179.724	52.198	52.135	- 0.063	0.777	0.942	0.728
206.154	54.518	54.480	- 0.039	0.800	0.952	0.759
243.156	56.987	57.015	0.028	0.825	0.962	0.792
280.158	58.826	58.924	0.099	0.845	0.968	0.818
301.302	59.871	59.811	- 0.060	0.854	0.971	0.830
327.732	60.806	60.758	- 0.048	0.864	0.974	0.843
343.590	61.177	61.256	0.079	0.870	0.975	0.850
			Π(2-BUTANOL) = 10.565 TORR			
47.574	43.071	43.155	0.084	0.818	0.884	0.614
52.860	45.408	45.541	0.134	0.833	0.903	0.644
63.432	49.809	49.833	0.023	0.857	0.930	0.699
68.718	51.716	51.717	0.001	0.867	0.940	0.723
84.576	56.348	56.322	- 0.027	0.889	0.959	0.783
			Π(2-BUTANOL) = 2.728 TORR			
58.146	57.281	57.239	- 0.041	0.955	0.963	0.795
63.432	59.762	59.663	- 0.099	0.959	0.971	0.828
74.004	63.136	63.256	0.120	0.964	0.981	0.879
			Π(2-BUTANOL) = 7.992 TORR			
52.860	47.806	47.777	- 0.029	0.869	0.918	0.673
58.146	50.195	50.131	- 0.064	0.879	0.932	0.703
74.004	55.802	55.931	0.129	0.903	0.958	0.778
84.576	58.706	58.755	0.048	0.914	0.968	0.815

TABLE IV-23 cont.

TFE/2-BUTANOL LIQUID-VAPOR DATA

AT 25.00 DEGREES CELSIUS

Π(TFE)	P(EXP)	PC	P(EXP)-PC	$\overline{X}$(TFE)	X^V(TFE)	X^L(TFE)
			Π(2-BUTANOL) = 5.274 TORR			
52.860	50.710	50.714	0.003	0.909	0.935	0.710
58.146	53.297	53.244	- 0.053	0.917	0.947	0.743
63.432	55.561	55.507	- 0.054	0.923	0.956	0.772
68.718	57.531	57.487	- 0.044	0.929	0.963	0.798
74.004	59.240	59.185	- 0.055	0.933	0.969	0.821
84.576	61.892	61.823	- 0.069	0.941	0.977	0.858
95.148	63.618	63.664	0.045	0.948	0.982	0.885
111.006	65.547	65.465	- 0.082	0.955	0.987	0.912

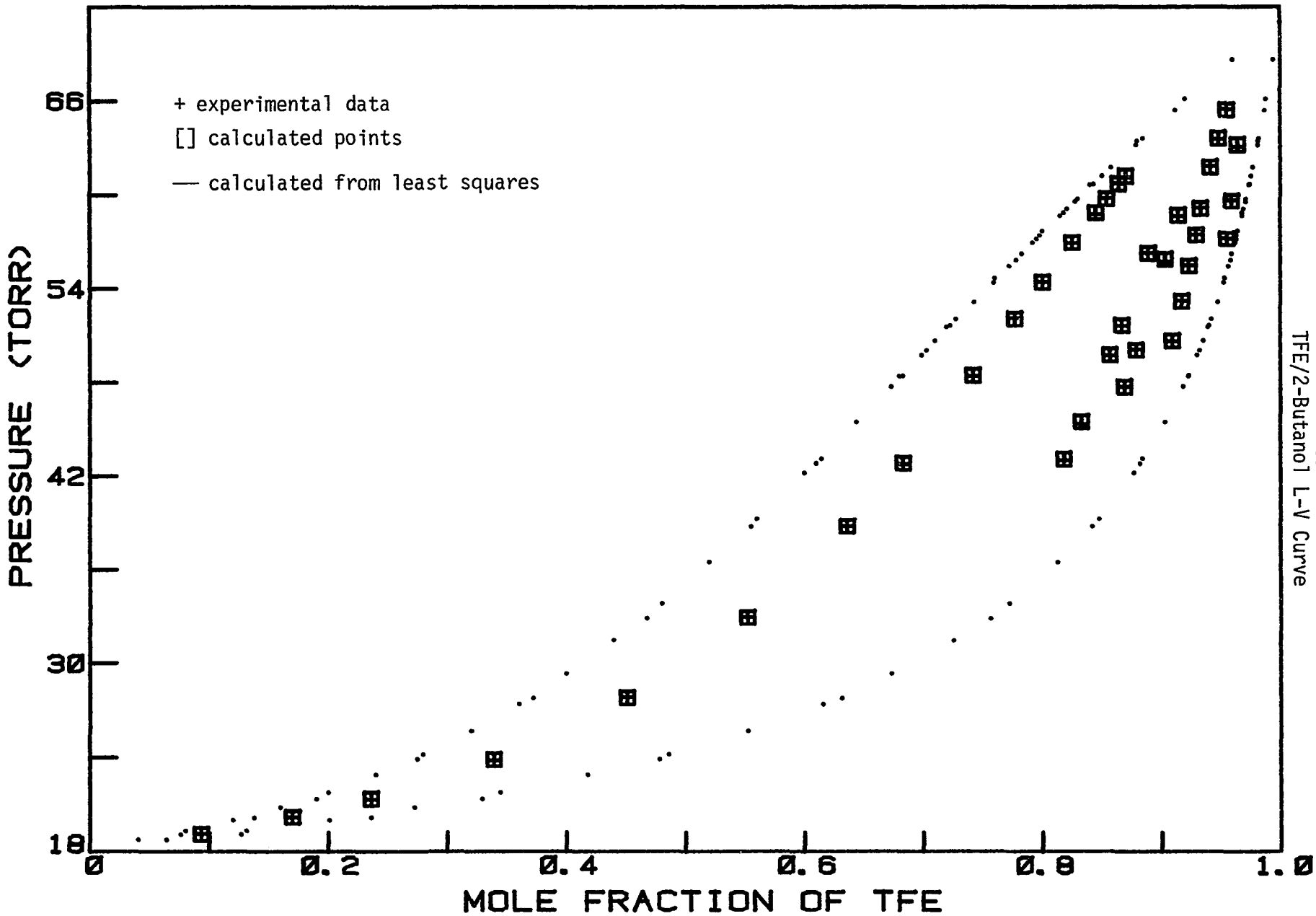

FIGURE IV-17

TFE/2-Butanol L-V Curve

viii-5. Acetone/Water

Vapor density data for acetone/water were collected at various temperatures between 15°C and 45°C using the automated vapor density apparatus. The data are presented in Tables IV-24 through IV-30. Graphs of the pressure differences vs. increments of acetone added at each temperature are presented in figures IV-18 through IV-24.

The data are quite unsatisfactory. In many acetone/water experiments, the pressure differences between consecutive additions of acetone increments are larger than the pressure differences in the corresponding sets of pure acetone data. This suggests that the water vapor was desorbing from the stainless steel walls of the sample cylinder as acetone was added to the system.

One difficulty in studying this system was introduction of the correct amount of water vapor to the sample cylinder. An excess amount of water vapor was introduced to the cylinder and then pumped out. After this was repeated several times to flush the system, the water vapor was pumped down to a predetermined pressure. The large amount of 1/16" tubing between the sample cylinder and pump and the large heat of vaporization of water made evacuation of the system very slow. Once an increment of acetone was added to the system, the very slow degassing of water

vapor was enhanced by displacement of adsorbed water molecules by acetone molecules.

No attempts were made to fit the data to an association model.

TABLE IV-24

ACETONE/WATER VAPOR DENSITY DATA

AT 15.04 DEGREES CELSIUS

# OF INC.	Π(WATER)	PRESSURE	PRESS. DIF.
1	6.120	16.432	10.312
2	6.120	26.672	10.240
3	6.120	36.870	10.198
4	6.120	47.033	10.163
5	6.120	57.154	10.121
6	6.120	67.240	10.086
7	6.120	77.275	10.035
8	6.120	87.253	9.978
9	6.120	97.158	9.905
1	8.774	19.086	10.312
2	8.774	29.322	10.236
3	8.774	39.523	10.201
4	8.774	49.682	10.159
5	8.774	59.796	10.114
6	8.774	69.879	10.083
7	8.774	79.914	10.035
8	8.774	89.889	9.975

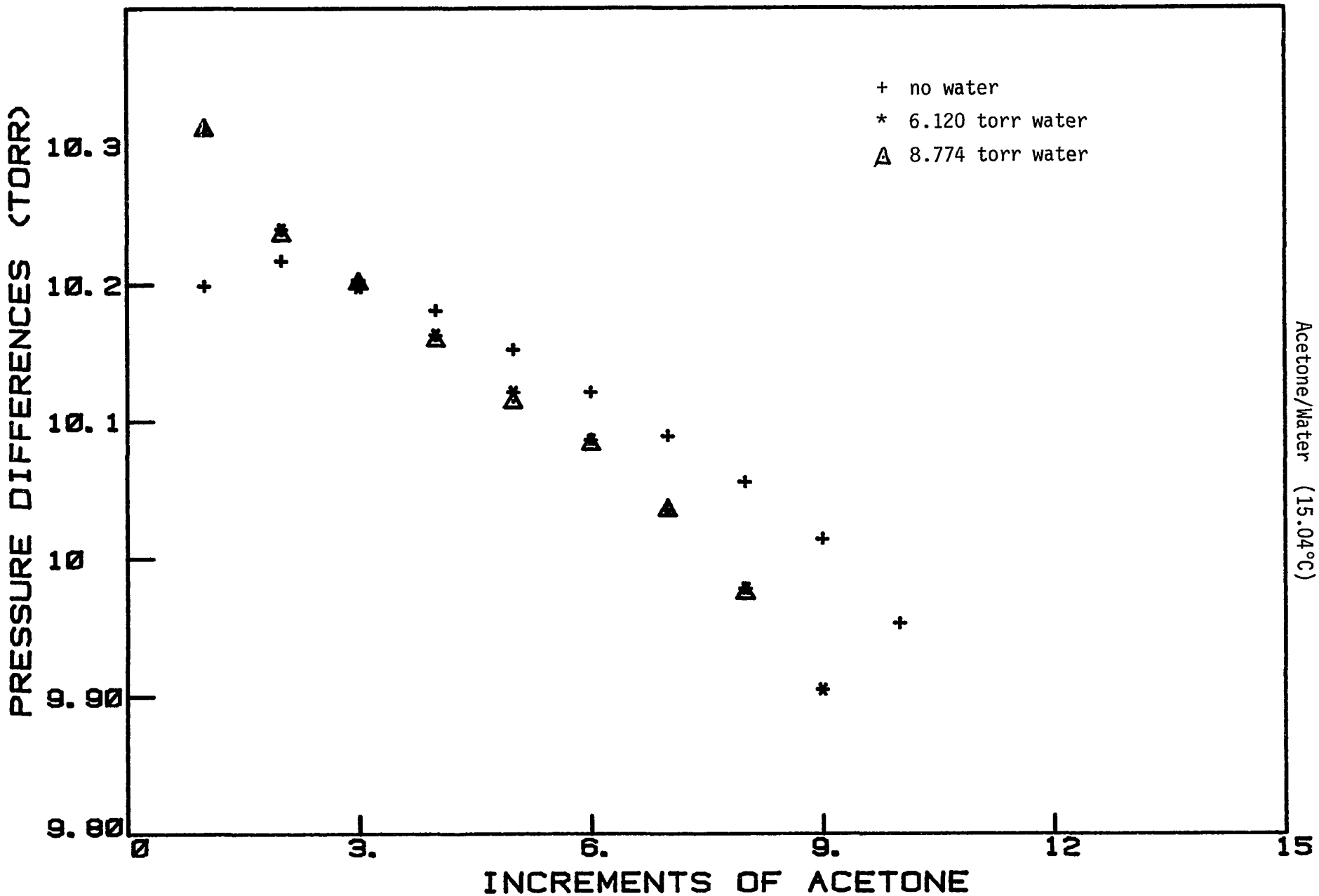

FIGURE IV-18

Acetone/Water (15.04°C)

TABLE IV-25

ACETONE/WATER VAPOR DENSITY DATA

AT 20.21 DEGREES CELSIUS

# OF INC.	Π(WATER)	PRESSURE	PRESS. DIF.
1	14.420	24.989	10.569
2	14.420	35.701	10.712
3	14.420	46.314	10.613
4	14.420	56.733	10.419
5	14.420	67.045	10.312
6	14.420	77.173	10.128
7	14.420	87.112	9.939
1	9.297	19.809	10.512
2	9.297	30.240	10.431
3	9.297	40.631	10.391
4	9.297	50.992	10.361
5	9.297	61.310	10.318
6	9.297	71.598	10.288
7	9.297	81.843	10.245
8	9.297	92.049	10.206
9	9.297	102.210	10.161
10	9.297	112.306	10.096
11	9.297	122.308	10.002
12	9.297	132.192	9.884

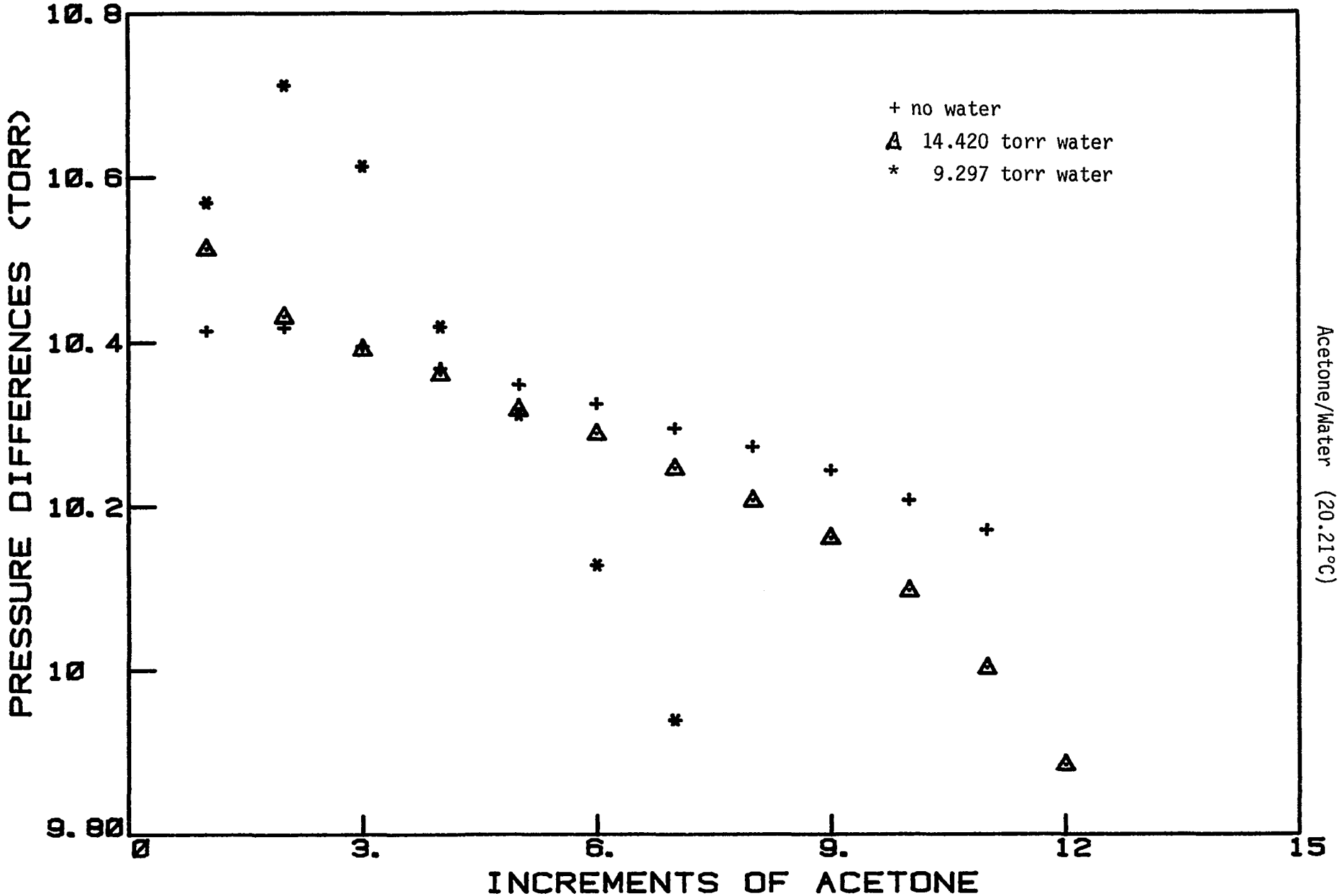

FIGURE IV-19

Acetone/Water (20.21°C)

TABLE IV-26

ACETONE/WATER VAPOR DENSITY DATA

AT 24.39 DEGREES CELSIUS

# OF INC.	π(WATER)	PRESSURE	PRESS. DIF.
1	10.059	20.803	10.744
2	10.059	31.464	10.661
3	10.059	42.080	10.616
4	10.059	52.661	10.581
5	10.059	63.217	10.556
6	10.059	73.742	10.525
7	10.059	84.235	10.493
8	10.059	94.703	10.468
9	10.059	105.120	10.417
10	10.059	115.506	10.386
11	10.059	125.855	10.349
12	10.059	136.154	10.299
13	10.059	146.406	10.252
14	10.059	156.583	10.177
15	10.059	166.663	10.080
16	10.059	176.574	9.911
1	14.948	25.615	10.667
2	14.948	36.184	10.569
3	14.948	46.702	10.518
4	14.948	57.185	10.483
5	14.948	67.624	10.439
6	14.948	78.026	10.402
7	14.948	88.371	10.345
8	14.948	98.670	10.299
9	14.948	108.922	10.252
10	14.948	119.109	10.187
11	14.948	129.211	10.102
12	14.948	139.223	10.012
1	5.103	15.816	10.713
2	5.103	26.420	10.604
3	5.103	37.019	10.599

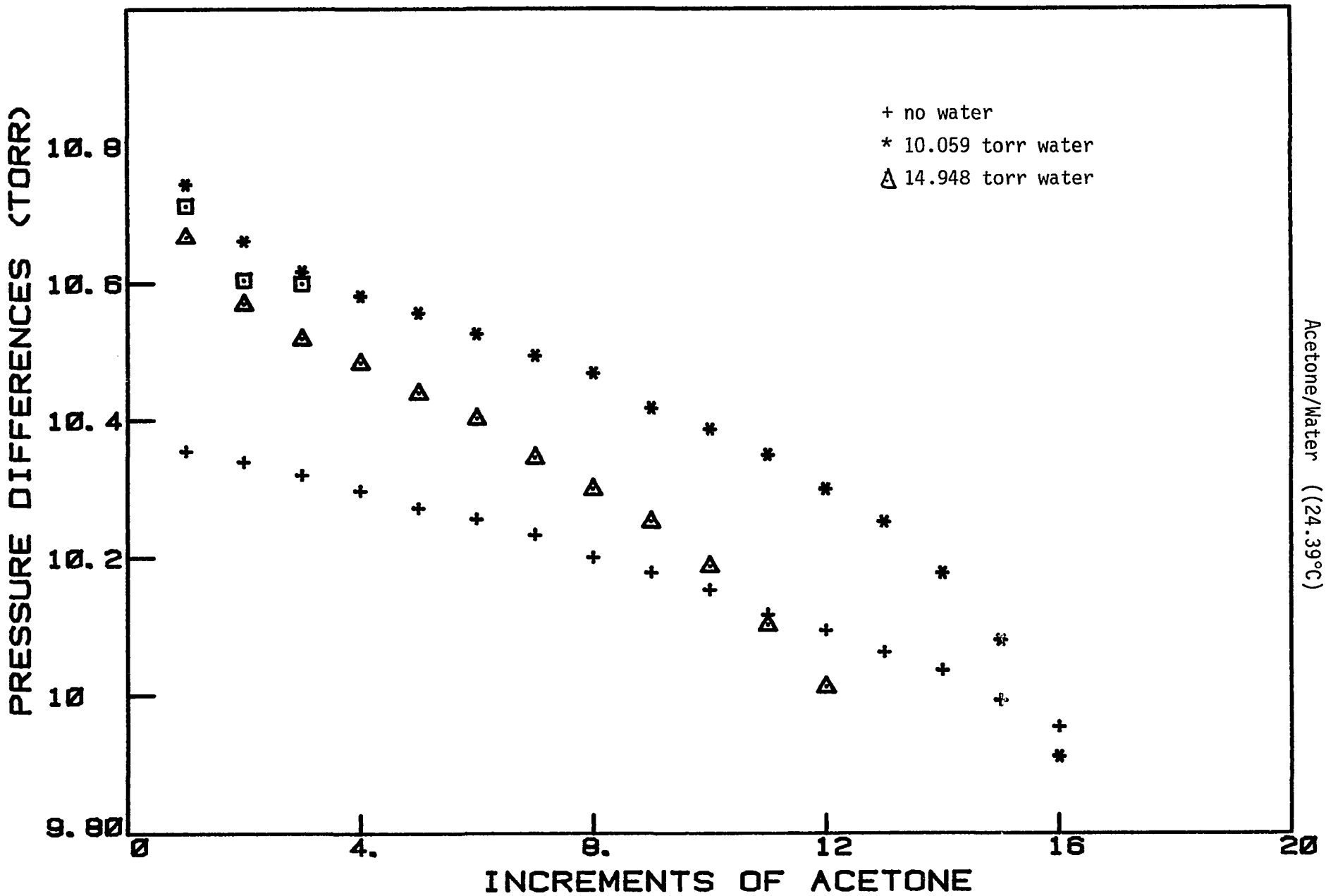

FIGURE IV-20

Acetone/Water ((24.39°C)

TABLE IV-27

ACETONE/WATER VAPOR DENSITY DATA

AT 30.00 DEGREES CELSIUS

# OF INC.	Π(WATER)	PRESSURE	PRESS. DIF.
1	5.009	15.598	10.589
2	5.009	26.126	10.528
3	5.009	36.626	10.500
4	5.009	47.099	10.473
5	5.009	57.551	10.452
6	5.009	67.979	10.428
7	5.009	78.383	10.404
8	5.009	88.763	10.380
9	5.009	99.103	10.340
10	5.009	109.419	10.316
11	5.009	119.720	10.301
12	5.009	129.997	10.277
13	5.009	140.254	10.257
14	5.009	150.468	10.214
15	5.009	160.677	10.209
1	9.978	20.578	10.600
2	9.978	31.110	10.532
3	9.978	41.608	10.498
4	9.978	52.075	10.467
5	9.978	62.518	10.443
6	9.978	72.933	10.415
7	9.978	83.331	10.398
8	9.978	93.698	10.367
9	9.978	104.041	10.343
10	9.978	114.350	10.309
11	9.978	124.645	10.295
12	9.978	134.913	10.268
13	9.978	145.154	10.241
14	9.978	155.364	10.210
15	9.978	165.560	10.196
16	9.978	175.726	10.166
17	9.978	185.865	10.139

TABLE IV-27 cont.

ACETONE/WATER VAPOR DENSITY DATA

AT 30.00 DEGREES CELSIUS

# OF INC.	π(WATER)	PRESSURE	PRESS. DIF.
1	14.447	25.073	10.626
2	14.447	35.624	10.551
3	14.447	46.154	10.530
4	14.447	56.597	10.443
5	14.447	67.068	10.471
6	14.447	77.482	10.414
7	14.447	87.911	10.429
8	14.447	98.251	10.340
9	14.447	108.628	10.377
10	14.447	118.978	10.350
11	14.447	129.310	10.332
12	14.447	139.605	10.295
13	14.447	149.866	10.261
14	14.447	160.122	10.256
15	14.447	170.347	10.225
16	14.447	180.545	10.198
17	14.447	190.716	10.171
18	14.447	200.856	10.140
19	14.447	210.960	10.104
20	14.447	221.040	10.080
1	18.592	29.229	10.637
2	18.592	39.791	10.562
3	18.592	50.315	10.524
4	18.592	60.808	10.493
5	18.592	71.273	10.465
6	18.592	81.717	10.444
7	18.592	91.986	10.269
8	18.592	102.378	10.392
9	18.592	112.626	10.248
10	18.592	122.963	10.337
11	18.592	133.270	10.307
12	18.592	143.565	10.295
13	18.592	153.830	10.265
14	18.592	164.067	10.237
15	18.592	174.274	10.207
16	18.592	184.460	10.186
17	18.592	194.622	10.162
18	18.592	204.741	10.119

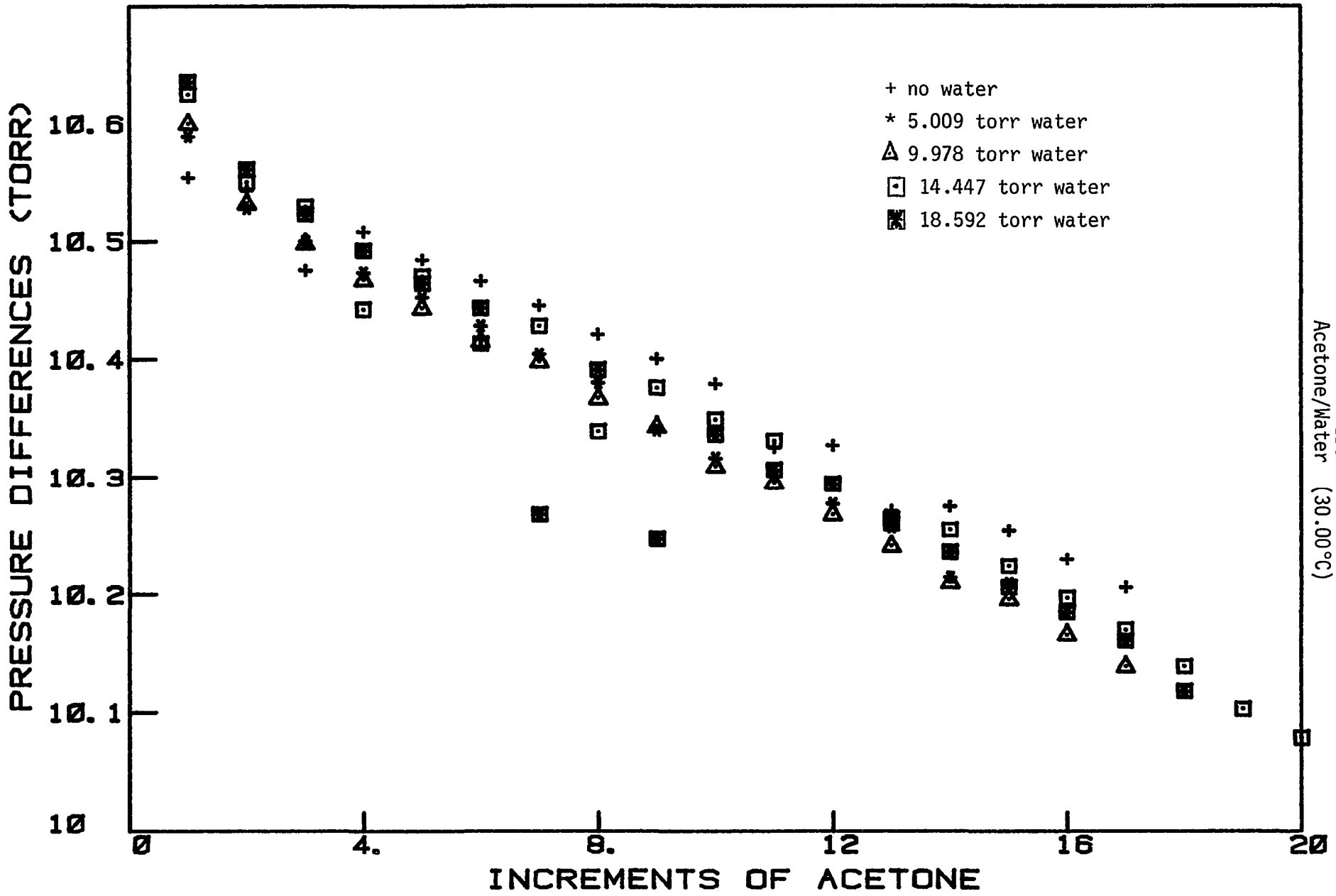

FIGURE IV-21

Acetone/Water (30.00°C)

TABLE IV-28

ACETONE/WATER VAPOR DENSITY DATA

AT 36.15 DEGREES CELSIUS

# OF INC.	Π(WATER)	PRESSURE	PRESS. DIF.
1	9.637	20.480	10.843
2	9.637	31.253	10.773
3	9.637	42.003	10.750
4	9.637	52.724	10.721
5	9.637	63.422	10.698
6	9.637	74.081	10.659
7	9.637	84.730	10.649
8	9.637	95.359	10.629
9	9.637	105.959	10.600
10	9.637	116.495	10.536
11	9.637	127.050	10.555
12	9.637	137.585	10.535
13	9.637	148.069	10.484
14	9.637	158.508	10.439
15	9.637	168.867	10.359
16	9.637	179.302	10.435
17	9.637	189.727	10.425
18	9.637	200.122	10.395
19	9.637	210.504	10.382
20	9.637	220.847	10.343
21	9.637	231.180	10.333
22	9.637	241.487	10.307
23	9.637	251.764	10.277
24	9.637	262.025	10.261
25	9.637	272.257	10.232
26	9.637	282.426	10.169
27	9.637	292.566	10.140
28	9.637	302.669	10.103
1	5.039	15.874	10.835
2	5.039	26.652	10.778
3	5.039	37.297	10.645
4	5.039	48.020	10.723
5	5.039	58.730	10.710
6	5.039	69.414	10.684
7	5.039	80.079	10.665
8	5.039	90.717	10.638
9	5.039	101.290	10.573
10	5.039	111.886	10.596
11	5.039	122.459	10.573

TABLE IV-28 cont.

ACETONE/WATER VAPOR DENSITY DATA

AT 36.15 DEGREES CELSIUS

# OF INC.	Π(WATER)	PRESSURE	PRESS. DIF.
12	5.039	133.003	10.544
13	5.039	143.524	10.521
14	5.039	154.025	10.501
15	5.039	164.503	10.478
16	5.039	174.955	10.452
17	5.039	185.381	10.426
18	5.039	195.797	10.416
19	5.039	206.183	10.386
20	5.039	216.550	10.367
21	5.039	226.844	10.294
22	5.039	237.097	10.253
23	5.039	247.407	10.310
24	5.039	257.679	10.272
25	5.039	267.891	10.212
26	5.039	278.093	10.202
27	5.039	288.281	10.188
28	5.039	298.413	10.132
1	14.931	25.797	10.866
2	14.931	36.539	10.742
3	14.931	47.252	10.713
4	14.931	57.965	10.713
5	14.931	68.655	10.690
6	14.931	79.309	10.654
7	14.931	89.842	10.533
8	14.931	100.464	10.622
9	14.931	111.057	10.593
10	14.931	121.624	10.567
11	14.931	132.174	10.550
12	14.931	142.689	10.515

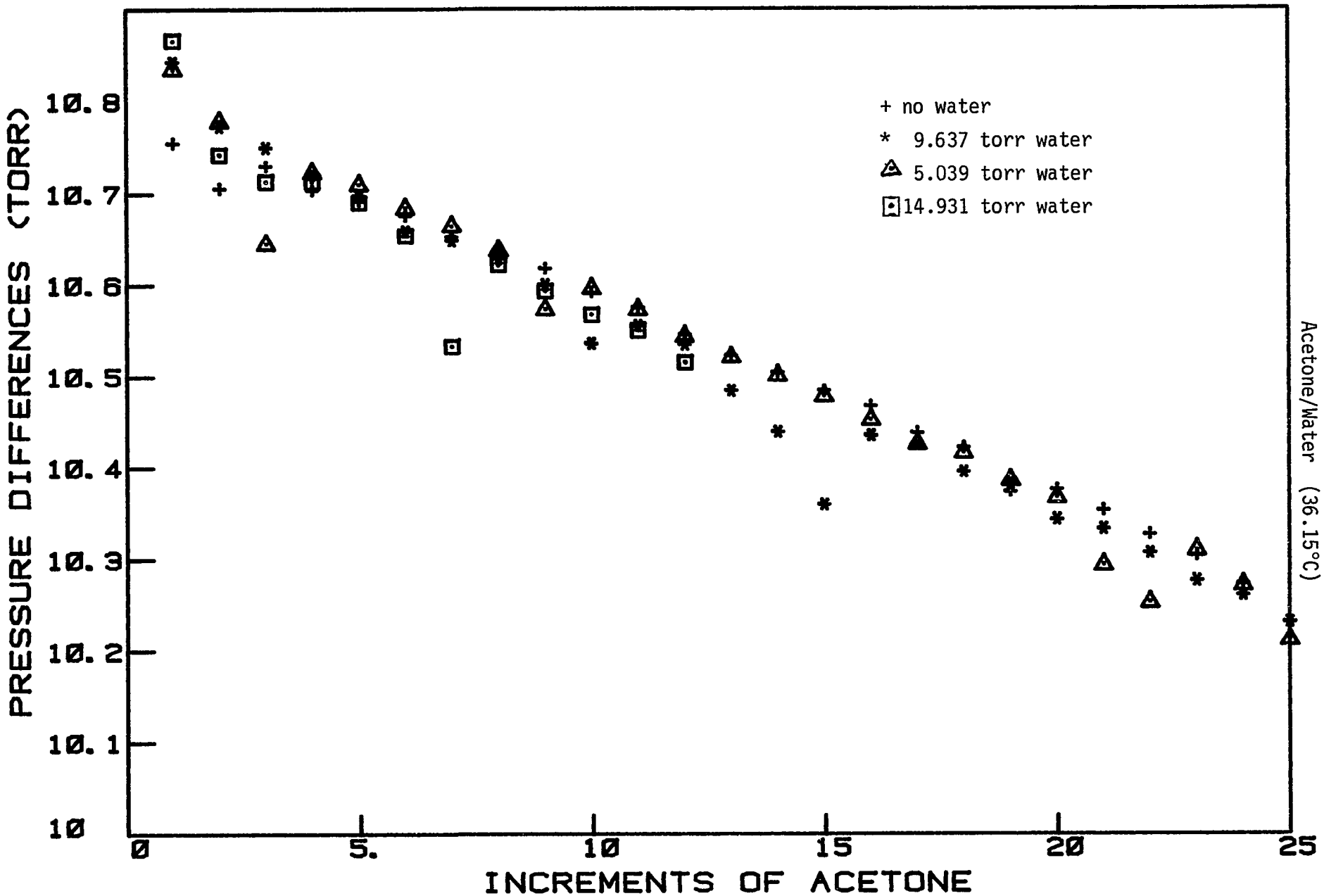

FIGURE IV-22

Acetone/Water (36.15°C)

TABLE IV-29

ACETONE/WATER VAPOR DENSITY DATA

AT 40.79 DEGREES CELSIUS

# OF INC.	Π(WATER)	PRESSURE	PRESS. DIF.
1	4.941	15.857	10.916
2	4.941	26.736	10.879
3	4.941	37.508	10.772
4	4.941	48.340	10.832
5	4.941	59.128	10.788
6	4.941	69.863	10.735
7	4.941	80.480	10.617
8	4.941	91.107	10.627
9	4.941	101.688	10.581
10	4.941	112.237	10.549
11	4.941	122.915	10.678
12	4.941	133.566	10.651
13	4.941	144.184	10.618
14	4.941	154.778	10.594
15	4.941	165.311	10.533
16	4.941	175.830	10.519
17	4.941	186.366	10.536
18	4.941	196.838	10.472
19	4.941	207.311	10.473
20	4.941	217.732	10.421
21	4.941	228.139	10.407
22	4.941	238.501	10.362
1	17.610	28.619	11.009
2	17.610	39.513	10.894
3	17.610	50.387	10.874
4	17.610	61.233	10.846
5	17.610	72.046	10.813
6	17.610	82.844	10.798
7	17.610	93.622	10.778
8	17.610	104.372	10.750
9	17.610	115.105	10.733
10	17.610	125.807	10.702
11	17.610	136.501	10.694
12	17.610	147.162	10.661
13	17.610	157.811	10.649
14	17.610	168.430	10.619
15	17.610	179.037	10.607
16	17.610	189.614	10.577
17	17.610	200.176	10.562

TABLE IV-29 cont.

ACETONE/WATER VAPOR DENSITY DATA

AT 40.79 DEGREES CELSIUS

# OF INC.	Π(WATER)	PRESSURE	PRESS. DIF.
18	17.610	210.576	10.400
19	17.610	220.931	10.355
20	17.610	231.285	10.354
21	17.610	241.640	10.355
22	17.610	251.960	10.320
1	9.897	20.870	10.973
2	9.897	31.772	10.902
3	9.897	42.437	10.665
4	9.897	53.083	10.646
5	9.897	63.899	10.816
6	9.897	74.681	10.782
7	9.897	85.459	10.778
8	9.897	96.174	10.715
9	9.897	106.917	10.743
10	9.897	117.627	10.710
11	9.897	128.332	10.705
12	9.897	138.965	10.633
13	9.897	149.625	10.660
14	9.897	160.217	10.592
15	9.897	170.674	10.457
16	9.897	181.199	10.525
17	9.897	191.647	10.448
18	9.897	202.022	10.375
1	14.244	25.196	10.952
2	14.244	36.101	10.905
3	14.244	46.972	10.871
4	14.244	57.822	10.850
5	14.244	68.648	10.826
6	14.244	79.450	10.802
7	14.244	90.143	10.693
8	14.244	100.895	10.752
9	14.244	111.441	10.546
10	14.244	122.152	10.711
11	14.244	132.758	10.606
12	14.244	143.427	10.669
13	14.244	154.072	10.645
14	14.244	164.696	10.624
15	14.244	175.182	10.486
16	14.244	185.768	10.586
17	14.244	196.160	10.392
18	14.244	206.539	10.379
19	14.244	217.060	10.521
20	14.244	227.544	10.484
21	14.244	238.023	10.479

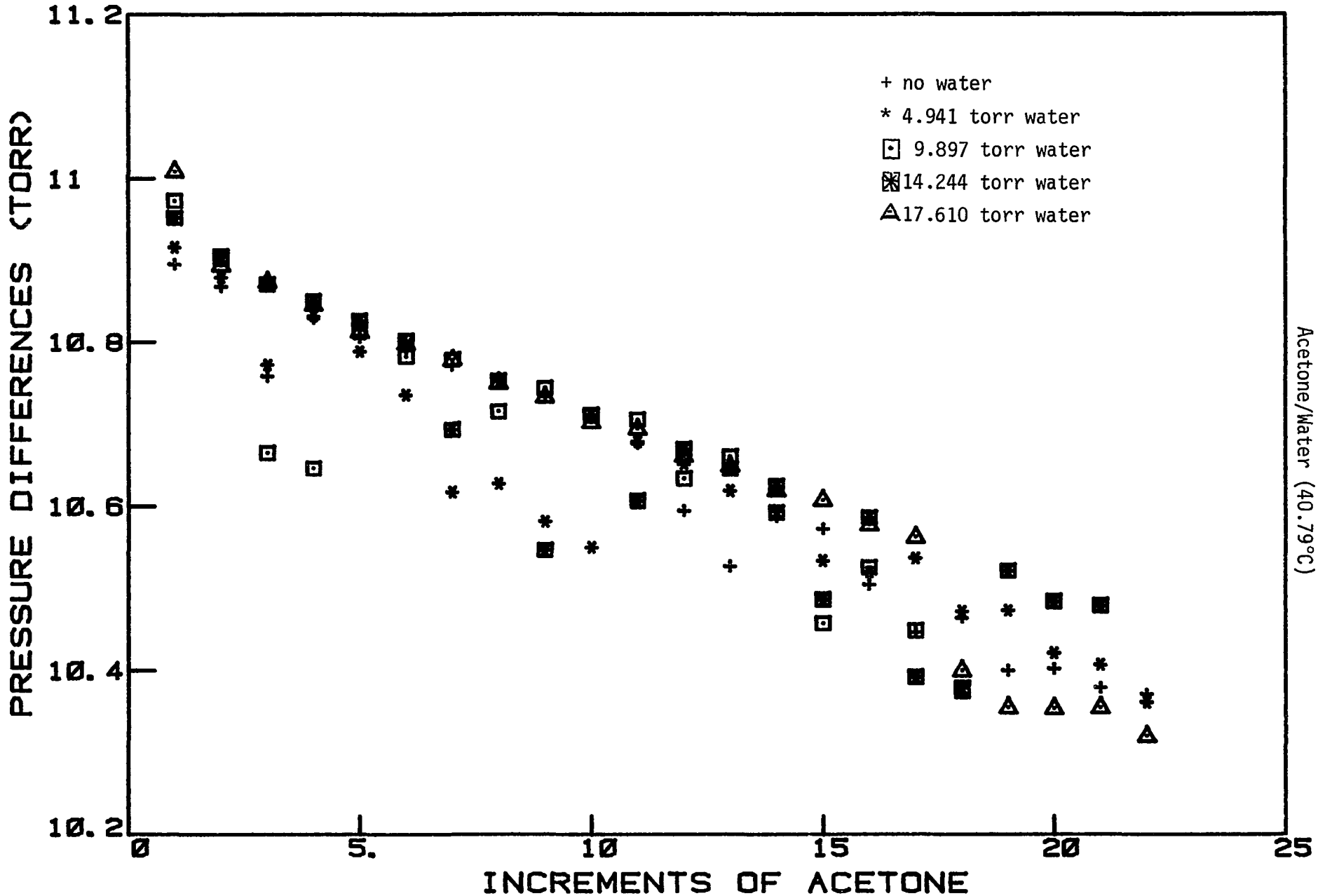

FIGURE IV-23

Acetone/Water (40.79°C)

TABLE IV-30

ACETONE/WATER VAPOR DENSITY DATA

AT 44.85 DEGREES CELSIUS

# OF INC.	Π(WATER)	PRESSURE	PRESS. DIF.
1	4.972	16.069	11.097
2	4.972	27.108	11.039
3	4.972	38.078	10.970
4	4.972	49.041	10.963
5	4.972	59.906	10.865
6	4.972	70.734	10.828
7	4.972	81.456	10.722
8	4.972	92.282	10.826
9	4.972	103.084	10.802
10	4.972	113.962	10.878
11	4.972	124.814	10.852
12	4.972	135.625	10.811
13	4.972	146.325	10.700
14	4.972	156.914	10.589
15	4.972	167.619	10.705
16	4.972	178.233	10.614
17	4.972	188.923	10.690
18	4.972	199.453	10.530
19	4.972	210.134	10.681
20	4.972	220.637	10.503
1	14.753	25.871	11.118
2	14.753	36.816	10.945
3	14.753	47.641	10.825
4	14.753	58.588	10.947
5	14.753	69.560	10.972
6	14.753	80.507	10.947
7	14.753	91.422	10.915
8	14.753	102.325	10.903
9	14.753	113.206	10.881
10	14.753	124.045	10.839
11	14.753	134.885	10.840
12	14.753	145.495	10.610
13	14.753	156.145	10.650
14	14.753	166.914	10.769
15	14.753	177.670	10.756
16	14.753	188.413	10.743
17	14.753	199.115	10.702
18	14.753	209.676	10.561
19	14.753	220.231	10.555

TABLE IV-30 cont.

ACETONE/WATER VAPOR DENSITY DATA

AT 44.85 DEGREES CELSIUS

# OF INC.	Π(WATER)	PRESSURE	PRESS. DIF.
20	14.753	230.699	10.468
1	9.715	20.830	11.115
2	9.715	31.739	10.909
3	9.715	42.747	11.008
4	9.715	53.564	10.817
5	9.715	64.536	10.972
6	9.715	75.368	10.832
7	9.715	86.304	10.936
8	9.715	97.211	10.907
9	9.715	108.097	10.886
10	9.715	118.883	10.786
11	9.715	129.735	10.852
12	9.715	140.564	10.829
13	9.715	151.375	10.811
14	9.715	162.157	10.782
15	9.715	172.872	10.715
16	9.715	183.607	10.735
17	9.715	194.200	10.593
18	9.715	204.784	10.584
19	9.715	215.362	10.578
20	9.715	225.953	10.591
21	9.715	236.525	10.572
22	9.715	247.053	10.528
1	17.388	28.371	10.983
2	17.388	39.306	10.935
3	17.388	50.104	10.798
4	17.388	60.889	10.785
5	17.388	71.650	10.761
6	17.388	82.394	10.744
7	17.388	93.102	10.708
8	17.388	103.786	10.684
9	17.388	114.460	10.674
10	17.388	125.113	10.653
11	17.388	135.723	10.610
12	17.388	146.320	10.597
13	17.388	156.893	10.573
14	17.388	167.439	10.546
15	17.388	177.962	10.523
16	17.388	188.496	10.534
17	17.388	199.003	10.507
18	17.388	209.486	10.483
19	17.388	219.958	10.472
20	17.388	230.396	10.438

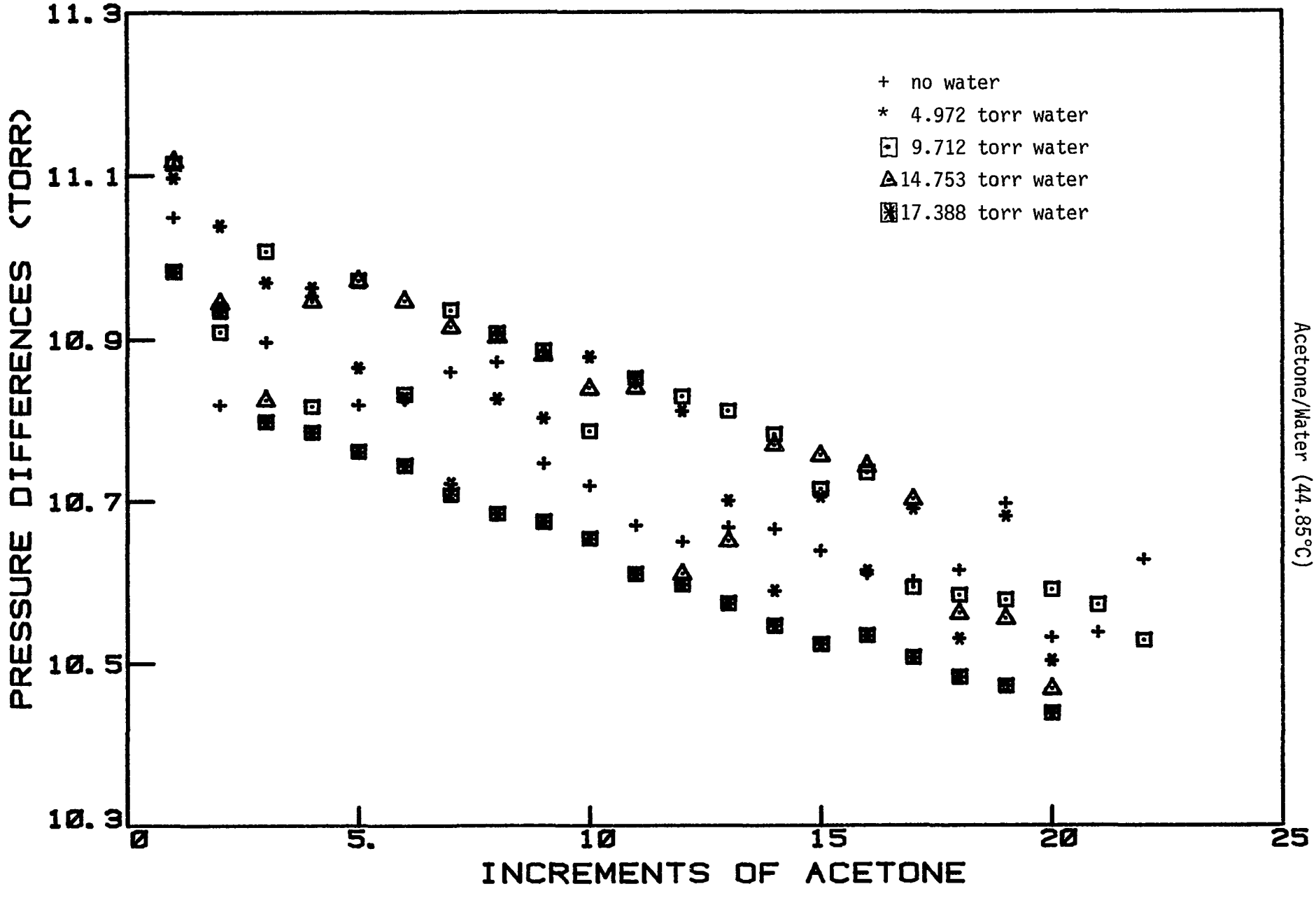

FIGURE IV-24
Acetone/Water (44.85°C)

viii-6. Acetone/Methanol

Pressure-density measurements for the acetone/methanol vapor system were collected on the automated vapor density apparatus at various temperatures between 15°C and 45°C. The data are presented in Tables IV-31 through IV-37. Kink corrections are not necessary for data collected on the automated vapor-density apparatus. Figures IV-25 through IV-31 are graphs of the incremental pressure change as increments of acetone are evaporated into the sample flask. Initial pressures of methanol were about 5 torr, 10 torr, 15 torr, and 20 torr in four experiments, respectively, conducted at seven different temperatures.

No evidence of methanol desorption is apparent after the first increment of acetone is added to the methanol in each experiment. Near saturation, adsorption problems become quite pronounced. Unfortunately, there is no way to calculate an anchor point for the mixed system. Instead, the data cut-off point for analysis purposes is chosen to be the same as the cut-off point in the pure acetone vapor study at each temperature. Actually, one would reach the dew point near this cut-off point in most of the experiments and so few vapor phase data points are ignored.

All of the mixed vapor data for acetone/methanol are fit simultaneously. Self-association of acetone is subtracted from

the total association to determine the pressure of hetero-complex. The amount of methanol dissociation is considered negligible. (See Table IV-38.) The amount of hetero-complex is fitted to a 1-infinity model. This requires determination of four parameters: an equilibrium constant ($K_{11}^{25°}$) for the formation of methanol-acetone at 25°C, a stepwise equilibrium constant ($K_{\infty}^{25°}$) for the addition of an acetone monomer to the $(acetone)_n$methanol complex at 25°C, and two heats of association constants (ΔH_{11},ΔH_{∞}) which are each temperature dependent parameters characteristic of one of the equilibrium constants. The 378 data points were fitted to an overall RMSD of 0.026 torr, where the RMSD is

$$RMSD = (\Sigma\ (\Delta\Pi\ (exp) - \Delta\Pi(calc)\ /(299\ points - 4\ parameters))^{\frac{1}{2}}$$

$\Delta\Pi$(exp) is the size of the loop parameter at a particular temperature. Values for the parameters are given in Table IV-13.

TABLE IV-31

ACETONE/METHANOL VAPOR DENSITY DATA

AT 14.96 DEGREES CELSIUS

INITIAL PRESSURE METHANOL	ACETONE PRESSURE	ACETONE IDEAL PRESSURE	$\Delta\Pi$(EXP)-$\Delta\Pi$(CALC)
5.208	9.640	9.669	- .008
5.208	19.262	19.339	- .000
5.208	28.867	29.008	.008
5.208	38.445	38.677	.007
5.208	47.992	48.347	.003
5.208	57.512	58.016	.003
5.208	67.004	67.686	.004
5.208	76.460	77.355	- .003
5.208	85.882	87.024	- .006
9.938	9.626	9.669	- .012
9.938	19.215	19.339	- .023
9.938	28.797	29.008	- .002
9.938	38.351	38.677	- .002
9.938	47.878	48.347	.000
9.938	57.379	58.016	.005
9.938	66.852	67.686	.009
9.938	76.291	77.355	.010
9.938	85.687	87.024	.004
14.865	9.612	9.669	- .017
14.865	19.177	19.339	- .036
14.865	28.718	29.008	- .031
14.865	38.232	38.677	- .027
14.865	47.716	48.347	- .025
14.865	57.173	58.016	- .019
14.865	66.599	67.686	- .013
14.865	75.990	77.355	- .009
14.865	85.353	87.024	.007

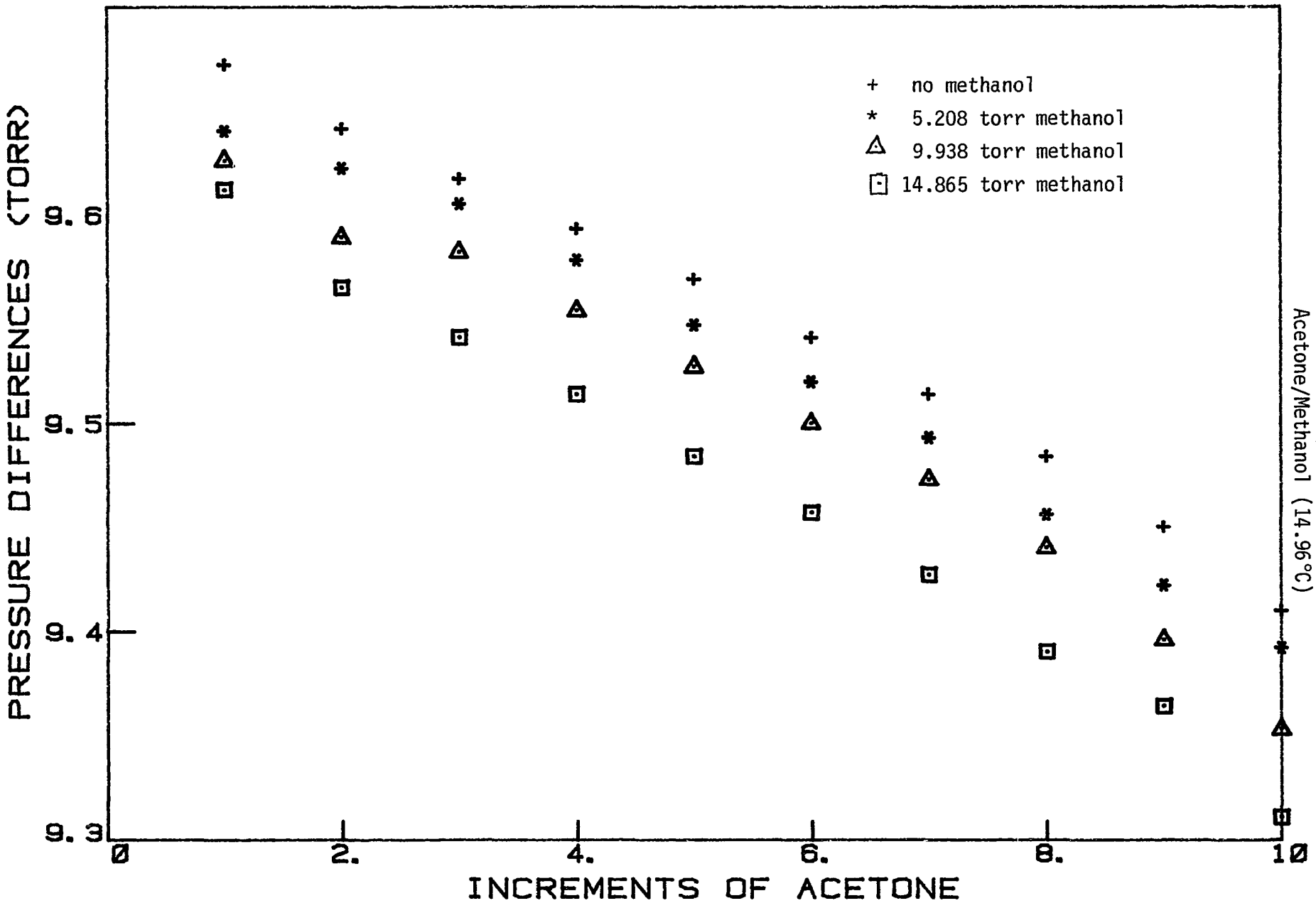

FIGURE IV-25

Acetone/Methanol (14.96°C)

TABLE IV-32

ACETONE/METHANOL VAPOR DENSITY DATA **

AT 20.29 DEGREES CELSIUS

INITIAL PRESSURE METHANOL	ACETONE PRESSURE	ACETONE IDEAL PRESSURE	$\Delta\Pi$(EXP)-$\Delta\Pi$(CALC)
5.235	9.909	9.848	.081
5.235	19.245	19.697	- .472
5.235	29.409	29.545	.384
5.235	38.981	39.393	- .189
5.235	48.486	49.241	- .233
5.235	57.719	59.090	- .487
5.235	67.069	68.938	- .345
5.235	76.208	78.786	- .537
5.235	85.348	88.634	- .514
5.235	94.452	98.483	- .527
10.147	9.861	9.848	.042
10.147	19.646	19.697	- .011
10.147	29.319	29.545	- .099
10.147	38.870	39.393	- .199
10.147	48.372	49.241	- .224
10.147	57.790	59.090	- .285
10.147	67.205	68.938	- .263
10.147	76.574	78.786	- .285
10.147	85.897	88.634	- .306
10.147	95.102	98.483	- .401
10.147	104.328	108.331	- .353

** These data were not included in data treatment.

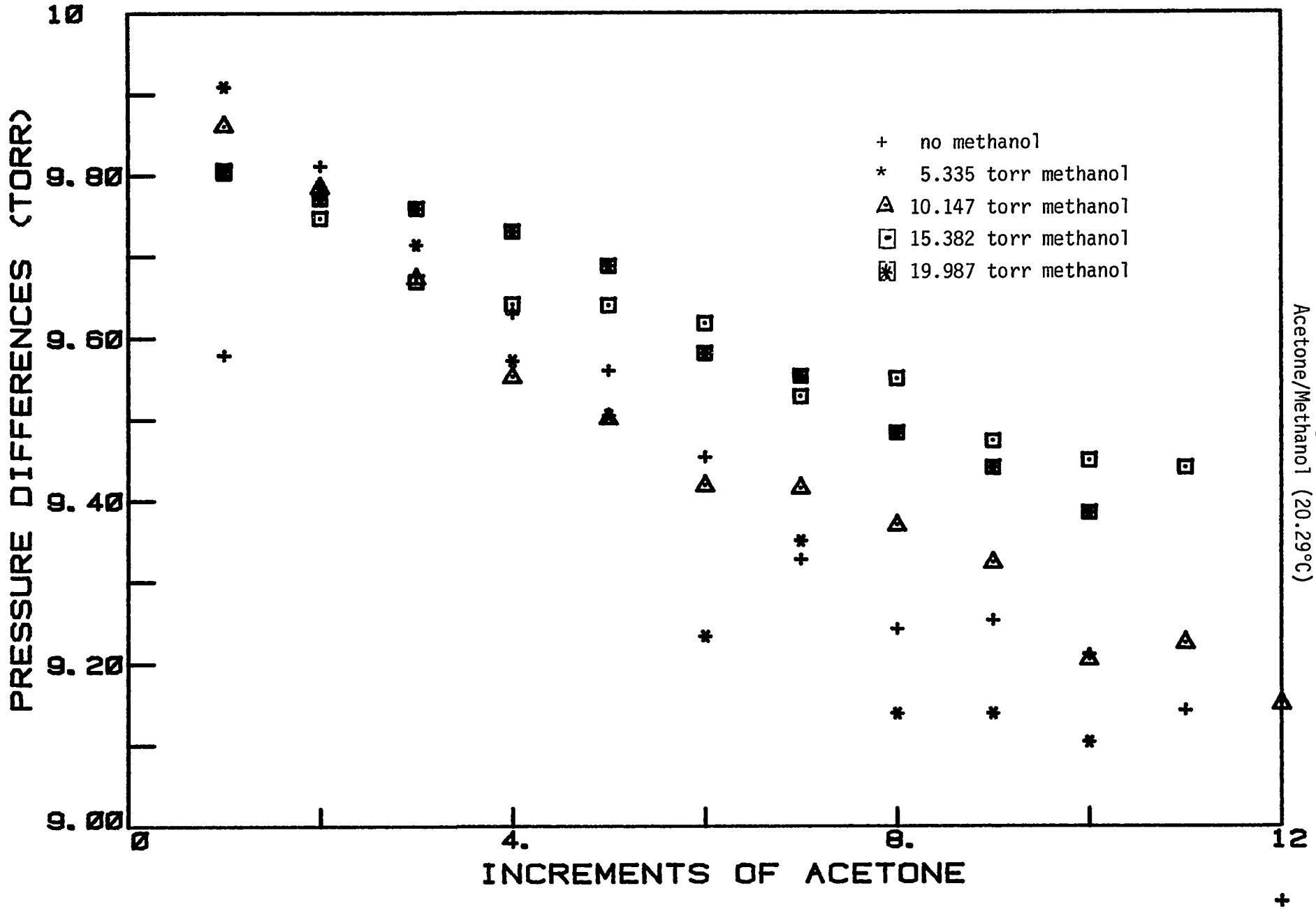

FIGURE IV-26

Acetone/Methanol (20.29°C)

TABLE IV-33

ACETONE/METHANOL VAPOR DENSITY DATA

AT 24.99 DEGREES CELSIUS

INITIAL PRESSURE METHANOL	ACETONE PRESSURE	ACETONE IDEAL PRESSURE	$\Delta\Pi$(EXP)-$\Delta\Pi$(CALC)
5.205	10.104	10.108	.016
5.205	20.181	20.215	.010
5.205	30.241	30.323	.015
5.205	40.276	40.431	.013
5.205	50.294	50.538	.018
5.205	60.282	60.646	.010
5.205	70.252	70.754	.015
5.205	80.201	80.861	.017
5.205	90.123	90.969	.013
5.205	100.018	101.077	.009
5.205	109.886	111.184	.005
5.205	119.730	121.292	.005
5.205	129.550	131.400	.004
5.205	139.343	141.507	.001
9.745	10.108	10.108	.027
9.745	20.182	20.215	.015
9.745	30.234	30.323	.016
9.745	40.260	40.431	.013
9.745	50.271	50.538	.021
9.745	60.255	60.646	.017
9.745	70.218	70.754	.019
9.745	80.154	80.861	.016
9.745	90.062	90.969	.012
9.745	99.947	101.077	.013
9.745	109.808	111.184	.013
9.745	119.645	121.292	.014
9.745	129.449	131.400	.006
9.745	139.232	141.507	.010
15.107	10.068	10.108	- .004
15.107	20.108	20.215	- .009
15.107	30.118	30.323	- .016
15.107	40.110	40.431	- .011
15.107	50.076	50.538	- .013
15.107	60.020	60.646	- .012

TABLE IV-33 cont.

ACETONE/METHANOL VAPOR DENSITY DATA

AT 24.99 DEGREES CELSIUS

INITIAL PRESSURE METHANOL	ACETONE PRESSURE	ACETONE IDEAL PRESSURE	$\Delta\Pi$(EXP)-$\Delta\Pi$(CALC)
15.107	69.935	70.754	- .017
15.107	79.829	80.861	- .013
15.107	89.699	90.969	- .012
15.107	99.540	101.077	- .016
15.107	109.356	111.184	- .016
15.107	119.152	121.292	- .010
15.107	128.915	131.400	- .017
15.107	138.655	141.507	- .014
20.159	10.066	10.108	.002
20.159	20.137	20.215	.031
20.159	30.145	30.323	- .009
20.159	40.132	40.431	- .006
20.159	50.101	50.538	.001
20.159	60.044	60.646	- .001
20.159	69.962	70.754	- .001
20.159	79.860	80.861	.005
20.159	89.725	90.969	- .003
20.159	99.575	101.077	.009
20.159	109.405	111.184	.015
20.159	119.202	121.292	.009
20.159	128.968	131.400	.006
20.159	138.708	141.507	.008

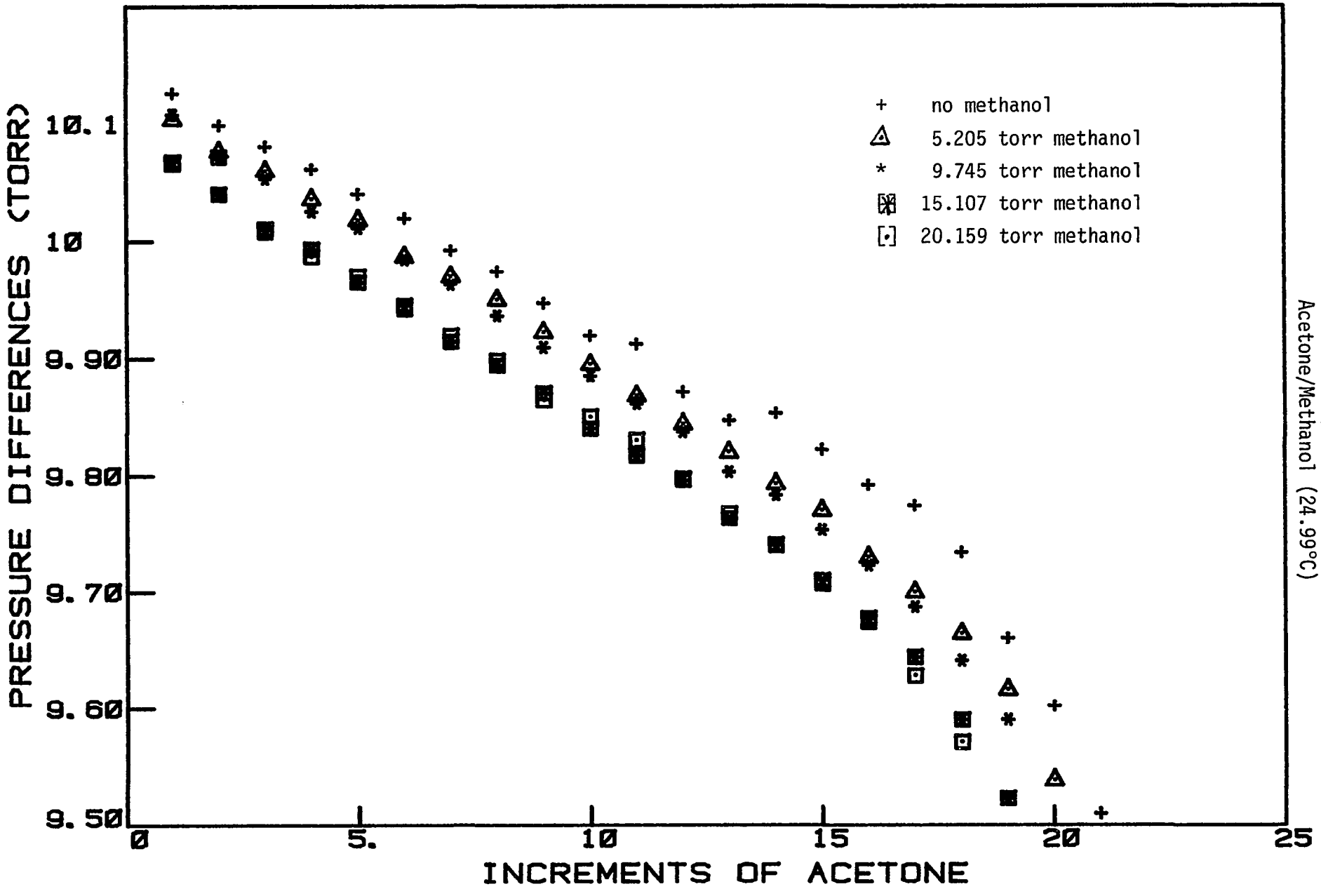

FIGURE IV-27

Acetone/Methanol (24.99°C)

TABLE IV-34

ACETONE/METHANOL VAPOR DENSITY DATA

AT 30.47 DEGREES CELSIUS

	INITIAL PRESSURE METHANOL	ACETONE PRESSURE	ACETONE IDEAL PRESSURE	$\Delta\Pi$(EXP)-$\Delta\Pi$(CALC)
	5.181	10.246	10.293	- .030
	5.181	20.470	20.587	- .031
	5.181	30.666	30.880	- .039
	5.181	40.846	41.174	- .035
	5.181	51.008	51.467	- .032
	5.181	61.155	61.761	- .026
	5.181	71.273	72.054	- .035
	5.181	81.373	82.348	- .032
	5.181	91.451	92.641	- .033
	5.181	101.500	102.934	- .041
	5.181	111.531	113.228	- .038
	5.181	121.527	123.521	- .052
	5.181	131.511	133.815	- .042
	5.181	141.477	144.108	- .039
	5.181	151.414	154.402	- .046
	10.170	10.248	10.293	- .020
	10.170	20.480	20.587	- .016
	10.170	30.683	30.880	- .024
	10.170	40.868	41.174	- .021
	10.170	51.031	51.467	- .022
	10.170	61.172	61.761	- .023
	10.170	71.294	72.054	- .021
	10.170	81.391	82.348	- .025
	10.170	91.467	92.641	- .024
	10.170	101.517	102.934	- .029
	10.170	111.548	113.228	- .026
**	14.622	10.590	10.293	.330
	14.622	20.810	20.587	- .020
	14.622	31.002	30.880	- .027
	14.622	41.182	41.174	- .018
	14.622	51.331	51.467	- .028
	14.622	61.463	61.761	- .023
	14.622	71.574	72.054	- .023
	14.622	81.660	82.348	- .026

TABLE IV-34 cont.

ACETONE/METHANOL VAPOR DENSITY DATA

AT 30.47 DEGREES CELSIUS

	INITIAL PRESSURE METHANOL	ACETONE PRESSURE	ACETONE IDEAL PRESSURE	$\Delta\Pi$(EXP)-$\Delta\Pi$(CALC)
	14.622	91.721	92.641	- .029
	14.622	101.763	102.934	- .026
	14.622	111.783	113.228	- .026
	14.622	121.778	123.521	- .029
	14.622	131.754	133.815	- .025
	14.622	141.705	144.108	- .028
	19.954	10.267	10.293	.014
	19.954	20.486	20.587	- .013
**	19.954	30.453	30.880	- .246
	19.954	40.635	41.174	- .008
	19.954	50.788	51.467	- .015
	19.954	60.932	61.761	- .002
	19.954	71.041	72.054	- .015
	19.954	81.125	82.348	- .018
	19.954	91.194	92.641	- .011
	19.954	101.233	102.934	- .018
	19.954	111.255	113.228	- .013
	19.954	121.254	123.521	- .013
	19.954	131.234	133.815	- .009
	19.954	141.189	144.108	- .011
	19.954	151.123	154.402	- .008

** These data were not included in the data treatment.

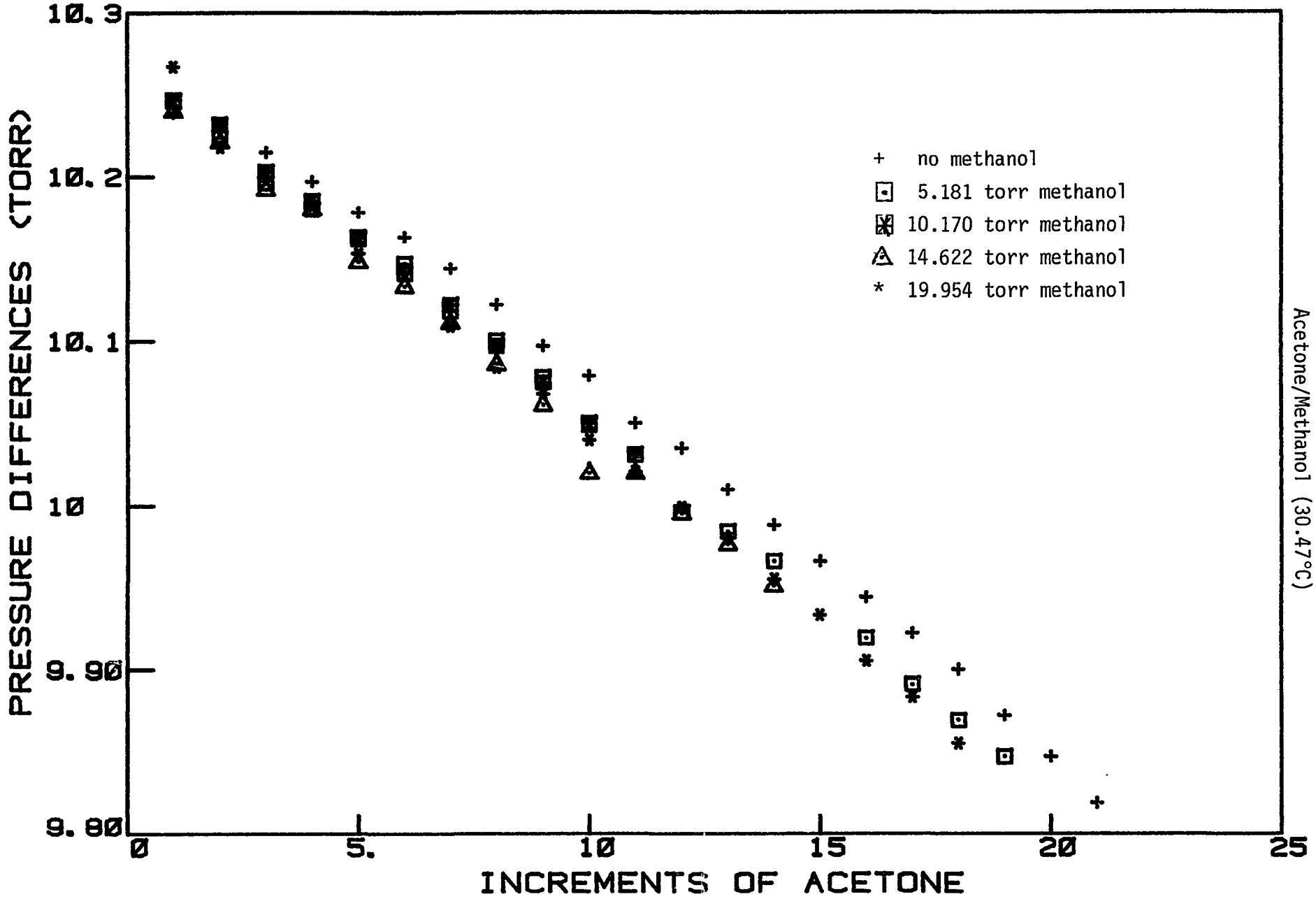

FIGURE IV-28

Acetone/Methanol (30.47°C)

TABLE IV-35

ACETONE/METHANOL VAPOR DENSITY DATA

AT 34.54 DEGREES CELSIUS

INITIAL PRESSURE METHANOL	ACETONE PRESSURE	ACETONE IDEAL PRESSURE	$\Delta\Pi$(EXP)-$\Delta\Pi$(CALC)
5.174	10.344	10.327	.034
5.174	20.655	20.653	.020
5.174	30.946	30.980	.020
5.174	41.216	41.306	.018
5.174	51.466	51.633	.017
5.174	61.700	61.959	.021
5.174	71.935	72.286	.042
5.174	82.140	82.612	.031
5.174	92.284	92.939	- .011
5.174	102.340	103.265	- .081
5.174	112.481	113.592	.026
5.174	122.603	123.918	.027
5.174	132.705	134.245	.027
5.174	142.791	144.571	.032
5.174	152.848	154.898	.023
5.174	162.882	165.224	.020
5.174	172.893	175.551	.017
5.174	182.882	185.877	.016
5.174	192.221	196.204	- .638
5.174	202.794	206.530	.665
10.167	10.355	10.327	.052
10.167	20.670	20.653	.032
10.167	30.960	30.980	.026
10.167	41.230	41.306	.026
10.167	51.471	51.633	.016
10.167	61.702	61.959	.026
10.167	71.915	72.286	.028
10.167	82.104	82.612	.024
10.167	92.271	92.939	.022
10.167	102.422	103.265	.026
10.167	112.554	113.592	.027
10.167	122.662	123.918	.023
10.167	132.749	134.245	.023
10.167	142.812	144.571	.019

TABLE IV-35 cont.

ACETONE/METHANOL VAPOR DENSITY DATA

AT 34.54 DEGREES CELSIUS

	INITIAL PRESSURE METHANOL	ACETONE PRESSURE	ACETONE IDEAL PRESSURE	$\Delta\Pi$(EXP)-$\Delta\Pi$(CALC)
	10.167	152.853	154.898	.017
	10.167	162.874	165.224	.018
	10.167	172.876	175.551	.020
	10.167	182.855	185.877	.017
	10.167	192.808	196.204	.012
	10.167	202.741	206.530	.013
	14.578	10.355	10.327	.059
	14.578	20.674	20.653	.042
	14.578	30.986	30.980	.055
	14.578	41.286	41.306	.063
	14.578	51.553	51.633	.050
	14.578	61.790	61.959	.040
	14.578	72.008	72.286	.041
	14.578	82.217	82.612	.052
	14.578	92.396	92.939	.042
	14.578	102.571	103.265	.059
	14.578	112.715	113.592	.048
	14.578	122.835	123.918	.045
	14.578	132.929	134.245	.039
	14.578	143.006	144.571	.043
	14.578	153.064	154.898	.045
	14.578	163.100	165.224	.044
	14.578	173.115	175.551	.044
	14.578	183.101	185.877	.036
	14.578	193.065	196.204	.035
	14.578	203.018	206.530	.046
	20.065	10.357	10.327	.069
	20.065	20.678	20.653	.052
	20.065	30.970	30.980	.043
	20.065	41.239	41.306	.040
	20.065	51.488	51.633	.040
**	20.065	60.371	61.959	- 1.325
	20.065	70.580	72.286	.038
	20.065	80.685	82.612	- .047

TABLE IV-35 cont.

ACETONE/METHANOL VAPOR DENSITY DATA

AT 34.54 DEGREES CELSIUS

INITIAL PRESSURE METHANOL	ACETONE PRESSURE	ACETONE IDEAL PRESSURE	$\Delta\Pi$(EXP)-$\Delta\Pi$(CALC)
20.065	90.845	92.939	.030
** 20.065	100.388	103.265	- .580
20.065	110.505	113.592	.027
20.065	120.606	123.918	.032
20.065	130.691	134.245	.037
20.065	140.753	144.571	.035
20.065	150.789	154.898	.030
20.065	160.809	165.224	.035
20.065	170.821	175.551	.049
20.065	180.805	185.877	.042
20.065	190.762	196.204	.037
20.065	200.691	206.530	.030

** These data were not included in the data treatment.

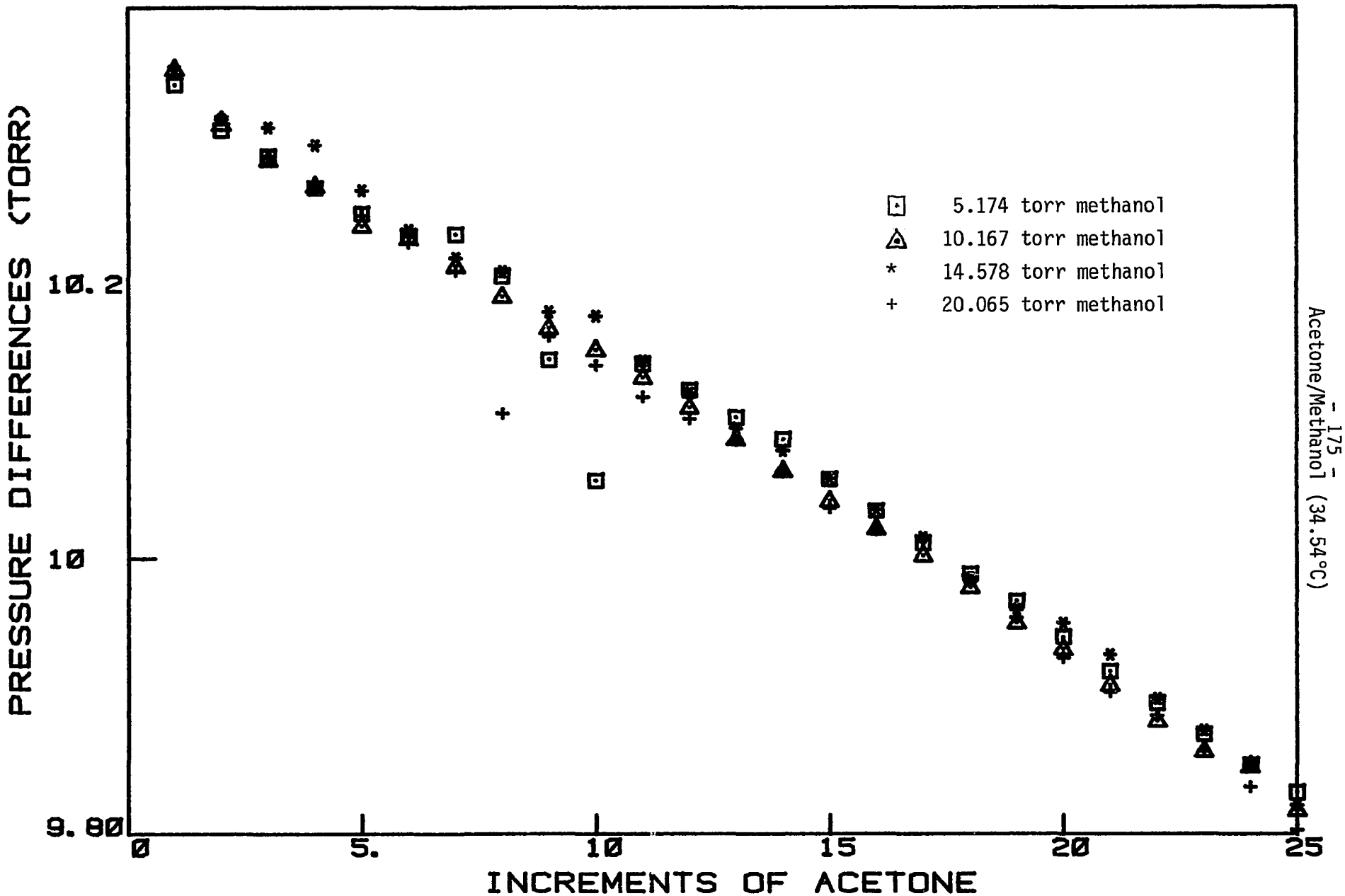

FIGURE IV-29

Acetone/Methanol (34.54°C)

TABLE IV-36

ACETONE/METHANOL VAPOR DENSITY DATA

AT 38.88 DEGREES CELSIUS

	INITIAL PRESSURE METHANOL	ACETONE PRESSURE	ACETONE IDEAL PRESSURE	$\Delta\Pi$(EXP)-$\Delta\Pi$(CALC)
	5.205	10.471	10.472	.015
	5.205	20.915	20.944	.006
	5.205	31.343	31.416	.008
	5.205	41.754	41.889	.010
	5.205	52.141	52.361	.004
	5.205	62.518	62.833	.013
	5.205	72.868	73.305	.004
	5.205	83.217	83.777	.022
	5.205	93.522	94.249	- .004
	5.205	103.801	104.722	- .011
	5.205	114.063	115.194	- .009
	5.205	124.304	125.666	- .011
	5.205	134.528	136.138	- .009
	5.205	144.732	146.610	- .010
	5.205	154.922	157.082	- .005
	5.205	165.090	167.555	- .008
	5.205	175.239	178.027	- .008
	5.205	185.360	188.499	- .016
	5.205	195.451	198.971	- .027
	5.205	205.553	209.443	.004
**	5.205	215.311	219.915	- .333
	5.205	225.338	230.388	- .034
	5.205	235.379	240.860	.001
	10.042	10.456	10.472	.006
	10.042	20.839	20.944	- .049
**	10.042	31.175	31.416	- .078
	10.042	41.521	41.889	- .049
	10.042	51.851	52.361	- .047
	10.042	62.210	62.833	.001
	10.042	72.552	73.305	.003
**	10.042	82.782	83.777	- .092
**	10.042	93.165	94.249	.083
	10.042	103.437	104.722	- .011
	10.042	113.694	115.194	- .007

TABLE IV-36 cont.

ACETONE/METHANOL VAPOR DENSITY DATA

AT 38.88 DEGREES CELSIUS

	INITIAL PRESSURE METHANOL	ACETONE PRESSURE	ACETONE IDEAL PRESSURE	$\Delta\Pi$(EXP)-$\Delta\Pi$(CALC)
	10.042	123.921	125.666	- .018
	10.042	134.134	136.138	- .013
	10.042	144.327	146.610	- .014
	10.042	154.496	157.082	- .019
	10.042	164.654	167.555	- .010
	10.042	174.795	178.027	- .008
	10.042	184.896	188.499	- .029
	10.042	194.986	198.971	- .020
	10.042	205.058	209.443	- .018
	10.042	215.107	219.915	- .022
	10.042	225.135	230.388	- .023
	10.042	235.142	240.860	- .024
	14.797	10.462	10.472	.019
	14.797	20.906	20.944	.019
	14.797	31.330	31.416	.018
	14.797	41.730	41.889	.012
	14.797	52.113	52.361	.014
	14.797	62.473	62.833	.010
	14.797	72.812	73.305	.007
	14.797	83.134	83.777	.009
	14.797	93.432	94.249	.004
	14.797	103.707	104.722	.000
	14.797	113.961	115.194	- .002
	14.797	124.194	125.666	- .003
	14.797	134.404	136.138	- .007
	14.797	144.587	146.610	- .015
	14.797	154.749	157.082	- .017
	14.797	164.887	167.555	- .021
	14.797	175.005	178.027	- .022
	14.797	185.109	188.499	- .016
**	14.797	195.132	198.971	- .080
**	14.797	205.277	209.443	.068
	14.797	215.331	219.915	- .006
	14.797	225.349	230.388	- .023

TABLE IV-36 cont.

ACETONE/METHANOL VAPOR DENSITY DATA

AT 38.88 DEGREES CELSIUS

INITIAL PRESSURE METHANOL	ACETONE PRESSURE	ACETONE IDEAL PRESSURE	$\Delta\Pi$(EXP)-$\Delta\Pi$(CALC)
14.797	235.349	240.860	- .021
19.416	10.467	10.472	.030
19.416	20.907	20.944	.021
19.416	31.316	31.416	.009
19.416	41.709	41.889	.012
19.416	52.087	52.361	.016
19.416	62.442	62.833	.011
19.416	72.780	73.305	.013
19.416	83.094	83.777	.008
19.416	93.384	94.249	.003
19.416	103.651	104.722	- .000
19.416	113.890	115.194	- .009
19.416	124.109	125.666	- .010
19.416	134.311	136.138	- .008
19.416	144.489	146.610	- .012
19.416	154.649	157.082	- .011
19.416	164.792	167.555	- .008
19.416	174.921	178.027	- .002
19.416	185.017	188.499	- .016
19.416	195.091	198.971	- .018
19.416	205.142	209.443	- .021
19.416	215.173	219.915	- .021
19.416	225.182	230.388	- .023
19.416	235.168	240.860	- .026

** These data were not included in the data treatment.

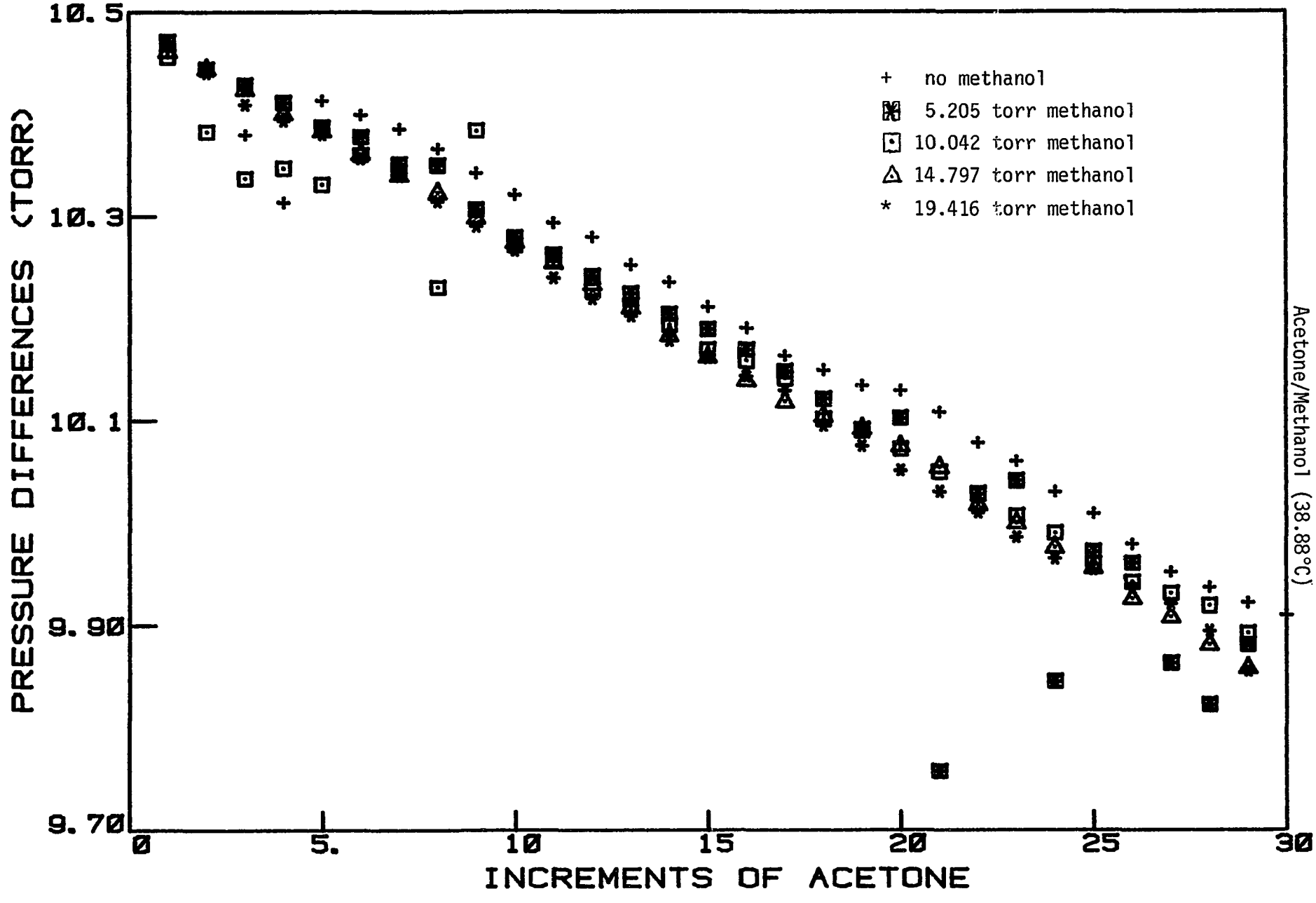

FIGURE IV-30
Acetone/Methanol (38.88°C)

TABLE IV-37

ACETONE/METHANOL VAPOR DENSITY DATA **

AT 44.84 DEGREES CELSIUS

INITIAL PRESSURE METHANOL	ACETONE PRESSURE	ACETONE IDEAL PRESSURE	$\Delta\Pi$(EXP)-$\Delta\Pi$(CALC)
5.225	10.687	10.672	.030
5.225	21.325	21.344	- .002
5.225	31.944	32.017	- .004
5.225	42.545	42.689	- .005
5.225	53.132	53.361	- .001
5.225	63.676	64.033	- .027
5.225	74.225	74.705	- .005
5.225	84.723	85.378	- .039
5.225	95.153	96.050	- .090
5.225	105.257	106.722	- .404
5.225	115.441	117.394	- .306
5.225	125.664	128.066	- .249
5.225	135.989	138.738	- .127
5.225	145.970	149.411	- .461
5.225	156.250	160.083	- .138
5.225	166.623	170.755	- .024
5.225	176.775	181.427	- .233
5.225	186.862	192.099	- .282
5.225	196.900	202.772	- .315
9.911	10.678	10.672	.027
9.911	21.308	21.344	- .004
9.911	31.912	32.017	- .013
9.911	42.452	42.689	- .060
9.911	53.020	53.361	- .015
9.911	63.520	64.033	- .066
9.911	74.035	74.705	- .033
9.911	84.398	85.378	- .170
9.911	94.785	96.050	- .128
9.911	105.248	106.722	- .033
9.911	115.463	117.394	- .268
9.911	125.810	128.066	- .116
9.911	136.131	138.738	- .124
9.911	146.378	149.411	- .182
9.911	156.698	160.083	- .089

TABLE IV-37 cont.

ACETONE/METHANOL VAPOR DENSITY DATA**

AT 44.84 DEGREES CELSIUS

INITIAL PRESSURE METHANOL	ACETONE PRESSURE	ACETONE IDEAL PRESSURE	$\Delta\Pi$(EXP)-$\Delta\Pi$(CALC)
9.911	167.051	170.755	- .037
9.911	177.217	181.427	- .211
9.911	187.526	192.099	- .045
9.911	197.779	202.772	- .084
15.272	10.634	10.672	- .011
15.272	21.186	21.344	- .076
15.272	31.584	32.017	- .214
15.272	41.998	42.689	- .181
15.272	52.157	53.361	- .421
15.272	62.281	64.033	- .440
18.996	10.676	10.672	.036
18.996	21.300	21.344	.001
18.996	31.630	32.017	- .277
18.996	42.109	42.689	- .110
18.996	52.198	53.361	- .487
18.996	62.235	64.033	- .524

** These data were not included in the data treatment.

FIGURE IV-31

Acetone/Methanol (44.84°C)

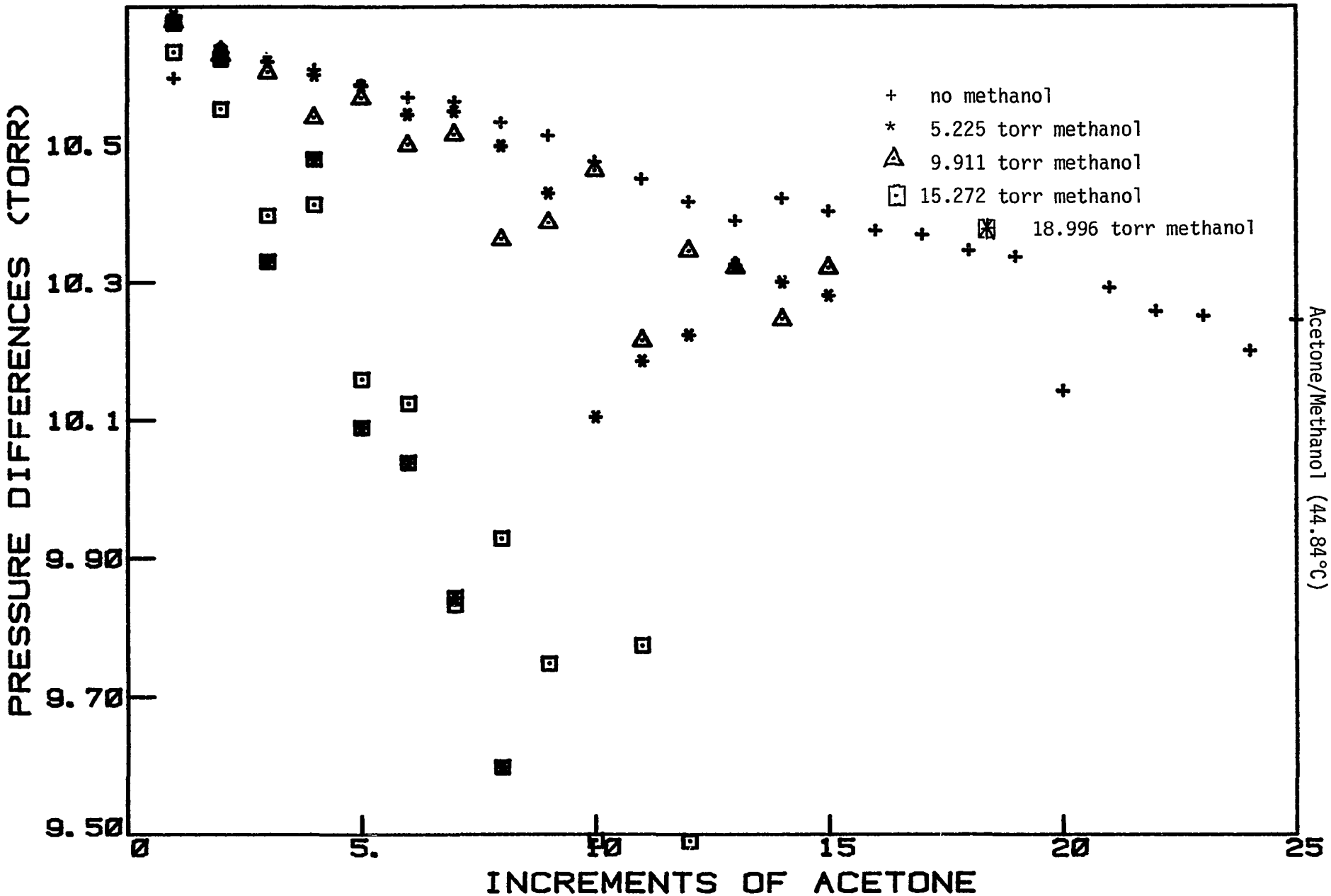

TABLE IV-38

METHANOL KEYES POINTS

T(°K)	Vapor P	Vapor II	Amount Associated (MeOH=20 torr)	Effect on A-MeOH (torr)
288.12	73.896	75.630	0.128	0.003
293.45	99.073	101.492	0.100	0.003
298.15	127.053	130.406	0.085	0.003
303.63	167.956	172.689	0.069	0.002
307.70	205.156	211.591	0.063	0.002
312.04	252.313	261.230	0.058	0.002
318.00	331.796	344.476	0.048	0.002

viii-7. Acetone/Ethanol

Vapor density data for the acetone/ethanol system were collected on the automated vapor density apparatus at temperatures between 15°C and 45°C. The initial amounts of ethanol in the sample flask at the beginning of each of four experiments for each temperature were about 5 torr, 10 torr, 15 torr, and 20 torr. The data are given in Tables IV-39 through IV-45 and are plotted as pressure difference vs. increments of acetone added in figure IV-32 through IV-38.

The pressure change after the first increment of acetone added was usually too high, suggesting desorption of ethanol from the stainless steel walls in the presence of acetone. For this reason, the first point of each experiment was neglected; the omitted points are included in the data tables.

Analysis of the 297 data points is identical to the data analysis of the acetone/methanol vapor system. The pressure of self-associated acetone is subtracted from the total pressure of complexed species to determine the pressure of $(acetone)_n$ethanol complex (n=1,2,...). The amount of ethanol association is considered negligible. (See Table IV-46.) Values of the four heteroassociation parameters ($K_{11}^{25°}$, $K_{\infty}^{25°}$, ΔH_{11}, ΔH_{∞}) are given in Table IV-13 . The RMSD between the incremental ideal pressure (or loop size) and the calculated change in the ideal pressure is

0.020 torr. The deviations for each point are given in the data tables.

TABLE IV-39

ACETONE/ETHANOL VAPOR DENSITY DATA

AT 14.97 DEGREES CELSIUS

	INITIAL PRESSURE ETHANOL	ACETONE PRESSURE	ACETONE IDEAL PRESSURE	$\Delta\Pi$(EXP)-$\Delta\Pi$(CALC)
**	15.443	11.858	11.950	- .038
	15.443	23.674	23.900	- .032
	15.443	35.442	35.850	- .027
	15.443	47.152	47.800	- .025
	15.443	58.792	59.751	- .023
	15.443	70.335	71.701	- .030
	15.443	81.707	83.651	- .082
**	9.653	11.890	11.950	- .019
	9.653	23.748	23.900	- .008
	9.653	35.568	35.850	.001
	9.653	47.336	47.800	.000
	9.653	59.049	59.751	.005
	9.653	70.701	71.701	.016
	9.653	82.274	83.651	.029
	9.653	93.724	95.601	.036
**	4.364	11.913	11.950	- .009
	4.364	23.798	23.900	.002
	4.364	35.647	35.850	.007
	4.364	47.452	47.800	.007
	4.364	59.214	59.751	.011
	4.364	70.921	71.701	.008
	4.364	82.565	83.651	.008
	4.364	94.128	95.601	.007

** These data were not included in the data treatment.

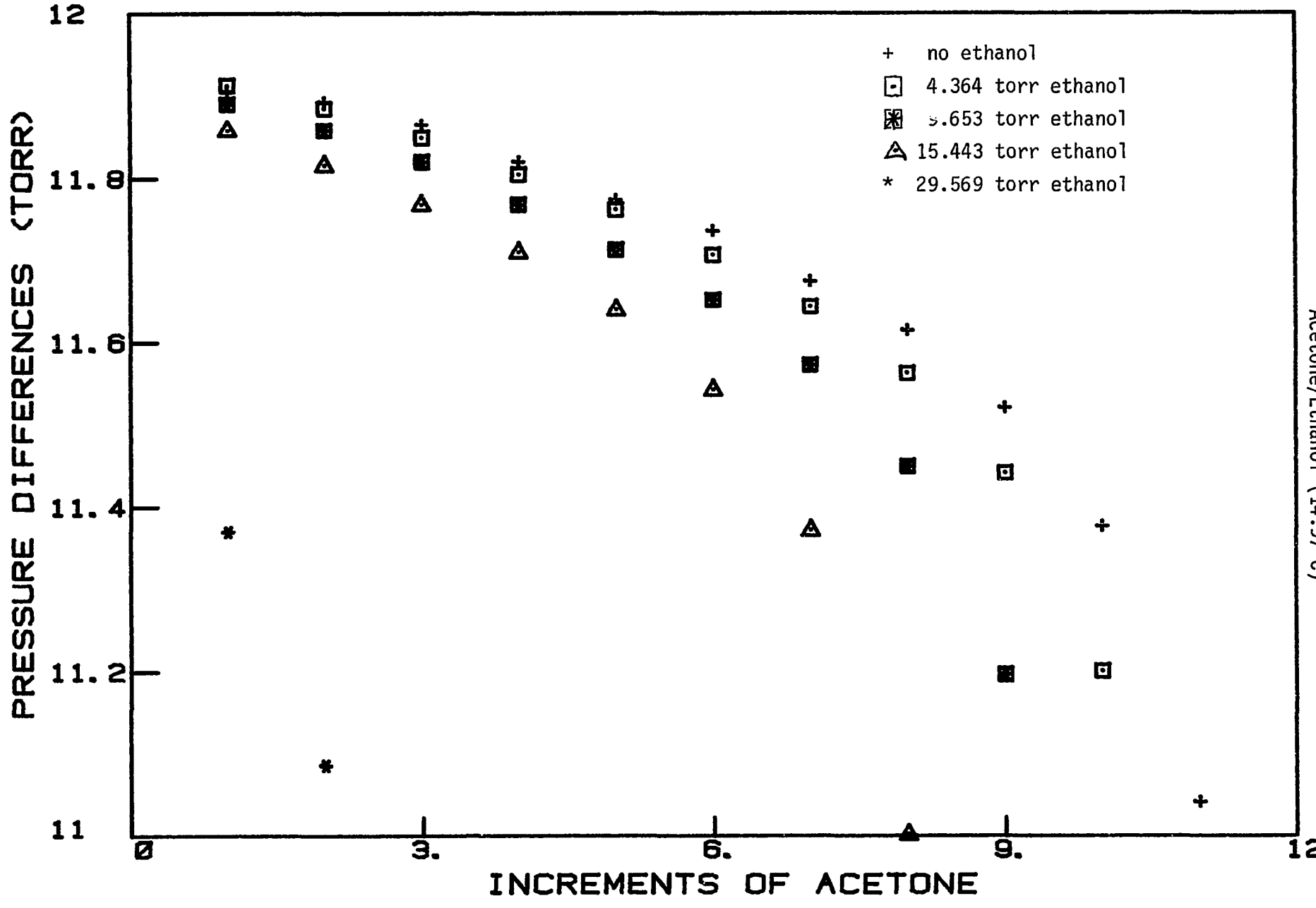

FIGURE IV-32

Acetone/Ethanol (14.97°C)

TABLE IV-40

ACETONE/ETHANOL VAPOR DENSITY DATA

AT 20.00 DEGREES CELSIUS

	INITIAL PRESSURE ETHANOL	ACETONE PRESSURE	ACETONE IDEAL PRESSURE	$\Delta\Pi$(EXP)-$\Delta\Pi$(CALC)
**	6.375	12.109	12.159	- .020
	6.375	24.202	24.317	.000
	6.375	36.261	36.476	.004
	6.375	48.282	48.635	.004
	6.375	60.267	60.794	.009
	6.375	72.211	72.952	.010
	6.375	84.111	85.111	.012
	6.375	95.962	97.270	.012
	6.375	107.754	109.429	.009
	6.375	119.477	121.587	.004
**	19.349	12.065	12.159	- .039
	19.349	24.090	24.317	- .037
	19.349	36.085	36.476	- .022
	19.349	48.036	48.635	- .019
	19.349	59.937	60.794	- .016
	19.349	71.789	72.952	- .007
	19.349	83.575	85.111	- .008
	19.349	95.270	97.270	- .022
**	14.749	12.099	12.159	- .014
	14.749	24.161	24.317	- .011
	14.749	36.189	36.476	- .003
	14.749	48.181	48.635	.006
	14.749	60.125	60.794	.006
	14.749	72.016	72.952	.006
	14.749	83.864	85.111	.022
	14.749	95.636	97.270	.014
	14.749	107.327	109.429	.013
**	12.576	12.099	12.159	- .018
	12.576	24.167	24.317	- .010
	12.576	36.202	36.476	- .002
	12.576	48.199	48.635	.003
	12.576	60.153	60.794	.006
	12.576	72.060	72.952	.010
	12.576	83.921	85.111	.019

TABLE IV-40 cont.

ACETONE/ETHANOL VAPOR DENSITY DATA

AT 20.00 DEGREES CELSIUS

INITIAL PRESSURE ETHANOL	ACETONE PRESSURE	ACETONE IDEAL PRESSURE	$\Delta\Pi$(EXP)-$\Delta\Pi$(CALC)
12.576	95.719	97.270	.019
12.576	107.442	109.429	.019

** These data were not included in the data treatment.

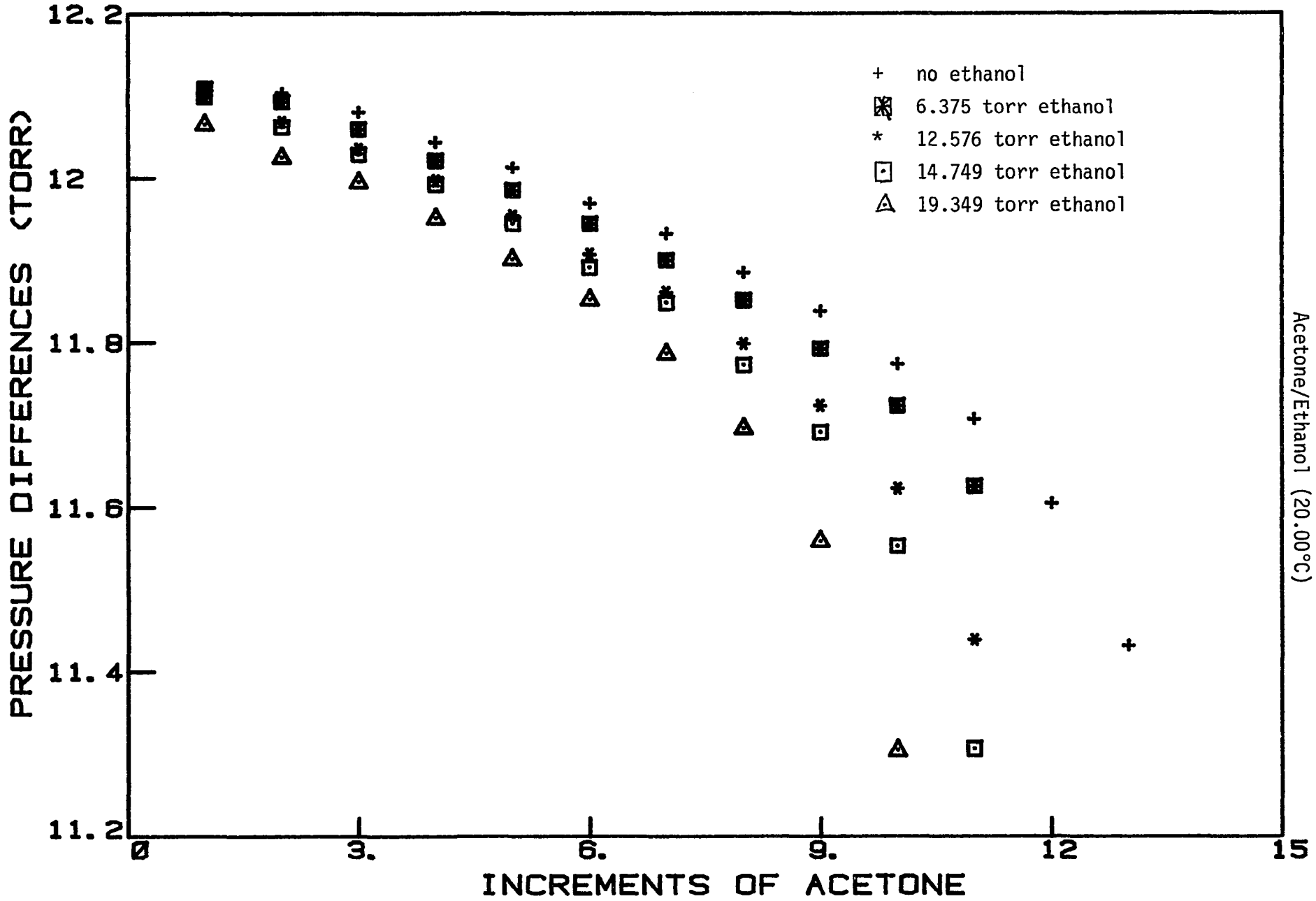

FIGURE IV-33

Acetone/Ethanol (20.00°C)

TABLE IV-41

ACETONE/ETHANOL VAPOR DENSITY DATA

AT 25.00 DEGREES CELSIUS

	INITIAL PRESSURE ETHANOL	ACETONE PRESSURE	ACETONE IDEAL PRESSURE	$\Delta\Pi$(EXP)-$\Delta\Pi$(CALC)
**	12.482	12.321	12.366	- .009
	12.482	24.615	24.732	- .001
	12.482	36.874	37.098	.000
	12.482	49.104	49.465	.008
	12.482	61.298	61.831	.010
	12.482	73.457	74.197	.015
	12.482	85.576	86.563	.016
	12.482	97.653	98.929	.017
	12.482	109.688	111.295	.020
	12.482	121.672	123.661	.018
	12.482	133.595	136.027	.009
	12.482	145.461	148.394	.010
**	13.961	12.317	12.366	- .010
	13.961	24.606	24.732	- .003
	13.961	36.865	37.098	.004
	13.961	49.091	49.465	.008
	13.961	61.282	61.831	.012
	13.961	73.440	74.197	.019
	13.961	85.552	86.563	.015
	13.961	97.623	98.929	.018
	13.961	109.648	111.295	.019
	13.961	121.629	123.661	.025
	13.961	133.548	136.027	.018
	13.961	145.404	148.394	.016
**	5.075	12.330	12.366	- .012
	5.075	24.648	24.732	.009
	5.075	36.937	37.098	.014
	5.075	49.197	49.465	.019
	5.075	61.421	61.831	.018
	5.075	73.609	74.197	.017
	5.075	85.762	86.563	.019
	5.075	97.878	98.929	.019
	5.075	110.024	111.295	.089
	5.075	121.979	123.661	- .067

TABLE IV-41 cont.

ACETONE/ETHANOL VAPOR DENSITY DATA

AT 25.00 DEGREES CELSIUS

INITIAL PRESSURE ETHANOL	ACETONE PRESSURE	ACETONE IDEAL PRESSURE	$\Delta\Pi$(EXP)-$\Delta\Pi$(CALC)
5.075	133.963	136.027	.006
5.075	145.889	148.394	- .009
** 26.416	12.284	12.366	- .023
26.416	24.526	24.732	- .026
26.416	36.735	37.098	- .019
26.416	48.906	49.465	- .015
26.416	61.040	61.831	- .008
26.416	73.127	74.197	- .009
26.416	85.165	86.563	- .008

** These data were not included in the data treatment.

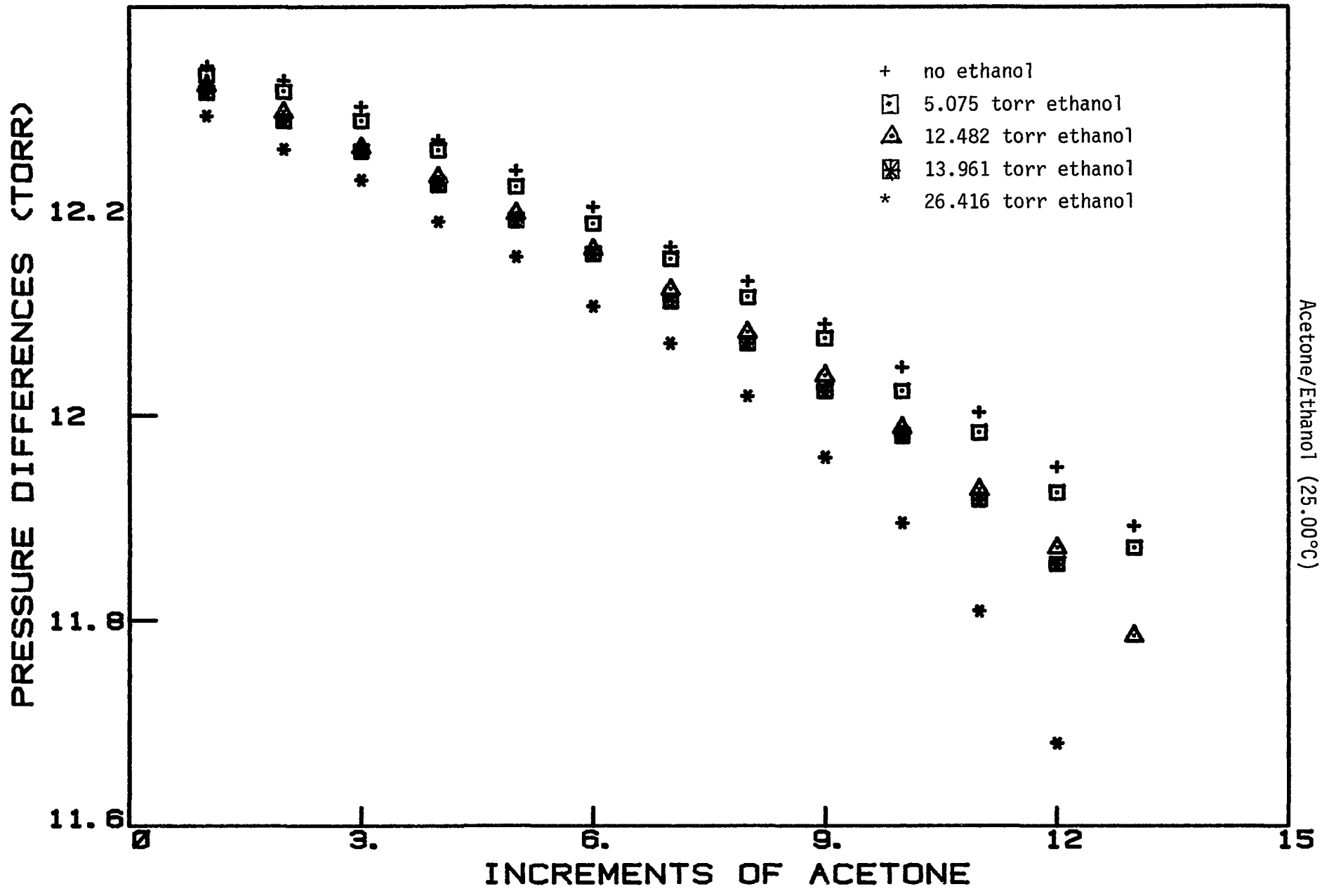

FIGURE IV-34

Acetone/Ethanol (25.00°C)

TABLE IV-42

ACETONE/ETHANOL VAPOR DENSITY DATA

AT 30.00 DEGREES CELSIUS

	INITIAL PRESSURE ETHANOL	ACETONE PRESSURE	ACETONE IDEAL PRESSURE	$\Delta\Pi$(EXP)-$\Delta\Pi$(CALC)
**	10.017	12.533	12.574	- .011
	10.017	25.046	25.147	.000
	10.017	37.540	37.721	.014
	10.017	50.000	50.294	.012
	10.017	62.429	62.868	.014
	10.017	74.823	75.441	.013
	10.017	87.192	88.015	.022
	10.017	99.517	100.588	.013
	10.017	111.810	113.162	.016
	10.017	124.069	125.735	.018
	10.017	136.281	138.309	.008
	10.017	148.462	150.882	.016
	10.017	160.598	163.456	.010
	10.017	172.688	176.029	.004
	10.017	184.722	188.603	- .010
**	21.916	12.495	12.574	- .033
	21.916	24.969	25.147	- .020
	21.916	37.409	37.721	- .020
	21.916	49.831	50.294	- .003
	21.916	62.215	62.868	- .005
	21.916	74.565	75.441	- .003
	21.916	86.883	88.015	.003
	21.916	99.161	100.588	.002
	21.916	111.404	113.162	.007
	21.916	123.600	125.735	.001
	21.916	135.765	138.309	.014
	21.916	147.870	150.882	- .002
	21.916	159.933	163.456	.004
	21.916	171.942	176.029	.001
	21.916	183.880	188.603	- .017
**	6.918	12.535	12.574	- .014
	6.918	25.058	25.147	.006
	6.918	37.557	37.721	.013
	6.918	50.024	50.294	.013

TABLE IV-42 cont.

ACETONE/ETHANOL VAPOR DENSITY DATA

AT 30.00 DEGREES CELSIUS

INITIAL PRESSURE ETHANOL	ACETONE PRESSURE	ACETONE IDEAL PRESSURE	$\Delta\Pi$(EXP)-$\Delta\Pi$(CALC)
6.918	62.464	62.868	.019
6.918	74.872	75.441	.019
6.918	87.246	88.015	.019
6.918	99.585	100.588	.017
6.918	111.892	113.162	.020
6.918	124.159	125.735	.014
6.918	136.391	138.309	.015
6.918	148.576	150.882	.003
6.918	160.730	163.456	.010
6.918	172.840	176.029	.004
6.918	184.900	188.603	- .007
** 15.567	12.515	12.574	- .022
15.567	25.012	25.147	- .007
15.567	37.481	37.721	- .002
15.567	49.922	50.294	.004
15.567	62.331	62.868	.006
15.567	74.700	75.441	.001
15.567	87.047	88.015	.015
15.567	99.354	100.588	.012
15.567	111.625	113.162	.013
15.567	123.856	125.735	.012
15.567	136.046	138.309	.011
15.567	148.279	150.882	.099
15.567	160.295	163.456	- .082
15.567	172.358	176.029	.014
15.567	184.361	188.603	.002

** These data were not included in the data treatment.

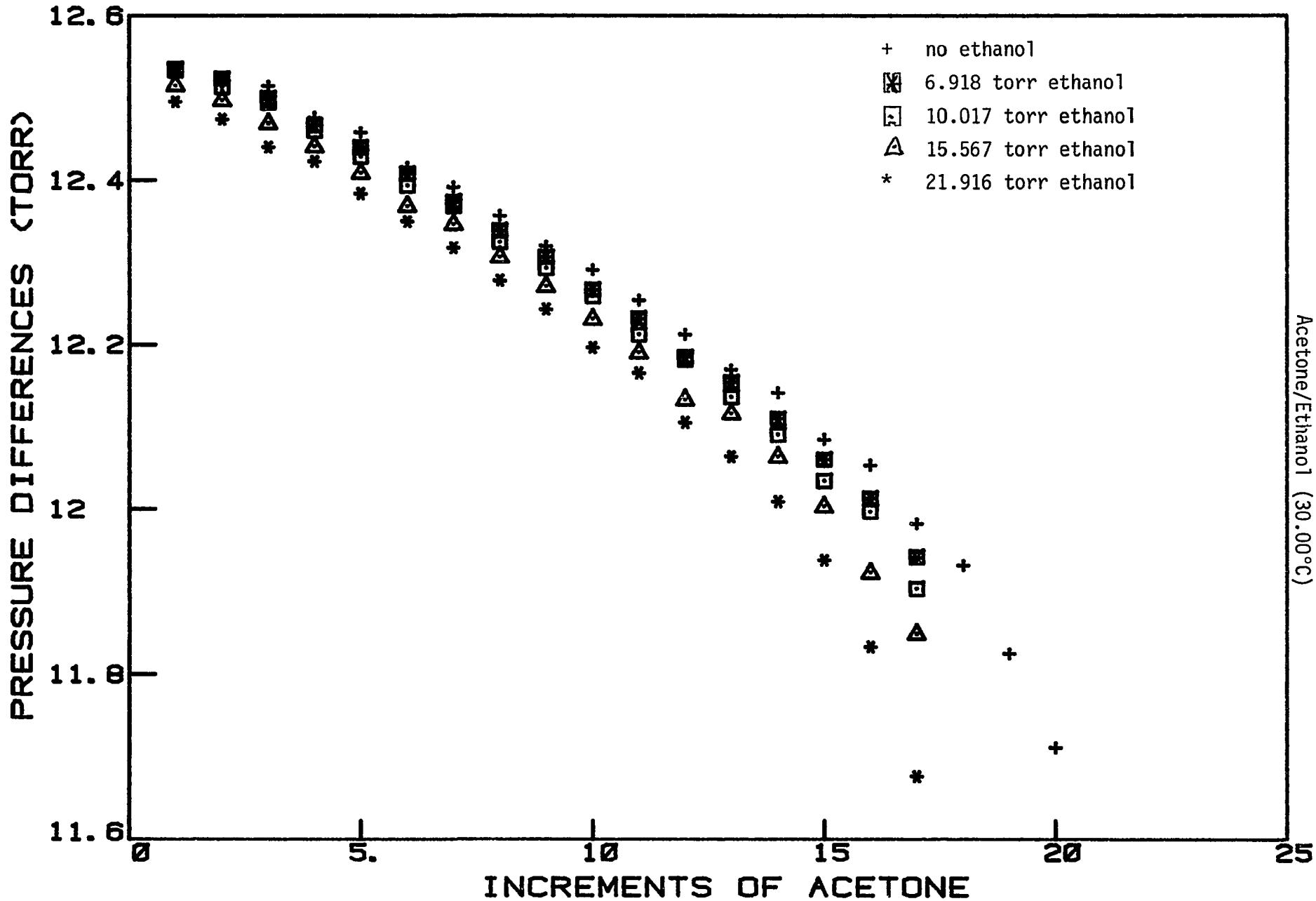

FIGURE IV-35

Acetone/Ethanol (30.00°C)

TABLE IV-43

ACETONE/ETHANOL VAPOR DENSITY DATA

AT 34.79 DEGREES CELSIUS

	INITIAL PRESSURE ETHANOL	ACETONE PRESSURE	ACETONE IDEAL PRESSURE	$\Delta\Pi$(EXP)-$\Delta\Pi$(CALC)
**	6.273	12.729	12.772	- .021
	6.273	25.449	25.544	- .001
	6.273	38.145	38.317	.005
	6.273	50.819	51.089	.013
	6.273	63.462	63.861	.012
	6.273	76.072	76.633	.009
	6.273	88.662	89.405	.020
	6.273	101.212	102.177	.010
	6.273	113.732	114.950	.011
	6.273	126.222	127.722	.013
	6.273	138.675	140.494	.007
	6.273	151.095	153.266	.006
	6.273	163.478	166.038	.001
	6.273	175.832	178.811	.005
	6.273	188.148	191.583	- .000
	6.273	200.425	204.355	- .006
**	9.670	12.719	12.772	- .027
	9.670	25.433	25.544	- .002
	9.670	38.120	38.317	.000
	9.670	50.784	51.089	.008
	9.670	63.418	63.861	.008
	9.670	76.023	76.633	.010
	9.670	88.600	89.405	.013
	9.670	101.144	102.177	.012
	9.670	113.655	114.950	.010
	9.670	126.129	127.722	.005
	9.670	138.576	140.494	.011
	9.670	150.980	153.266	.000
	9.670	163.355	166.038	.005
	9.670	175.702	178.811	.011
	9.670	188.000	191.583	- .005
	9.670	200.271	204.355	.003
**	15.059	12.721	12.772	- .019
	15.059	25.423	25.544	- .007

TABLE IV-43 cont.

ACETONE/ETHANOL VAPOR DENSITY DATA

AT 34.79 DEGREES CELSIUS

	INITIAL PRESSURE ETHANOL	ACETONE PRESSURE	ACETONE IDEAL PRESSURE	$\Delta\Pi$(EXP)-$\Delta\Pi$(CALC)
	15.059	38.098	38.317	- .004
	15.059	50.750	51.089	.004
	15.059	63.369	63.861	.002
	15.059	75.958	76.633	.004
	15.059	88.517	89.405	.006
	15.059	101.045	102.177	.007
	15.059	113.541	114.950	.008
	15.059	126.003	127.722	.007
	15.059	138.425	140.494	.001
	15.059	150.814	153.266	.002
	15.059	163.173	166.038	.007
	15.059	175.494	178.811	.004
	15.059	187.778	191.583	.003
	15.059	200.025	204.355	.003
**	19.591	12.703	12.772	- .031
	19.591	25.387	25.544	- .020
	19.591	38.047	38.317	- .013
	19.591	50.682	51.089	- .006
	19.591	63.286	63.861	- .005
	19.591	75.864	76.633	.001
	19.591	88.405	89.405	- .004
	19.591	100.925	102.177	.009
	19.591	113.397	114.950	- .006
	19.591	125.838	127.722	- .003
	19.591	138.253	140.494	.006
	19.591	150.627	153.266	.000
	19.591	162.966	166.038	.002
	19.591	175.261	178.811	- .006
	19.591	187.521	191.583	- .003
	19.591	199.744	204.355	- .001

** These data were not included in the data treatment.

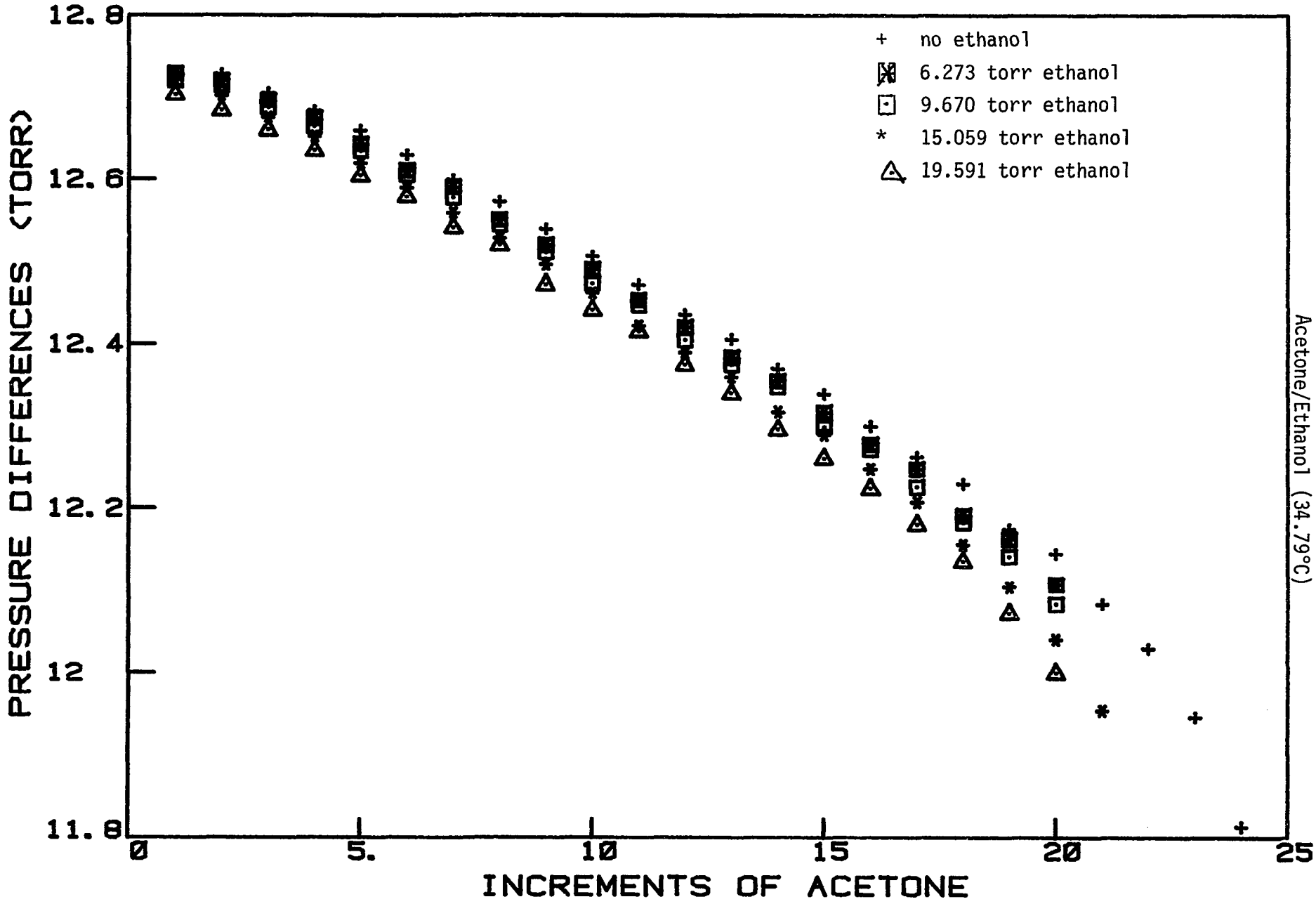

FIGURE IV-36

Acetone/Ethanol (34.79°C)

TABLE IV-44

ACETONE/ETHANOL VAPOR DENSITY DATA

AT 40.06 DEGREES CELSIUS

	INITIAL PRESSURE ETHANOL	ACETONE PRESSURE	ACETONE IDEAL PRESSURE	$\Delta\Pi$(EXP)-$\Delta\Pi$(CALC)
**	6.152	12.954	12.991	- .017
	6.152	25.901	25.982	.004
	6.152	38.819	38.972	.003
	6.152	51.715	51.963	.009
	6.152	64.583	64.954	.009
	6.152	77.424	77.945	.010
	6.152	90.237	90.935	.011
	6.152	103.024	103.926	.014
	6.152	115.779	116.917	.010
	6.152	128.495	129.908	.000
	6.152	141.191	142.898	.010
	6.152	153.848	155.889	- .000
	6.152	166.476	168.880	.000
	6.152	179.074	181.871	.000
	6.152	191.637	194.861	- .005
	6.152	204.173	207.852	- .002
	6.152	216.674	220.843	- .007
	6.152	229.147	233.834	- .004
	6.152	241.579	246.824	- .015
**	15.520	12.930	12.991	- .031
	15.520	25.842	25.982	- .021
	15.520	38.749	38.972	.003
	15.520	51.630	51.963	.005
	15.520	64.473	64.954	- .004
	15.520	77.290	77.945	- .001
	15.520	90.078	90.935	- .001
	15.520	102.856	103.926	.019
	15.520	115.579	116.917	- .006
	15.520	128.277	129.908	- .001
	15.520	140.942	142.898	- .004
	15.520	153.580	155.889	- .000
	15.520	166.193	168.880	.006
	15.520	178.766	181.871	- .004
	15.520	191.313	194.861	.002

TABLE IV-44 cont.

ACETONE/ETHANOL VAPOR DENSITY DATA

AT 40.06 DEGREES CELSIUS

	INITIAL PRESSURE ETHANOL	ACETONE PRESSURE	ACETONE IDEAL PRESSURE	$\Delta\Pi$(EXP)-$\Delta\Pi$(CALC)
	15.520	203.818	207.852	- .009
	15.520	216.308	220.843	.009
	15.520	228.735	233.834	- .023
	15.520	241.148	246.824	- .004
**	11.069	12.938	12.991	- .028
	11.069	25.871	25.982	- .005
	11.069	38.793	38.972	.012
	11.069	51.679	51.963	.005
	11.069	64.552	64.954	.020
	11.069	77.397	77.945	.021
	11.069	90.193	90.935	.001
	11.069	102.979	103.926	.020
	11.069	115.717	116.917	.002
	11.069	128.444	129.908	.021
	11.069	141.117	142.898	- .004
	11.069	153.783	155.889	.019
	11.069	166.419	168.880	.020
	11.069	179.022	181.871	.017
	11.069	191.589	194.861	.012
	11.069	204.127	207.852	.014
	11.069	216.632	220.843	.012
	11.069	229.088	233.834	- .006
	11.069	241.508	246.824	- .010

** These data were not included in the data treatment.

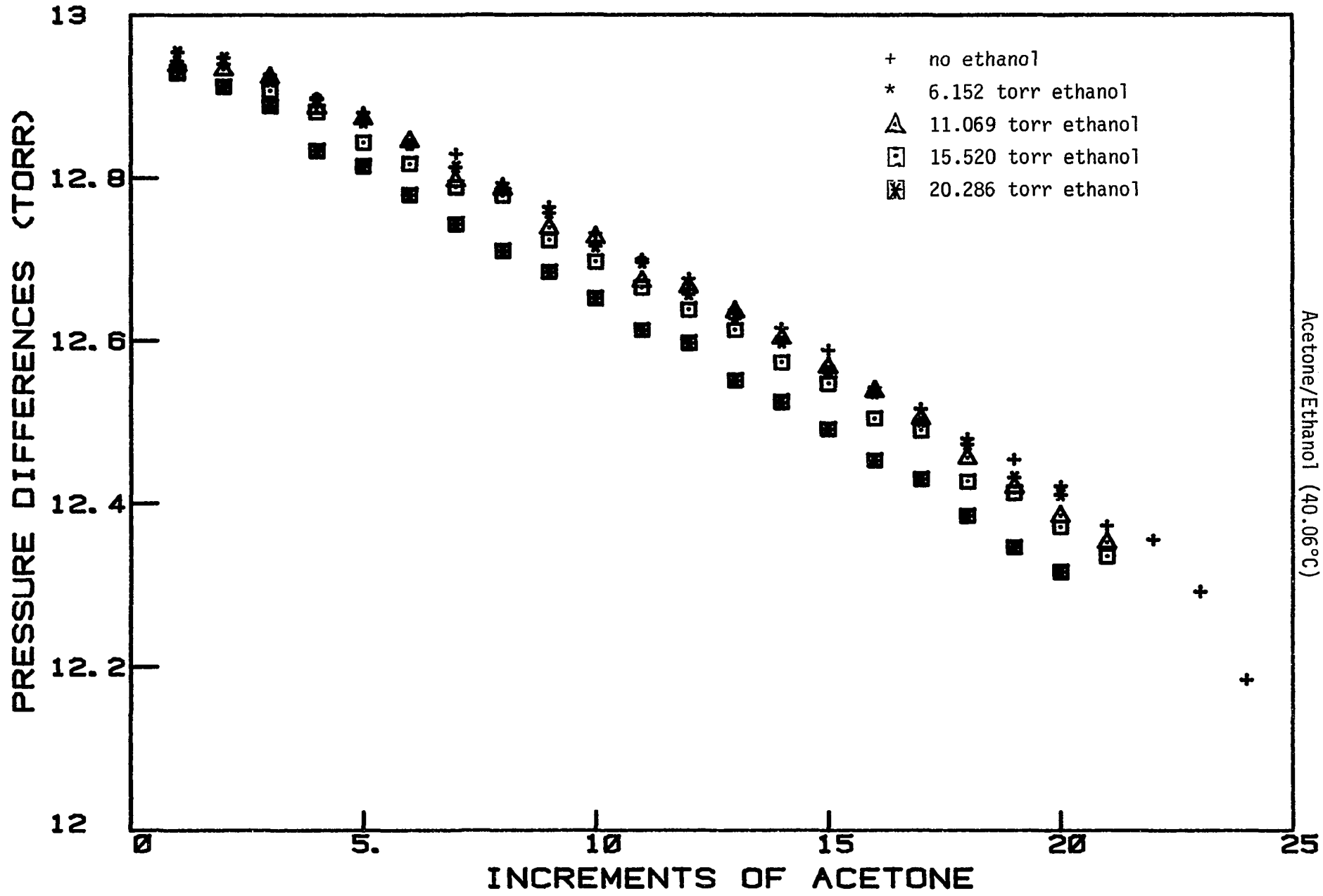

FIGURE IV-37

Acetone/Ethanol (40.06°C)

TABLE IV-45

ACETONE/ETHANOL VAPOR DENSITY DATA

AT 44.96 DEGREES CELSIUS

INITIAL PRESSURE ETHANOL	ACETONE PRESSURE	ACETONE IDEAL PRESSURE	$\Delta\Pi$(EXP)-$\Delta\Pi$(CALC)
** 19.385	13.150	13.194	- .013
19.385	26.269	26.388	- .018
19.385	39.377	39.582	- .002
19.385	52.444	52.776	- .016
19.385	65.494	65.970	- .005
19.385	78.532	79.164	.010
19.385	91.523	92.358	- .009
19.385	104.489	105.552	- .006
19.385	117.444	118.746	.011
19.385	130.350	131.940	- .010
19.385	143.228	145.134	- .010
19.385	156.116	158.328	.030
19.385	168.956	171.522	.010
19.385	181.745	184.716	- .013
19.385	194.509	197.910	- .008
19.385	207.238	211.104	- .014
19.385	219.934	224.298	- .018
19.385	232.602	237.492	- .016
19.385	245.277	250.686	.022
** 10.638	13.165	13.194	- .006
10.638	26.292	26.388	- .018
10.638	39.407	39.582	- .003
10.638	52.493	52.776	- .006
10.638	65.556	65.970	- .002
10.638	78.598	79.164	.004
10.638	91.611	92.358	.003
10.638	104.594	105.552	- .000
10.638	117.545	118.746	- .005
10.638	130.392	131.940	- .083
10.638	143.367	145.134	.077
10.638	156.228	158.328	- .011
10.638	169.066	171.522	- .006
10.638	181.869	184.716	- .013
10.638	194.647	197.910	- .009

TABLE IV-45 cont.

ACETONE/ETHANOL VAPOR DENSITY DATA

AT 44.96 DEGREES CELSIUS

INITIAL PRESSURE ETHANOL	ACETONE PRESSURE	ACETONE IDEAL PRESSURE	$\Delta\Pi$(EXP)-$\Delta\Pi$(CALC)
10.638	207.397	211.104	- .009
10.638	220.114	224.298	- .013
10.638	232.806	237.492	- .009
10.638	245.471	250.686	- .007

** These data were not included in the data treatment.

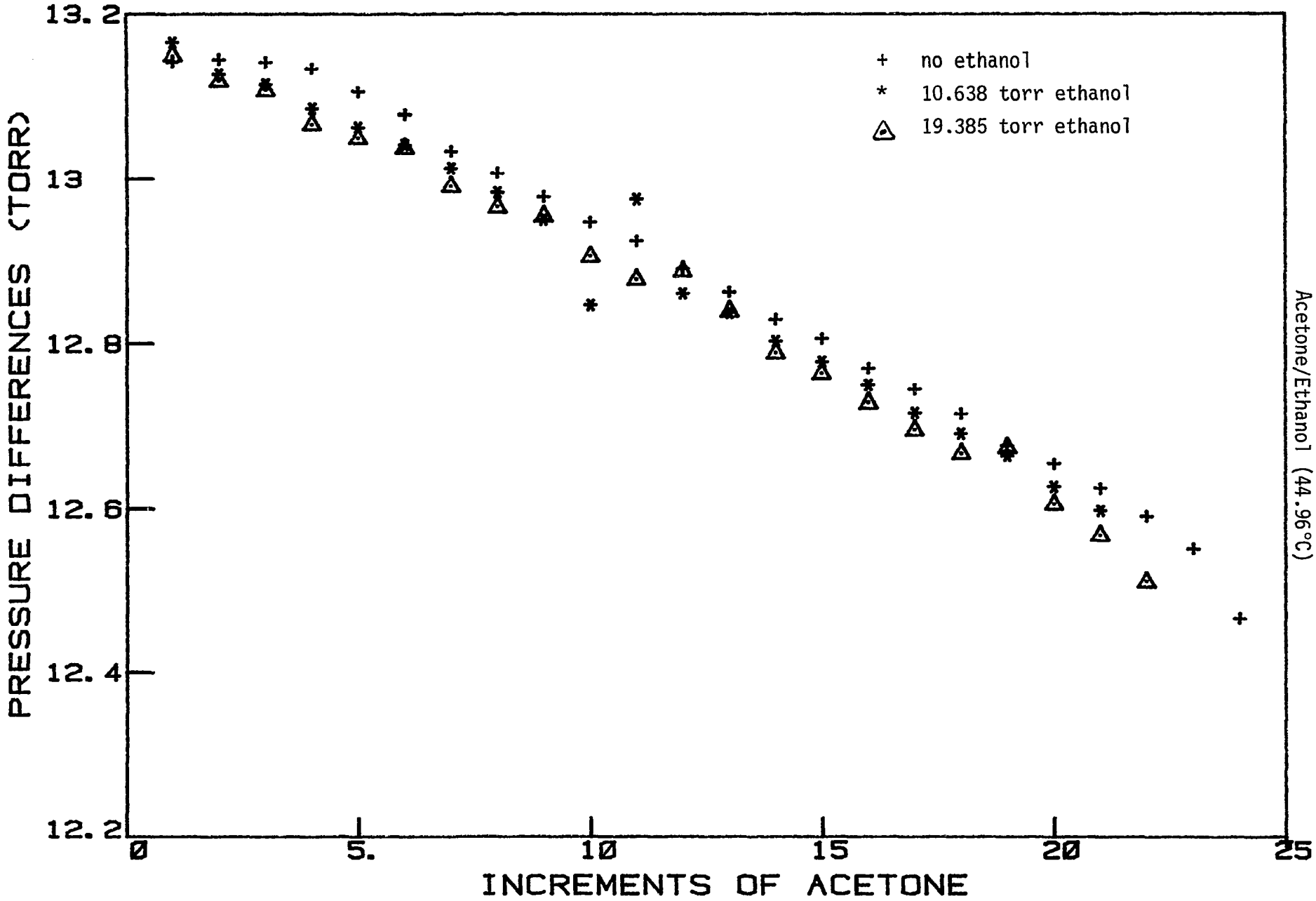

FIGURE IV-38

Acetone/Ethanol (44.96°C)

TABLES IV-46

ETHANOL KEYES POINTS

T(°K)	Vapor P	Vapor II	Amounted Associated (EtOH=20 torr)	Effect on A-EtOH (torr)
288.12	32.172	32.624	0.174	0.006
293.15	43.886	44.476	0.123	0.004
298.15	59.023	59.817	0.092	0.003
303.15	78.470	79.570	0.072	0.002
307.94	102.038	103.579	0.060	0.002
313.21	134.745	137.026	0.051	0.002
318.11	172.817	176.113	0.045	0.001

viii-8. Acetone/2-Butanol

Pressure-density data for the acetone/2-butanol system were collected on the automated vapor-density apparatus at temperatures between 25°C and 45°C. Initial pressures of 2-butanol for three experiments at each temperature were about 5 torr, 10 torr, and 15 torr. Data are presented in Tables IV-47 through IV-51 and are plotted as difference in pressure vs. increments of acetone added at each temperature in figures IV-39 through IV-43.

The first two points of each data set are omitted in the data analysis. The pressure differences at these points were greater than the pressure differences of the first two points of the pure acetone, indicating a desorption of 2-butanol from the stainless steel walls of the sample cylinder in the presence of acetone.

Analysis of the 252 vapor density measurements is, again, identical to the analysis of the acetone/methanol system. Values of $K_{11}^{25°}$, $K_{\infty}^{25°}$, ΔH_{11}, and ΔH_{∞} are obtained using the NLLSQ program and are presented in Table IV-13. Deviations between the calculated ideal pressure differences and the experimental ideal pressure differences (i.e. loop size) for each point are included in the data tables. The overall RMSD is 0.015 torr.

TABLE IV-47

ACETONE/2-BUTANOL VAPOR DENSITY DATA

AT 25.00 DEGREES CELSIUS

INITIAL PRESSURE 2-BUTANOL	ACETONE PRESSURE	ACETONE IDEAL PRESSURE	$\Delta\Pi$(EXP)-$\Delta\Pi$(CALC)
** 11.140	10.534	10.538	.022
** 11.140	21.017	21.077	- .003
11.140	31.469	31.615	- .007
11.140	41.898	42.153	- .003
11.140	52.292	52.691	- .010
11.140	62.660	63.230	- .006
11.140	72.998	73.768	- .004
11.140	83.302	84.306	- .005
11.140	93.569	94.845	- .005
11.140	103.794	105.383	- .007
11.140	113.969	115.921	- .012
11.140	124.070	126.459	- .033
** 12.327	10.536	10.538	.026
** 12.327	21.021	21.077	.001
12.327	31.482	31.615	.004
12.327	41.909	42.153	- .002
12.327	52.309	52.691	- .000
12.327	62.679	63.230	.000
12.327	73.021	73.768	.004
12.327	83.330	84.306	.006
12.327	93.603	94.845	.008
12.327	103.836	105.383	.010
12.327	114.019	115.921	.008
12.327	124.141	126.459	.004
12.327	134.182	136.998	- .010
** 15.978	10.512	10.538	.007
** 15.978	20.976	21.077	- .014
15.978	31.410	31.615	- .016
15.978	41.810	42.153	- .022
15.978	52.170	52.691	- .031
15.978	62.499	63.230	- .030
15.978	72.786	73.768	- .038
15.978	83.013	84.306	- .061
15.978	93.182	94.845	- .078

** These data were not included in the data treatment.

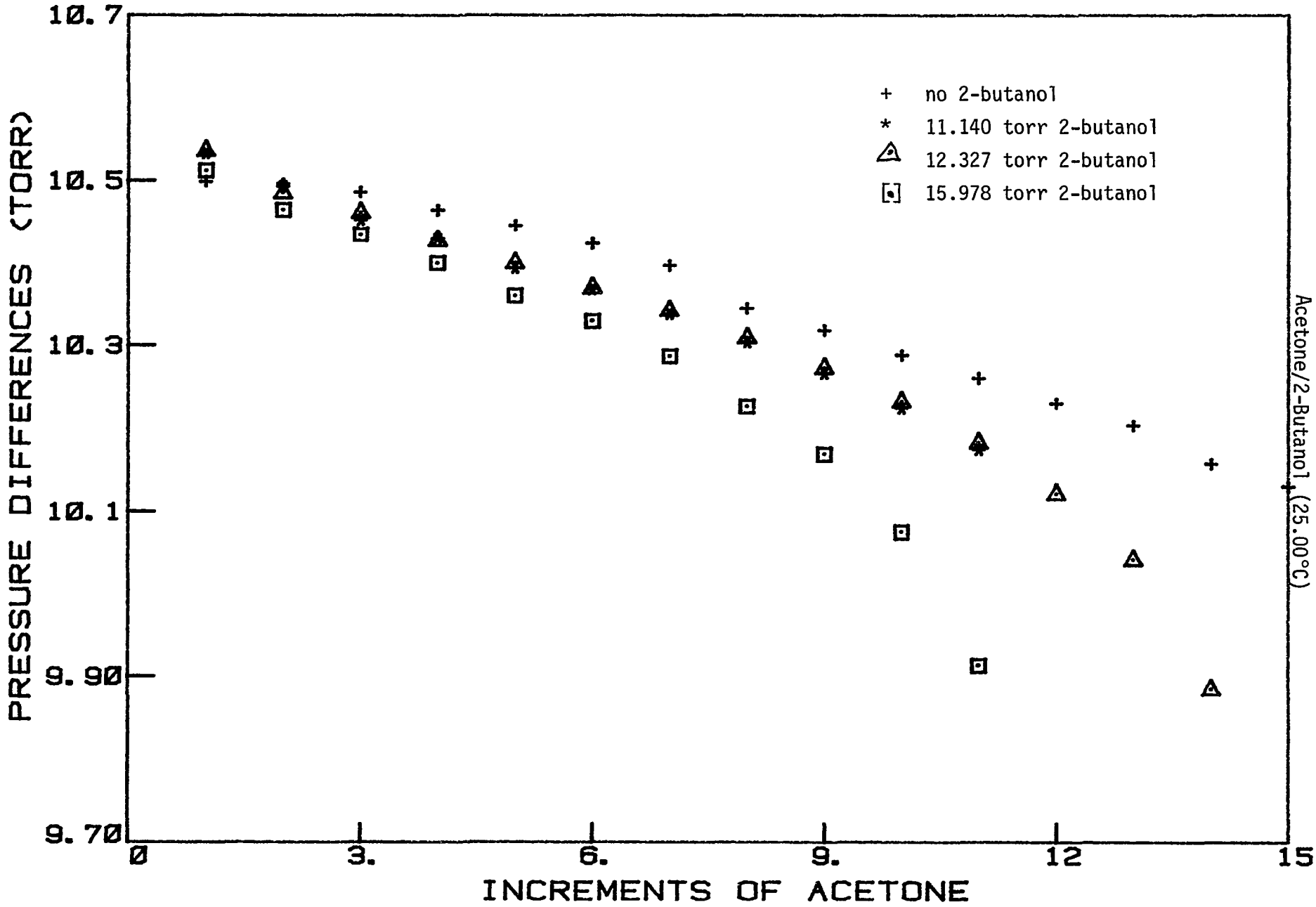

FIGURE IV-39

Acetone/2-Butanol (25.00°C)

TABLE IV-48

ACETONE/2-BUTANOL VAPOR DENSITY DATA

AT 29.93 DEGREES CELSIUS

	INITIAL PRESSURE 2-BUTANOL	ACETONE PRESSURE	ACETONE IDEAL PRESSURE	$\Delta\Pi$(EXP)-$\Delta\Pi$(CALC)
**	6.486	10.767	10.790	- .004
**	6.486	21.525	21.580	.010
	6.486	32.261	32.370	.012
	6.486	42.974	43.160	.013
	6.486	53.667	53.950	.017
	6.486	64.334	64.740	.015
	6.486	74.982	75.531	.021
	6.486	85.604	86.321	.021
	6.486	96.200	97.111	.021
	6.486	106.770	107.901	.021
	6.486	117.314	118.691	.023
	6.486	127.829	129.481	.022
	6.486	138.324	140.271	.031
	6.486	148.784	151.061	.027
	6.486	159.215	161.851	.030
	6.486	169.617	172.641	.036
	6.486	179.994	183.431	.048
**	11.302	10.772	10.790	.007
**	11.302	21.507	21.580	- .006
	11.302	32.217	32.370	- .007
	11.302	42.907	43.160	- .002
	11.302	53.572	53.950	- .002
	11.302	64.211	64.740	- .002
	11.302	74.827	75.531	.002
	11.302	85.417	86.321	.003
	11.302	95.985	97.111	.009
	11.302	106.520	107.901	.005
	11.302	117.027	118.691	.007
	11.302	127.511	129.481	.015
	11.302	137.956	140.271	.010
	11.302	148.373	151.061	.017
	11.302	158.745	161.851	.010
**	14.517	10.775	10.790	.014
**	14.517	21.508	21.580	- .003

TABLE IV-48 cont.

ACETONE/2-BUTANOL VAPOR DENSITY DATA

AT 29.93 DEGREES CELSIUS

INITIAL PRESSURE 2-BUTANOL	ACETONE PRESSURE	ACETONE IDEAL PRESSURE	$\Delta\Pi$(EXP)-$\Delta\Pi$(CALC)
14.517	32.212	32.370	- .007
14.517	42.893	43.160	- .005
14.517	53.555	53.950	.002
14.517	64.194	64.740	.006
14.517	74.807	75.531	.007
14.517	85.398	86.321	.014
14.517	95.956	97.111	.010
14.517	106.488	107.901	.014
14.517	116.995	118.691	.022
14.517	127.473	129.481	.027
14.517	137.918	140.271	.030
14.517	148.332	151.061	.038
14.517	158.711	161.851	.046

** These data were not included in the data treatment.

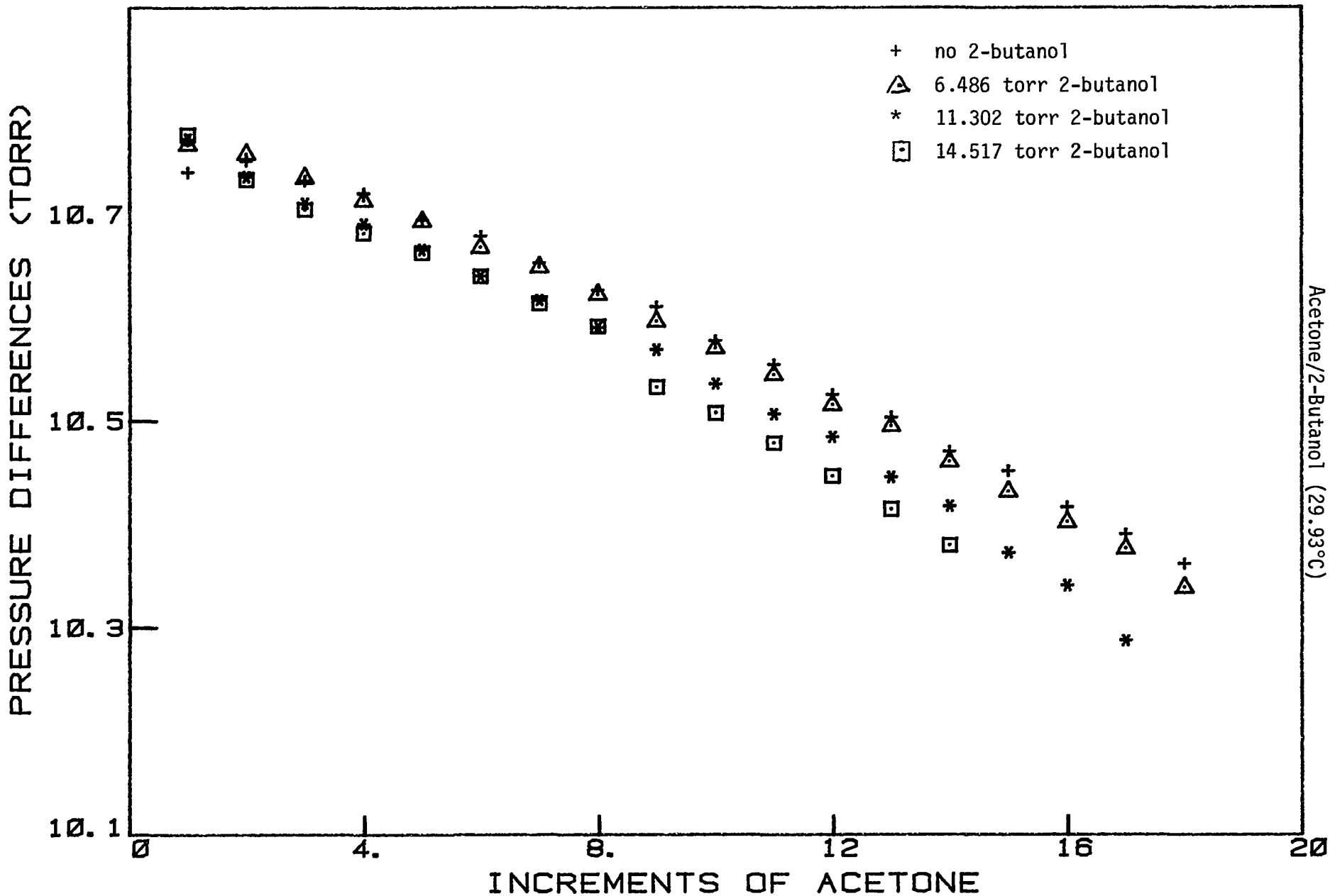

FIGURE IV-40

Acetone/2-Butanol (29.93°C)

TABLE IV-49

ACETONE/2-BUTANOL VAPOR DENSITY DATA

AT 33.94 DEGREES CELSIUS

INITIAL PRESSURE 2-BUTANOL	ACETONE PRESSURE	ACETONE IDEAL PRESSURE	$\Delta\Pi$(EXP)-$\Delta\Pi$(CALC)
** 7.904	10.927	10.933	.014
** 7.904	21.823	21.866	.005
7.904	32.701	32.799	.010
7.904	43.559	43.731	.012
7.904	54.400	54.664	.018
7.904	65.217	65.597	.017
7.904	76.007	76.530	.014
7.904	86.773	87.463	.013
7.904	97.518	98.396	.016
7.904	108.230	109.328	.007
7.904	118.917	120.261	.007
7.904	129.584	131.194	.012
7.904	140.220	142.127	.006
7.904	150.833	153.060	.009
7.904	161.422	163.993	.012
7.904	171.987	174.925	.015
7.904	182.518	185.858	.009
7.904	193.022	196.791	.010
7.904	203.494	207.724	.008
7.904	213.932	218.657	.005
7.904	224.334	229.590	.001
7.904	234.694	240.522	- .008
** 12.542	10.932	10.933	.025
** 12.542	21.819	21.866	.002
12.542	32.685	32.799	.004
12.542	43.535	43.731	.012
12.542	54.357	54.664	.007
12.542	65.156	65.597	.008
12.542	75.930	76.530	.007
12.542	86.681	87.463	.009
12.542	97.401	98.396	.002
12.542	108.094	109.328	.001
12.542	118.767	120.261	.007
12.542	129.409	131.194	.002

TABLE IV-49 cont.

ACETONE/2-BUTANOL VAPOR DENSITY DATA

AT 33.94 DEGREES CELSIUS

	INITIAL PRESSURE 2-BUTANOL	ACETONE PRESSURE	ACETONE IDEAL PRESSURE	$\Delta\Pi$(EXP)-$\Delta\Pi$(CALC)
	12.542	140.025	142.127	.003
	12.542	150.616	153.060	.006
	12.542	161.177	163.993	.005
	12.542	171.708	174.925	.004
	12.542	182.210	185.858	.006
	12.542	192.674	196.791	- .000
	12.542	203.097	207.724	- .008
	12.542	213.468	218.657	- .026
**	16.086	10.910	10.933	.007
**	16.086	21.779	21.866	- .011
	16.086	32.629	32.799	- .007
	16.086	43.458	43.731	- .004
	16.086	54.259	54.664	- .008
	16.086	65.044	65.597	.000
	16.086	75.801	76.530	- .003
	16.086	86.535	87.463	- .001
	16.086	97.245	98.396	.001
	16.086	107.927	109.328	- .001
	16.086	118.586	120.261	.003
	16.086	129.218	131.194	.004
	16.086	139.823	142.127	.005
	16.086	150.398	153.060	.004
	16.086	160.952	163.993	.014
	16.086	171.470	174.925	.009
	16.086	181.954	185.858	.008
	16.086	192.406	196.791	.011
	16.086	202.809	207.724	- .002
	16.086	213.164	218.657	- .012

** These data were not included in the data treatment.

FIGURE IV-41

Acetone/2-Butanol (33.94°C)

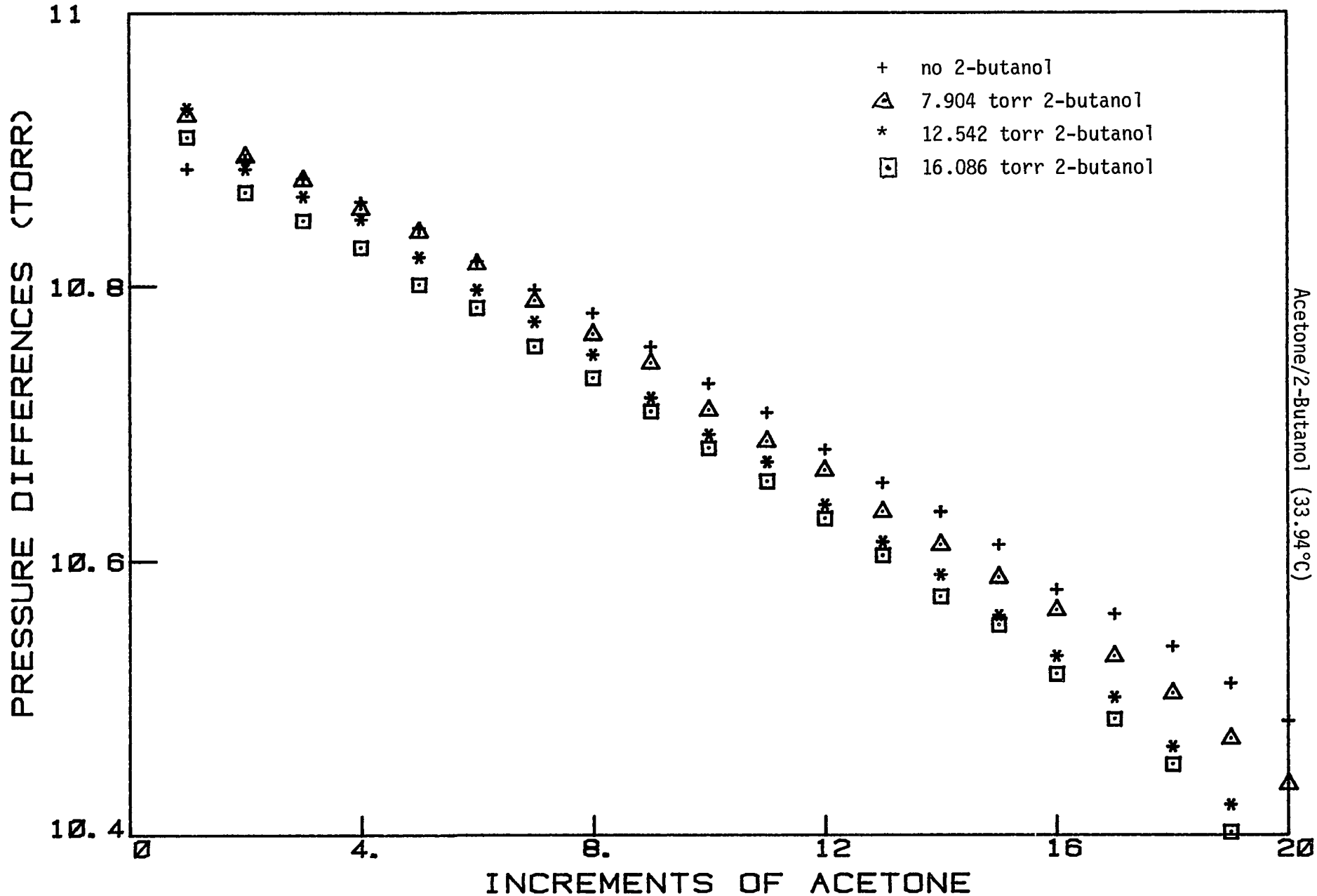

TABLE IV-50

ACETONE/2-BUTANOL VAPOR DENSITY DATA

AT 39.95 DEGREES CELSIUS

INITIAL PRESSURE 2-BUTANOL		ACETONE PRESSURE	ACETONE IDEAL PRESSURE	$\Delta\Pi$(EXP)-$\Delta\Pi$(CALC)
**	5.006	11.120	11.147	- .011
**	5.006	22.228	22.294	- .003
	5.006	33.317	33.440	- .001
	5.006	44.394	44.587	.007
	5.006	55.452	55.734	.009
	5.006	66.490	66.881	.010
	5.006	77.510	78.028	.013
	5.006	88.504	89.174	.008
	5.006	99.482	100.321	.013
	5.006	110.427	111.468	.002
	5.006	121.360	122.615	.011
	5.006	132.266	133.762	.006
	5.006	143.151	144.908	.007
	5.006	154.018	156.055	.011
	5.006	164.857	167.202	.005
	5.006	175.679	178.349	.010
	5.006	186.471	189.496	.002
	5.006	197.245	200.642	.007
	5.006	207.992	211.789	.002
	5.006	218.713	222.936	- .001
	5.006	229.414	234.083	.002
	5.006	240.092	245.230	.002
	5.006	250.744	256.376	- .000
	5.006	261.370	267.523	- .003
**	9.288	11.129	11.147	.002
**	9.288	22.240	22.294	.005
	9.288	33.328	33.440	.003
	9.288	44.400	44.587	.008
	9.288	55.454	55.734	.011
	9.288	66.481	66.881	.005
	9.288	77.493	78.028	.012
	9.288	88.483	89.174	.011
	9.288	99.446	100.321	.006
	9.288	110.387	111.468	.006

TABLE IV-50 cont.

ACETONE/2-BUTANOL VAPOR DENSITY DATA

AT 39.95 DEGREES CELSIUS

INITIAL PRESSURE 2-BUTANOL	ACETONE PRESSURE	ACETONE IDEAL PRESSURE	$\Delta\Pi$(EXP)-$\Delta\Pi$(CALC)
9.288	121.309	122.615	.009
9.288	132.207	133.762	.007
9.288	143.083	144.908	.007
9.288	153.937	156.055	.008
9.288	164.767	167.202	.007
9.288	175.578	178.349	.011
9.288	186.363	189.496	.008
9.288	197.119	200.642	.002
9.288	207.849	211.789	- .000
9.288	218.552	222.936	- .004
9.288	229.236	234.083	.002
9.288	239.900	245.230	.006
9.288	250.532	256.376	- .001
** 15.422	11.131	11.147	.011
** 15.422	22.223	22.294	- .007
15.422	33.293	33.440	- .008
15.422	44.347	44.587	- .002
15.422	55.378	55.734	- .004
15.422	66.391	66.881	.000
15.422	77.378	78.028	- .004
15.422	88.349	89.174	.002
15.422	99.294	100.321	- .002
15.422	110.214	111.468	- .004
15.422	121.114	122.615	- .001
15.422	131.991	133.762	- .001
15.422	142.843	144.908	- .003
15.422	153.675	156.055	.000
15.422	164.481	167.202	- .002
15.422	175.262	178.349	- .003
15.422	186.022	189.496	.000
15.422	196.757	200.642	- .000
15.422	207.466	211.789	- .001
15.422	218.142	222.936	- .009
15.422	228.796	234.083	- .005
15.422	239.421	245.230	- .008

** These data were not included in the data treatment.

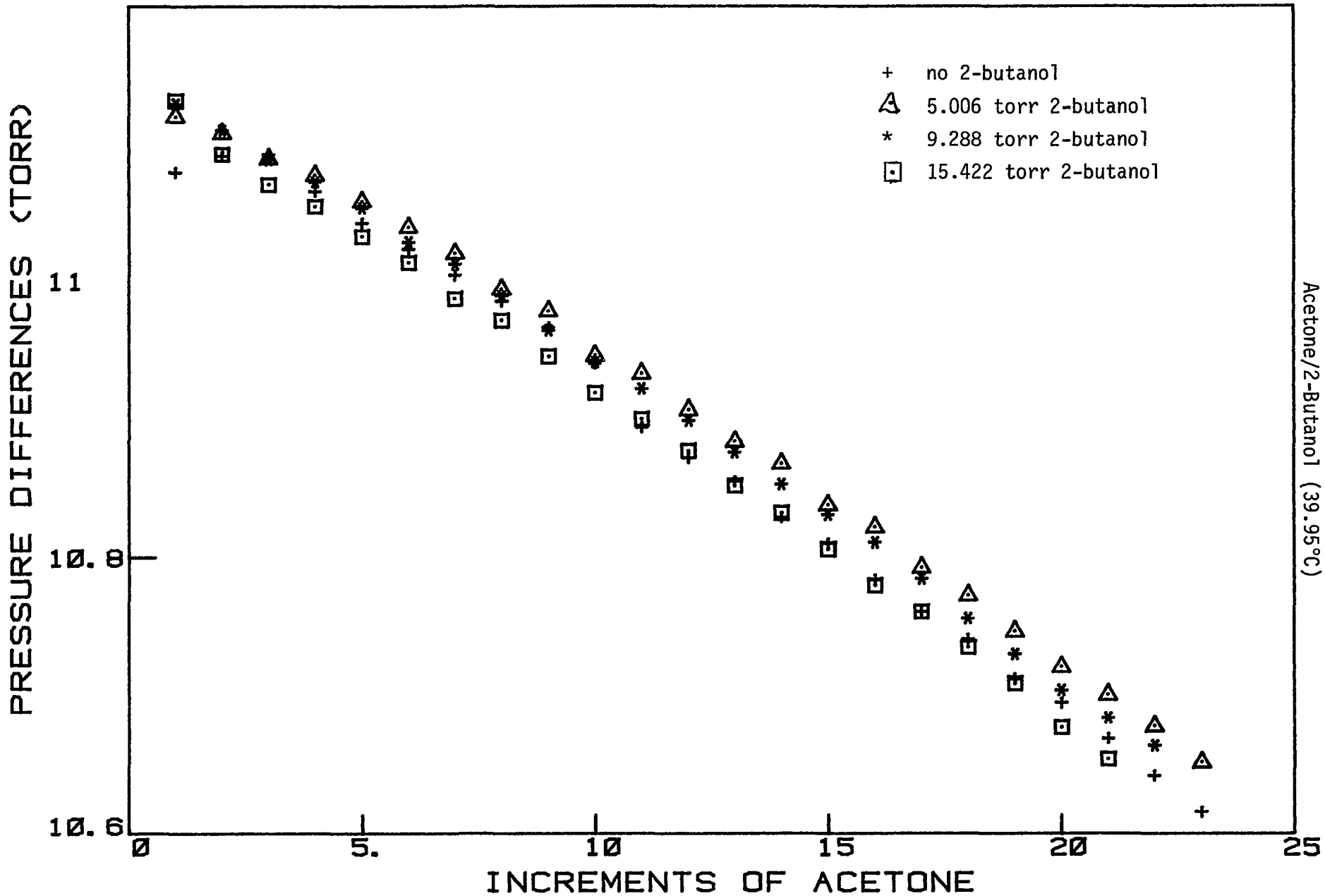

FIGURE IV-42

Acetone/2-Butanol (39.95°C)

TABLE IV-51

ACETONE/2-BUTANOL VAPOR DENSITY DATA

AT 44.91 DEGREES CELSIUS

INITIAL PRESSURE 2-BUTANOL	ACETONE PRESSURE	ACETONE IDEAL PRESSURE	$\Delta\Pi$(EXP)-$\Delta\Pi$(CALC)
** 7.003	11.310	11.323	.003
** 7.003	22.603	22.647	.006
7.003	33.879	33.970	.008
7.003	45.138	45.294	.011
7.003	56.376	56.617	.010
7.003	67.597	67.940	.013
7.003	78.801	79.264	.016
7.003	89.984	90.587	.015
7.003	101.149	101.910	.017
7.003	112.287	113.234	.010
7.003	123.410	124.557	.016
7.003	134.502	135.881	.005
7.003	145.586	147.204	.018
7.003	156.642	158.527	.011
7.003	167.655	169.851	- .012
7.003	178.665	181.174	.006
7.003	189.648	192.497	.000
7.003	200.616	203.821	.006
7.003	211.565	215.144	.009
7.003	222.495	226.468	.011
7.003	233.404	237.791	.012
7.003	244.282	249.114	.002
7.003	255.147	260.438	.011
** 9.612	11.316	11.323	.012
** 9.612	22.602	22.647	.002
9.612	33.873	33.970	.006
9.612	45.122	45.294	.004
9.612	56.356	56.617	.009
9.612	67.569	67.940	.008
9.612	78.765	79.264	.011
9.612	89.937	90.587	.007
9.612	101.092	101.910	.011
9.612	112.228	113.234	.012
9.612	123.341	124.557	.010

TABLE IV-51 cont.

ACETONE/2-BUTANOL VAPOR DENSITY DATA

AT 44.91 DEGREES CELSIUS

	INITIAL PRESSURE 2-BUTANOL	ACETONE PRESSURE	ACETONE IDEAL PRESSURE	$\Delta\Pi$(EXP)-$\Delta\Pi$(CALC)
	9.612	134.429	135.881	.005
	9.612	145.502	147.204	.011
	9.612	156.554	158.527	.011
	9.612	167.556	169.851	- .019
	9.612	178.559	181.174	.004
	9.612	189.540	192.497	.003
	9.612	200.497	203.821	.001
	9.612	211.433	215.144	.001
	9.612	222.353	226.468	.007
	9.612	233.248	237.791	.004
	9.612	244.125	249.114	.008
	9.612	254.980	260.438	.008
	9.612	265.806	271.761	.000
**	15.641	11.294	11.323	- .004
**	15.641	22.565	22.647	- .007
	15.641	33.815	33.970	- .008
	15.641	45.045	45.294	- .008
	15.641	56.261	56.617	- .002
	15.641	67.456	67.940	- .003
	15.641	78.631	79.264	- .002
	15.641	89.788	90.587	.000
	15.641	100.917	101.910	- .007
	15.641	112.029	113.234	- .003
	15.641	123.120	124.557	- .003
	15.641	134.187	135.881	- .006
	15.641	145.242	147.204	.003
	15.641	156.270	158.527	- .003
	15.641	167.279	169.851	- .000
	15.641	178.270	181.174	.004
	15.641	189.237	192.497	.001
	15.641	200.176	203.821	- .005
	15.641	211.097	215.144	- .001
	15.641	221.999	226.468	.003
	15.641	232.873	237.791	- .003
	15.641	243.728	249.114	.000
	15.641	254.559	260.438	- .001

** These data were not included in the data treatment.

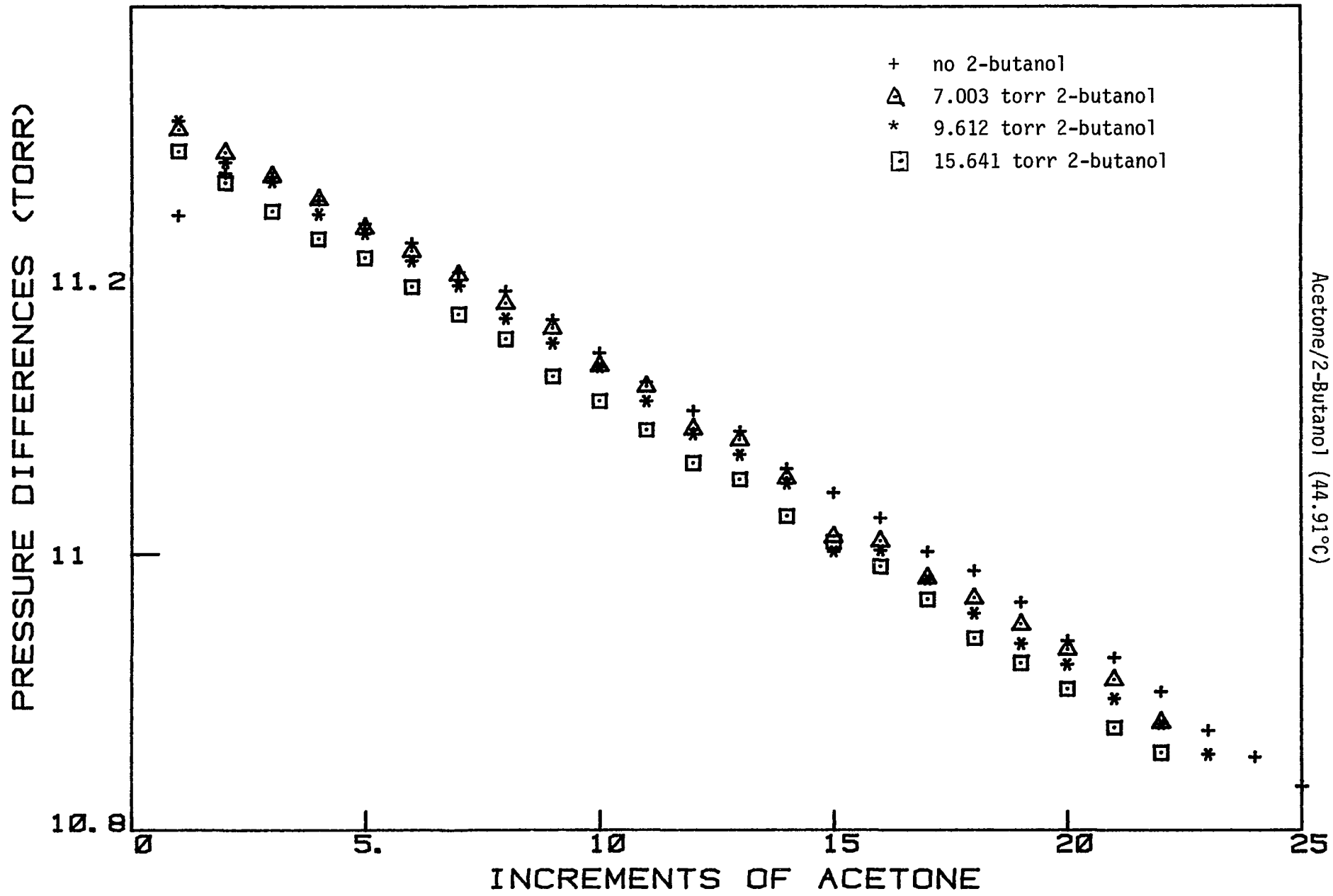

FIGURE IV-43

Acetone/2-Butanol (44.91°C)

CHAPTER V

DISCUSSION

i. General

The significant result of this dissertation research is the development of an appartus capable of studying a wide range of phenomena. One may obtain highly precise data from the manually-operated vapor density apparatus, heretofore not possible. Molecular behavior in both the vapor and solution phases, as well as at the dew point, is readily observed through effects of complexation on pressure. The automated version of this apparatus makes the versatility of this technique even more appealing. Literally hundreds of data points are quickly and easily obtained through operation of this apparatus. In other techniques for studying molecular association, both the time to collect good data and the complexity of treating these data are deterrents to studying a large number of systems. One hopes that with the advent of such apparatuses as have resulted from this work, many more vapor systems will be thoroughly studied with the goal of developing an adequate theory of solution behavior.

The most important information one wishes to obtain from vapor phase studies is the value of the second virial coefficient. Theoretical values of the second virial coefficient may be

compared with the experimental values (the dimer equilibrium constant) with the purpose of confirming or rejecting equations of state used to model vapor behavior. One may determine very reliable second virial coefficients from data obtained from this apparatus. Unfortunately, higher order terms are subject to considerable error due to adsorption problems.

Adsorption effects have been mentioned throughout this dissertation: (1) Experiments carried out by other investigators to study the adsorption of various compounds on glass are referred to in the Introduction. (2) Experiments performed by this investigator on adsorption effects are described in Chapter III and a graph of water/TFE adsorption on pyrex glass given in figure IV-9. (3) The necessity to ignore the first data point of each set of acetone/ethanol vapor density experiments and the first two data points of each acetone/2-butanol vapor density data set is blamed on adsorption effects. In fact, the acetone/water vapor density data were not analyzed because of the overwhelming adsorption problem. (4) A calculated point based on literature experimental results, the Keyes point, was added to the acetone vapor density results at each of the seven temperatures. Use of this point made it possible to observe the effect of adsorption on data obtained near the saturation point.

Previous attempts to separate adsorption effects from association effects in PVT data have not been very successful. Anderson, Kudchadker, and Eubank[93] studied the association of

acetone vapor for the temperature range 25°C to 150°C using a Burnett PVT apparatus.[85] After each expansion, they waited 10 to 12 hours to reach equilibrium. The data were then corrected for adsorption using a Langmuir model and analyzed for chemical association with a model including 2nd, 3rd, and 4th virial coefficients. In comparing the second virial coefficients of Anderson et al. with those obtained by other scientists[93] and this study, the second virial coefficients of Anderson et al. are at almost every temperature the largest values reported. In most studies, values of second virial coefficients tend to be too large due to neglect of higher-order terms in the association model or adsorption effects. Anderson and co-workers included a sufficient number of higher-order terms in treating their data. However, acetone vapor is so weakly associated, it is very difficult to separate the adsorption effects from association effects.

Cheam, Farnham, and Christian[48] also tried to eliminate adsorption effects during the course of a PVT experiment in a study of methanol vapor association at 25°C. A silica microbalance was placed in a chamber, to which methanol vapor samples could be added. At one end of the balance beam was a closed bulb and at the other end an open bulb having nearly the same total surface area. The change in gas density in the chamber was detected by observing a change in height of the closed bulb. Changes due to adsorption on the closed bulb would be countered by the same amount of adsorption on the open bulb. Yet, the authors

still found adsorption effects a problem near the saturation pressure.

The point is, when adsorption effects become too large relative to association, the two cannot be readily separated. Necessarily, great care must be taken when analyzing the data of a very weakly associated vapor with a propensity to adsorb to the flask wall. It is very difficult to compensate for adsorption effects; rather, it is easier to avoid them all together. The method of introducing a Keyes point when analyzing PVT data and using only the vapor density data free from significant adsorption effects seems an excellent choice to avoid this nagging adsorption problem. Heats of vaporization data and studies of vapor pressure as a function of temperature are not available in the literature for many compounds that might be interesting subjects for vapor density experiments. Moreover, no comparable information for mixed vapor systems exists.

Regardless of whether or not a Keyes point is determined, PVT data at pressures below 2/3 of the vapor pressure of many compounds may be analyzed to obtain a very good value of the second virial coefficient or dimer equilibrium constant. Equilibrium constants for the formation of species larger than the dimer are very sensitive to data near the saturation pressure.

ii.- Self-Association

ii.1 - 2,2,2-Trifluoroethanol

Results from the PVT studies of TFE vapor indicate that little association occurs between monomers of TFE at 25°C and pressures as large as 50 torr. Data were fitted with several different association models. A single-parameter fit, whether a stepwise equilibrium constant, K_∞, or a dimer or trimer constant, K_2 or K_3, did not adequately fit the data. The combination of either a dimer or trimer equilibrium constant with a stepwise constant, K_∞, gave equally good fits and consistent equilibrium constants for the formation of a trimer and the sequential addition of monomer. (See Table IV-2.) K_3 from the 1-3-infinity model is $2.7X10^{-7}$ $torr^{-2}$; calculation of K_3 from the 1-2-infinity model is obtained from the product of the dimer constant and the stepwise addition constant,

$$K_2 * K_\infty = 2.11X10^{-5} * 1.04X10^{-2} = 2.12X10^{-7} torr^{-2}.$$

Fitting the data to a 1-2-3-infinity model resulted in a negative value for the trimer constant. This is a data fitting problem and not a physical one.

Several other studies have been reported on TFE association. S. Farnham [64] used a monomer-trimer-octamer model (1-3-8) to fit TFE PVT data at 25°C. The results of his study are

in accord with this work insofar as he suggests that TFE is little associated up to pressures of about 50 torr. Farnham's trimer constant is 7.46×10^{-7}, about 2.7 times larger than those obtained from the 1-2-infinity or 1-3-infinity models in this study. Thermal conductivity studies of TFE vapor are reported by Curtiss, Frurip, and Blander.[58] They studied the association of TFE at several temperatures between 65°C and 112°C. Extrapolation of their results to 25°C yields a dimer constant of 3.2×10^{-4} $torr^{-1}$, an order of magnitude greater than the results of this work. Their data were fit with a model accounting for dimer, trimer, tetramer, and pentamer formation, however it was concluded that only dimers are present in TFE vapor.

The results of the present study do not agree at all with the findings of Curtiss et al. The results of the 1-2-infinity and 1-3-infinity models indicate that no single associated species is responsible for a major fraction of the deviation from ideality. The relative contribution of an n-mer does, however, decrease as n increases.

According to Curtiss et al.,[58] the most stable dimer structure predicted by molecular orbital theory is cyclic,

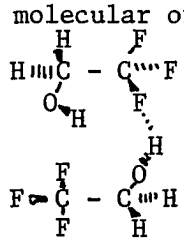

The data depicted in Figure IV-1 imply that the dimer is not an important species, inasmuch as the limiting slope of the plot of

average molecular weight vs. pressure is not significantly greater than zero. Another possible structure would be an open chain of TFE molecules linked by hydrogen bonds, O-H...O,

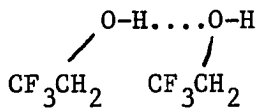

The oxygen atom of a single TFE molecule is a weaker proton acceptor than the oxygen of the corresponding hydrocarbon alcohol, ethanol. Consistent with this is the fact that ethanol has a larger dimer constant, K_2=2-3X10^{-4} $torr^{-1}$, than TFE.

Hydrogen bonding between hydroxyl groups will increase the electron density of the oxygen on the terminal TFE molecule, thereby increasing the hydrogen-bonding ability of the oxygen. This cooperative effect causes higher-order aggregates to form in preference to dimers.

ii.2 - Acetone

Association of acetone in the vapor phase has been studied extensively. There is a considerable discrepancy between reported values. In most cases, analysis of the data assumed all association due to dimer formation. A few studies included terms to account for larger polymers in addition to the dimer. A fairly complete table (V-1) of equilibrium constants reported in the literature is provided in this chapter.

At 25°C, vapor density pressures up to 63% of the vapor pressure and the Keyes point were used to determine the dimer equilibrium constant, $K_2=1.034X10^{-4}$ $torr^{-1}$, and the stepwise addition constant, $K_\infty=2.92X10^{-4}$ $torr^{-1}$. At the vapor density data cut-off pressure, 146.1 torr, 12 increments of acetone had been added. The ratio of ideal pressure to true pressure (Π/P) is 1.0157. At this pressure, dimer formation is responsible for 95.8% (2.140 torr) of the association. Trimer species represent 4% of the nonideal behavior. Near saturation, the contribution of each associated species to the nonideal behavior is

dimer	93.4%	(5.254 torr)
trimer	6.2%	(0.346 torr)
tetramer	.4%	(0.023 torr)

pressure of associated species = 5.624 torr.

Assuming only dimer formation, K_2=1.184X10^{-4} torr^{-1}.

Admittedly, the formation of the dimer is by far the most significant contribution to the nonideal behavior of acetone vapor. For many purposes, neglecting higher-order constants than the dimer in modeling acetone vapor will still yield good results. Due to the predominance of the dimeric species, the second virial coefficient or dimer constant for acetone should be very reliable. On the other hand, higher-order constants are dependent on data collected in the pressure region where adsorption effects are so critical. Or, as in the case of this work, the higher-order constant, K_∞, is almost totally dependent on the value of the Keyes point.

A heat of association was calculated for each equilibrium constant. Both ΔH_2 and ΔH_∞ are negative indicating that the amount of association decreases with increasing temperature.

Comparing the chemical structure of acetone with that of TFE is instructive in understanding the very different behavior of associated species in the two vapors. Association of two TFE molecules enhances the hydrogen bonding ablility of the hydroxyl groups. This cooperative effect leads to further association and, thus, no single species predominates.

Frurip, Curtiss, and Blander[60] have proposed geometric structures for the acetone dimer stabilized by weak hydrogen bonds.

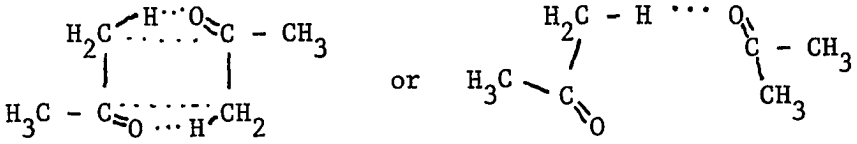

Molecular orbital calculations were made on several possible structures and these two were found to be the most stable.

An antiparallel configuration discussed by C. Lin[37]

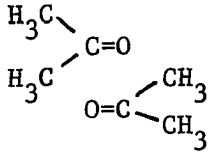

may be described as a "random dipole pair".[99] There is less rigidity in such a dimer than in a hydrogen bonded complex. In either proposed structure, further association is not likely to be greatly enhanced by formation of the dimer.

TABLE V-1

REFERENCES TO ACETONE VAPOR STUDIES

Reference	Experimental Technique	Temperature	Model	Results
35	PVT	40-130°C	1-2	ΔH_2= -3.2-(-8.0) kcal/mole
116	PVT	70-100°C	1-2	only graphs
117	PVT	30-160°C	1-2	K_2(31.48°C)=9.45X10^{-5} torr^{-1} ;K_2(157.19°C)=1.84X10^{-5}torr^{-1}
118	differential compressibility	22°C & 55°C	1-2	K_2(22°C)=1.15X10^{-4} torr^{-1}; K_2(55°C)=714X10^{-5} torr^{-1}
93	PVT-Burnett apparatus	25-150°C	1-2-3-4	ΔH_2=-3.9kcal/mole; K_2(25°C)=1.1467X10^{-4}torr^{-1}
60	Thermal Conductivity	66-105°C	1-2	ΔH_2=-3.22 kcal/mole; K_2(67.65°C)=7.76X10^{-5} torr^{-1}
119	PVT	40-100°C	1-2	K_2(40°C)=8.65X10^{-5} torr^{-1}; K_2(100°C)=3.58X10^{-5} torr^{-1}
82	Thermal Conductivity	98 & 109.4°C	1-2	ΔH_2= >-5.0 kcal/mole
120	Theoretical Stockmayer Pot.	25°C	dimer	K_2=1.138X10^{-4} torr^{-1}
121	PVT-quartz microbalance	22°C	data suggests higher order terms needed.	Π/P(150 torr)=1.018
122	PVT	22°C	1-2	K_2=8.34X10^{-5} torr^{-1}
this work	PVT	15-45°C	1-2-∞	ΔH_2= -3.14 kcal/mole; ΔH_∞=2.65 kcal/mole; K_2(25°C)=1.03X10^{-4} torr^{-1} K_∞(25°C)=2.92X10^{-4} torr^{-1}

iii. HETEROASSOCIATION

iii.1 TFE/ROH

The mixed vapor density data for the TFE/ROH system were fitted with several models. No single-parameter models were sufficient in fitting the data. A 1-infinity model was used and, in the case of TFE/water, worked very well. Fitting the TFE/alcohol data required the inclusion of a third parameter representing the formation of the 2:1 trimer,

$$TFE + 2ROH \overset{K_{21}}{\rightleftharpoons} TFE(ROH)_2 .$$

See Table IV-2 for results.

Unlike the case of TFE, where no single species predominates, the TFE-ROH dimer is present in a significant amount. Near saturation and at the largest partial pressure of ROH, the following pressures of 1:1 complexes were calculated using the K_{11} equilibrium constant.

ROH	partial pressure of TFE-ROH	% of total heteroassociation
Water	0.10 torr	49%
Methanol	0.10 torr	25%
Ethanol	0.10 torr	38%

2-Butanol	0.03 torr	26%

The predominant species in the TFE/ethanol and TFE/2-butanol systems is the $TFE(ROH)_2$ trimer. 51% of the TFE/ethanol and 72% of the TFE/2-butanol heteroassociation is due to the formation of this trimer. In the case of TFE/methanol, the $TFE(MeOH)_2$ trimer and 1:1 dimer are present in equal amounts.

An interesting result of this study is the observation that the K_∞ values for each TFE mixed system and self-association system are remarkably similar. K_∞ increases very slightly in the order

TFE< water< methanol< ethanol< 2-butanol

Values of the trimer equilibrium constant increase in the same order,

methanol< ethanol< 2- butanol

One can expect to obtain a more reliable heteroassociation dimer constant than was possible for the self-association dimer constant for this system. In the latter case, TFE monomers are not as attracted to one another as they are to dimers. Dimeric species are readily converted to trimers, tetramers, etc. In the mixed vapor system the TFE monomers and ROH monomers have a greater affinity for one another than in the TFE self-association case. Just as K_2 for ethanol is greater than K_2

for TFE, K_{11} for ethanol and TFE would also be expected to be larger than K_2 for TFE.

There is an increase in the strength of the 1:1 interaction with an increase in molecular weight of ROH in the series

water< methanol< ethanol< 2-butanol

This order is the expected one, assuming that the TFE hydroxyl proton forms hydrogen bonds to the oxygen of ROH.

Both the polarizability and the inductive effects increase with addition of CH_3 groups. One expects these effects to combine to strengthen the 1:1 interaction as R increases in size.

The results of the TFE system (both self-association and mixed vapor systems) have been published in a recent article.[63] In that paper, a proposal of Taft et al.[11] is cited. With modifications, his proposal is applied to the TFE studies. The work of Taft et al. discusses the role of polarizability effects (P) and inductive effects (I) in the gas phase proton-transfer equilibria, e.g.

$$ROH + CH_3OH_2^+ = ROH_2^+ + CH_3OH \quad (a)$$

$$ROH + CH_3O^- = RO^- + CH_3OH \quad (b)$$

In each of these reactions, a proton has been completely

transferred. Analogous to these reactions is the partial transfer of a proton involved in the hydrogen bonding reactions,

$$ROH + HA = R\overset{H}{O}...HA \quad (a')$$

$$ROH + B = RO\text{-}H...B \quad (b')$$

The polarizability is a measure of the ease with which the electron density around a molecule can be deformed by an external field (e.g. the dipole of another molecule). As the size of R increases, the polarizability of ROH increases. The inductive effect refers to the electron donating ability (+I) or the electron withdrawing ability (-I) of the R substituent. The inductive effect of R follows the order

$$H<CH_3<CH_3CH_2<CH_3CH(CH_3) \qquad \text{for } +I$$

or

$$H>CH_3>CH_3CH_2>CH_3CH(CH_3) \qquad \text{for } -I$$

Reactions (a) and (a') are enhanced by P and +I. Reactions (b) and (b') are favored by P and -I. The association of TFE and ROH is an (a') reaction since TFE is a proton donor. Complexation should increase with increasing polarizability of the R group and with increasing electron donating ability (+I) of the R group. The increase in K_{11} and K_∞ with increasing molecular weight of R is consistent with this theory.

iii.2 Acetone/ROH

Vapor density data of acetone/ROH at 25°C were fitted to several different models before choosing the 1-infinity model. One might expect that a model containing a 1:1 constant and a 2:1 constant (i.e. $(ROH)_2$acetone) would adequately fit the data since two alcohols might hydrogen bond with one another. The most probable structure of the 1:1 dimer is

$$>\!=O\ldots H\text{-}O\text{-}R.$$

A model which assumes addition of an acetone monomer to this dimer gives 1/3 of the RMSD obtained by assuming an ROH monomer adds to this dimer. Acetone behaves as a Lewis base in the presence of alcohol. The association of acetone and ROH is described by reaction (b') in the previous section.

Equilibrium constants and heats of association constants were calculated using the 1-infinity model. K_{11} decreases slightly with increasing molecular weight of ROH,

methanol>ethanol>2-butanol.

This is also the order in which the electron withdrawing ability of R (-I) increases. The formation of the dimer is stabilized by the inductive effect (-I) of the R group on the -O-H...O= bond. Further association occurs by the addition of acetone monomers to the 1:1 dimer. This would be an induced dipole interaction since

there is no available hydrogen bonding site. It is stabilized by polarizability effects. Again, the larger the size of R in the R-O-H...O=< complex, the more polarizable the molecule. The results of the acetone/ROH studies are consistent with this theory since K_∞ increases in the order

methanol<ethanol<2-butanol

Table V-2 gives the total pressure of associated molecules and the relative contributions of dimers, trimers, and tetramers to the overall nonideality of the mixed vapors at 25°C. These values are calculated using the least squares values of K_{11} and K_∞ obtained from the 1-infinity fit of mixed vapor data at all temperatures. Table IV-13 gives the results of the data treatment. The amount of alcohol is 15 torr and the amount of acetone is 50, 100, and 150 torr. At 50 torr partial pressure of acetone, the amount of total deviation is about the same for each mixed vapor system. This suggests that the effects of P and -I tend to cancel one another. Near saturation, the overall deviation increases with increasing molecular weight of R. This may be attributed to the predominance of polarizability effects. It is interesting to note that a reversal in order is found in condensed phases. Apparently the longer range polarizability effects are attenuated to a greater degree in solvents than the shorter range inductive effects.[11]

TABLE V-2

PRESSURE OF ACETONE/ROH COMPLEXES

ROH	Pressure of Acetone	Total Pressure of Complexes	Dimer Pressure	% of Complexes	Trimer Pressure	%of Complexes	Tetramer Pressure	% of Complexes
Methanol	50 torr	0.131 torr	0.119	90.6	0.011	8.5	0.001	0.8
Methanol	100 "	0.292 "	0.237	81.2	0.045	15.3	0.008	2.9
Methanol	150 "	0.496 "	0.356	71.8	0.100	20.2	0.028	5.7
Ethanol	50 torr	0.111 torr	0.093	84.03	0.015	13.4	0.002	2.0
Ethanol	100 "	0.275 "	0.187	68.07	0.060	21.74	0.019	6.9
Ethanol	150 "	0.538 "	0.280	52.1	0.134	25.0	0.064	12.0
2-Butanol	50 torr	0.111 torr	0.088	79.2	0.018	16.5	0.004	3.4
2-Butanol	100 "	0.302 "	0.177	58.5	0.073	24.3	0.030	10.1
2-Butanol	150 "	0.703 "	0.265	37.7	0.165	23.5	0.103	14.6

All alcohol pressures = 20 torr.

iii.3 Acetone Compared with TFE/ROH

The overall deviations from ideality are greater in the TFE/ROH system than in the acetone/ROH system. The 1:1 constants for both systems fall in the range of $1\text{-}5\times10^{-4}$ $torr^{-1}$, where the dimer is stabilized by hydrogen bond formation. Larger aggregates form much more readily in the TFE/ROH vapors since P and +I effects work together. P and -I effects work against one another in the complexation of ROH and acetone. The stepwise addition constant for the Lewis base system is only 1/5-1/10 as large as K_∞ for the TFE/ROH vapor.

IV. Liquid-Vapor Equilibrium

An ideal vapor in equilibrium with its ideal liquid obeys the relationship

$$P_i = X_i P_i^\circ$$

known as Raoult's law. P_i is the pressure of component i whose mole fraction in solution is X_i. P_i° is the vapor pressure of the pure component. For the binary TFE/ROH system, the relationship is

$$P = P_{TFE} + P_{ROH} = X_{TFE} P^\circ_{TFE} + X_{ROH} P^\circ_{ROH}$$

where P is the total pressure consisting of the partial pressures of TFE and ROH, P_{TFE} and P_{ROH}.

A pronounced positive deviation from Raoult's law is observed in the TFE/water liquid-vapor curve. At high mole fractions of TFE, this positive deviation begins to diminish and in the limit (as $X_{TFE} \rightarrow 1$) the system is consistent with Raoult's law.

The liquid-vapor equilibrium curves of TFE/methanol, TFE/ethanol, and TFE/2-butanol all display negative deviation from Raoult's law. This negative deviation may be attributed to relatively strong hydrogen bonding in the liquid phase. In the cases of TFE/methanol and TFE/ethanol, an azeotrope is observed at P=66.7 torr, $\overline{X}_{TFE}$=0.74 and P=48.10 torr, $\overline{X}_{TFE}$=0.41, respectively.

CHAPTER VI.

CONCLUSIONS

The highly precise vapor density technique allows one to study a wide range of gas phase interactions. From these studies, one can get a better understanding of effects contributing to association. The problems of adsorption are still troublesome and, although not prohibitive to vapor phase studies, limit the amount of meaningful information one is able to obtain from data near the saturation pressure.

In the homogeneous vapor systems, K_∞, is well determined from TFE vapor data and K_2 is the more reliable parameter determined from acetone vapor data. All of the constants in the mixed vapor studies are believed to be reliable. ΔH_∞ for the acetone/ROH systems is quite large and is most probably affected by adsorption problems.

Collection of liquid-vapor eqiulibrium data is both rapid and convenient. A very small amount of substance is used in each experimental run; a complete curve may require several experimental runs in order to cover the entire mole fraction range.

Inclusion of a Keyes point in analyzing vapor density data provides a very good check for adsorption problems. However, producing the data to calculate the single Keyes point requires some effort. The vapor pressure at different temperatures must be measured. Very reliable P(T) data are already available in the literature for many compounds. Published heat of vaporization data are more scarce and might have to be determined by the investigator.

The concepts of polarizability effects and inductive effects may provide a powerful tool in predicting the modification of molecular complexes formed in condensed phase. For example, polarizability effects frequently appear to predominate in the vapor phase; they have considerably less impact on complexation in the solution phase where the shorter range inductive effects become more important.

More vapor phase association studies are needed before trying to make any correlations with solution phase studies. For example, a comparison of F_3C-CH_2OH, F_2CH-CH_2-OH, and FCH_2-CH_2-OH associated with acetone would give a more definitive understanding of inductive effects in the vapor phase. K_{11} for the formation of TFE:acetone in the vapor phase at 25°C is $2.55X10^{-3}$ $torr^{-1}$ according to the vapor density studies of E. E. Tucker and S. D. Christian.[102] This value is almost 20 times the K_{11} value obtained for acetone/ethanol. The strong electron withdrawing ability of the $-CH_2CF_3$ substituent (-I) is much more effective in stabilizing

the 1:1 complex than is $-CH_2CH_3$. Vapor density studies of a series of primary, secondary, and tertiary alcohols with a Lewis acid and a Lewis base would provide further insight into the effects of polarizability on gas phase reactions.

Overall, the vapor density technique is capable of excellent results in studying association in the vapor phase (or solution phase). The straightforward method of data treatment and the repeatability of data sets render it superior to other experimental techniques used to study molecular complexes.

Several suggestions for choosing systems to be studied with this method follow:

1)The compounds chosen should be compatible with the surfaces of the apparatus. Avoid corrosive vapors and vapors notorious for adsorption (e.g. tetrahydrofuran).

2)Choose a compound whose vapor pressure at the experimental temperature is high enough that a reasonable number of increments may be introduced to the flask.

3)In the study of solution phase interactions, the solvent should have a fairly low vapor pressure.

4)Choose systems in which the degree of association is suspected to be great enough so as not to be masked by adsorption effects.

BIBLIOGRAPHY

1. E. Hall, J. Pick, V. Fried, O. Vilim, "Vapour-Liquid Equilibrium", Pergamon Press: New York, 1958.
2. F.T. Wall, "Chemical Thermodynamics", 3rd ed.; W.H. Freeman and Co: San Fransisco, 1947; pp 382-384.
3. J.W. Gibbs, "Collected Works", Vol.1; Longmans, Green: New York, 1928; p. 55
4. See p. 372 in reference 3.
5. J.O. Hirschfelder, F.T. McClure and I.F. Weeks, J. Chem. Phys., 10, 201(1942).
6. J. Timmerman, J. Chim. Physique, 19, 169(1921).
7. J.J. Van Laar, Z. Physik. Chem., 72, 723(1910).
8. J.J. Van Larr, Z. Physik. Chem., 83, 599(1913).
9. F. Dolezalek, Z. Physik. Chem., 64, 727(1908).
10. J.M. Prausnitz and W.B. Carter, Am. Inst. Chem. Eng. J., 6, 611(1960).
11. R.W. Taft, M. Taagepera, J.L. Abboud, J.F. Wolf, D.J. DeFrees, W.J. Hehre, J.E. Bartmess, R.T. McIver, Jr., J. Am. Chem, 100, 7765(1978).
12. F. London, Z. Physik. Chem., B11, 222(1930); Trans. Faraday Soc., 33, 8(1937).
13. J.J. Sudborough, J. Chem. Soc., 79, 522(1901).
14. J.J. Weiss, Nature London, 147, 512(1941).

15. J.H. Hildebrand and R.L. Scott, "Solubility of Nonelectrolytes", 3rd ed.; Reinhold Publishers: New York, 1950.

16. C.A. Coulson, "Valence", 2nd ed.; Oxford University Press: Oxford, 1961.

17. See p. 182 in reference 16.

18. L. Pauling, "The Nature of the Chemical Bond", 2nd ed.; Cornell University Press: New York, 1940; p. 3.

19. D. Berthelot, Trav. Bur. Int. Poids Mes., 13 (1907).

20. S.D. Christian and E.H. Lane in "Solutions and Solubilities", M.R.J. Dack, Editor; Wiley: New York, 1975, Chapter 6.

21. J.D. Lambert, Disc. Faraday Soc., 15, 226(1953).

22. S.D. Christian and J. Grundnes, Acta Chem. Scand., 22, 1702(1968).

23. S.D. Christian, J.R. Johnson, H.E. Affsprung and P.J. Kilpatrick, J.Phys. Chem., 70, 3376(1966).

24. S.D. Christian, R. Frech and K.O. Yeo, J. Phys. Chem., 77, 813(1966).

25. K.M.C. Davis in "Molecular Association", Vol.1; R. Foster, Editor; Academic Press:1975; Chapter 3.

26. M.J. Cook, A.R. Katritzky, M. Taagerpa, T.D. Singh and R.W. Taft, J. Am. Chem. Soc., 98, 6048(1976).

27. P. Beak, Acc. Chem. Res., 10, 186(1977).

28. P. Beak, J.B. Covington and S.G. Smith, J. Am. Chem. Soc., 98, 8284(1976).

29. P. Beak, F.S. Fry, Jr., J. Lee and F. Steele, J. Am. Chem. Soc., 98, 171(1976).

30. E. Hirano and K. Kozima, Bull. Chem. Soc. Japan, 39, 1216(1966).

31. R.S. Mulliken and W.B. Person, "Molecular Complexes", Wiley: New York, 1969; p.307.

32. E.A. Mason and T.H. Spurling,"The Virial Equation of State", 1st ed.; Pergamon Press: New York, 1969, p.3.

33. E.E. Tucker, E.H Lane and S.D. Christian, J. Solution Chem., 10, 1(1981).

34. P.J. McElroy, T.W. Shannon, A.G. Williamson, J. Chem. Thermodyn., 12, 371(1980).

35. J.D. Lambert, G.H.A. Roberts,J.S. Rowlinson and V.S. Wilkinson, Proc. Roy. Soc. London, A196, 113(1949).

36. J.O. Hirschfelder, C.F. Curtiss and R.B. Bird, "Molecular Theory of Gases and Liquids", 2nd ed.; Wiley: New York, 1964, p.917.

37. C. Lin, Ph.D. Dissertation, TheUniversity of Oklahoma, 1964.

38. L. Pauling, "The Nature of the Chemical Bond", 2nd ed.; Cornell University Press: New York, 1940, Chapter 1.

39. R.S. Mulliken, J. Am. Chem. Soc., 74, 811(1952).

40. M. Kroll, J. Am. Chem. Soc., 90, 1097(1968).

41. R. Foster, "Organic Charge-Transfer Complexes", Academic Press: New York, 1970; Chapter 7.

42. G.M. Barrow, J. Chem. Phys., 20, 1739(1952).

43. A. Werner, Ber., 36, 147(1903).

44. P. Pfeiffer, Ann., 137(1913).

45. W.M. Latimer and W.H Rodebush, J. Am. Chem. Soc., 42, 1419(1920).

46. E.F. Fiock, D.C. Ginning, W.B. Holton, U.S. Bur. Standards J. Res., 6, 881(1931).

47. L. Pauling, "The Nature of the Chemical Bond", 2nd ed.; Cornell University Press: New York, 1940, p. 431.

48. V.C. Cheam, S.B. Farnham, S.D. Christian, J. Phys. Chem., 74, 4157(1970).

49. E. Lippert in "The Hydrogen Bond", P. Schuster, G. Zundel and C. Sdandorfy, Editors; North Holland Publishing Co.: Amsterdam, 1976; Chapter 1.

50. D. Ambrose, C.H.S. Sprake, J. Chem. Thermodyn., 2, 631(1970).

51. G.C. Pimentel and A.L. McClellan, "The Hydrogen Bond", W.H. Freeman: San Fransisco, 1960.

52. J.D. van der Waals (Leiden 1873); cited in Ref. 15.

53. N. Davidson, "Statistical Mechanics", McGraw-Hill: New York, 1962, Chapter 15.

54. See Chapter 6 in reference 36.

55. J.H. Dymond and E.B. Smith, "The Virial Coefficient of Pure Gases and Mixtures", Clarendon Press: Oxford, 1980.

56. See p. 14 in reference 32.

57. See p. 325 in reference 53.

58. L.A. Curtiss, D.J. Frurip and M. Blander, J. Am. Chem. Soc., 100, 79(1978).

59. T.A. Renner, G.H. Kuccra and M. Blander, J. Chem. Phys., 66, 177(1977).

60. D.J. Frurip, L.A. Curtiss and M. Blander, J. Phys. Chem., 82, 2555(1978).

61. J. Del Bene, . Chem. Phys., 60, 3812(1974).

62. L.A. Curtiss, J. Chem. Phys., 67, 1144(1977).

63. L.S. Smith, E.E. Tucker and S.D. Christian, J. Phys. Chem., 85, 1120(1981).

64. S. Farnham, Ph.D. Dissertation, The University of Oklahoma, Norman, OK, 1971.

65. R.H. Wood, T.H. Lilley and P.T. Thompson, J. Solution Chem., 6, 1301(1977).

66. O.R. Wulf and V. Liddel, J. Am. Chem. Soc., 57, 1464(1953).

67. G.E. Hilbert, O.R. Wulf, S.B. Hendricks and V. Liddel, Nature, 135, 147(1935).

68. G.E. Hilbert, O.R. Wulf, S.B. Hendricks and V. Liddel, J. Am. Chem. Soc., 58, 548(1936).

69. G.E. Hilbert, O.R. Wulf, S.B. Hendricks and V. Liddel, J. Am. Chem. Soc., 58, 1991(1936).

70. O.R. Wulf, V. Liddel and S.B. Hendricks, J. Am. Chem. Soc., 58, 2287(1936).

71. O.R. Wulf and L.S. Deming, J. Chem. Phys., 6, 702(1938).

72. V. Liddel and O.R. Wulf, J. Am. Chem. Soc., 55, 3574(1938).

73. R.M. Badger and S.H. Bauer, J. Chem. Phys., 4, 711(1936).

74. W. Brackmann, Rev. Trav. Chim., 68, 147(1949).

75. R.S. Mulliken, J. Phys. Chem., 56, 801(1952).

76. C. Reid and R.S. Mulliken, J. Am. Chem. Soc., 76, 3869(1954)

77. L.E. Orgel and R.S. Mulliken, J. Am. Chem. Soc., 79, 4839(1957).

78. H.H. Willard, L.L. Merritt and J.A. Dean, "Instrumental Methods of Analysis", 5th ed.; Van Nostrand: Princeton, 1974; p.83,86.

79. E.M. Engler, P. Laszlo, J. Am. Chem. Soc., 93, 1317(1971); P. Laszlo and J.L. Soong, Jr., J. Chem. Phys., 47, 4472(1967).

80. A.J. Pesce, C.G. Rosen, T.L. Pasby, "Fluoroscence Spectroscopy", M. Dekker: New York, 1971; Chapter 7.

81. for example see A.D.H. Clague, G. Govil and H.J. Bernstein, Can. J. Chem., 47, 625(1969).

82. R.G. Vines, Aust. J. Chem., 6, 1(1969).

83. See p. 8 in reference 38.

84. V.S. Touloukian, P.E. Liley and S.C. Saxena, "Thermal Physical Properties of Matter", IFI Plenum: 1970; Vol.3, p.24A.

85. E.S. Burnett, J. Appl. Mech., 58, A-136(1936).

86. E.E. Tucker and S.D. Christian, J. Chem. Thermodyn., 11, 1137(1979).

87. M. Folman and D.J.C. Yates, Trans. Faraday Soc., 54, 1684(1958).

88. G.A. Bottomley, I.H. Coopes, L. Nyberg and T.H. Spurling, Austr. J. Chem., 18, 1105(1965).

89. T. Devries and B.T. Collins, J. Am. Chem. Soc., 63, 1343(1941).

90. C. Ener, A. Busala and J.C. Hubbard, J. Chem. Phys., 23, 155(1955).

91. R.G. Inskeep, F.E. Dickson and J.M. Kelliher, J. Mol. Spectroscopy, 4, 477(1960).

92. D.J. Millen and J. Zabicky, J. Chem. Soc., 3080(1960).

93. L.N. Anderson, A.P. Kudchadker and P.T. Eubank, J. Chem. Eng. Data, 13, 321(1968).

94. J.D. Lambert, E.N. Staines and S.D. Woods, Proc. Roy. Soc., 200A, 262(1950).

95. E.H. Lane, Ph.D. Dissertation, The University of Oklahoma, Norman, OK, 1977.

96. C.B. Kretschmer and R. Wiebe, J. Am. Chem. Soc., 76, 2579(1954).

97. F. Cracco and P. Huyskens, Bull. Soc. Chim. Belg., 69, 255(1960).

98. J.D. Cox, Trans. Faraday Soc., 57, 1674(1961).

99. A.M. Saum, J. Polymer Sci., 42, 57(1960).

100. B.R. Lentz, A.T. Hagler, H.A. Scheraga, J. Phys. Chem., 78, 1531(1974).

101. L.A. Curtiss, D.J. Frurip and M. Blander, Chem. Phys. Letter, 54, 575(1978).

102. E.E. Tucker and S.D. Christian, J. Am. Chem. Soc., 98, 6109(1976).

103. Cited in Ref. 58: (a) D.R. Miller, "Rankine Working Fluids for Solar to Electrical Conversion", Monsanto Research Corporation MRC-SL-399, 1974; (b) J.G. Davoud, "Proof of Principle Study of the D-cycle: a Thermodynamic Cycle using Mechanical Compression of a Condensable Vapor", DCR No 741, D-Cycle Power Systems Inc., Richmond, VA, 1974.

104. C.H. Rochester and J.R. Symonds, J. Chem. Soc Faraday Trans.I, 1267(1973).

105. A.I. Vogel, "Practical Organic Chemistry", 3rd ed.; Longman: London, 1965, p.171.

106. See p. 169 in reference 105.

107. K.B. Wiberg, "Laboratory Techniques in Organic Chemistry", McGraw-Hill: New York 1960, pp.243-245.

108. F.G. Keyes, J. Chem. Phys., 15, 602(1947).

109. R.S. Hansen, F.A. Miller, J. Phys. Chem., 58, 193(1954).

110. S.D. Christian, J. Chem. Educ. 39, 521(1962).

111. E.E. Tucker, E.D. Becker, J. Phys. Chem., 77, 1783(1973).

112. D.W. Marquardt, J. Soc. Ind. Appl. Math., 11, 431(1963).

113. R.E. Pennington, K.A. Kobe, J. Am. Chem. Soc., 79, 300(1957).

114. R.B. Bird, W.E. Stewart, E.N. Lightfoot, "Transport Phenomena", John Wiley & Sons, Inc.: New York, 1960.

115. D. Ambrose, C.H.S. Sprake, R. Townsend, J. Chem. Thermodyn., 6, 693(1974).

116. A. Eucken, L. Meyer, Z. Physik. Chem., B5, 452(1929).

117. G.A. Bottomley, T.H. Spurling, Australian J. Chem., 20, 1789(1967).

118. G.A. Bottomley, T.H. Spurling, Nature, 195, 900(1962).

119. D.H. Knoebel, W.C. Edminister, J. Chem. Engr. Data, 14, 377(1969).

120. J.S. Rowlinson, Trans. Faraday Soc., 45, 974(1949).

121. F.L. Cassado, D.S. Massie, R. Whytlaw-Gray, Proc. Roy. Soc., A214, 466(1952).

122. Sh.D. Zaalishvilli, L.E. Kolysko, J. Phys. Chem (Russian), 34, 1223(1960).